TFW-SH12-96-001
USGS WRIR 95-4219

SIMULATION OF WATER AVAILABLE FOR RUNOFF IN CLEARCUT FOREST OPENINGS DURING RAIN-ON-SNOW EVENTS IN THE WESTERN CASCADE RANGE OF OREGON AND WASHINGTON

By

Marijke van Heeswijk
John S. Kimball
Danny Marks
U.S. Geological Survey

1996

U.S. DEPARTMENT OF THE INTERIOR

BRUCE BABBITT, Secretary

U.S. GEOLOGICAL SURVEY

Gordon P. Eaton, Director

For additional information write to:

District Chief
U.S. Geological Survey
1201 Pacific Avenue Suite 600
Tacoma, Washington 98402

Copies of this report may he **purchased** from:

U.S. Geological Survey
Earth Science Information Center
Open-File Reports Section
Box 25286, MS 517
Denver Federal Center
Denver, Colorado 80225

Simulation of Water Available for Runoff in Clearcut Forest Openings During Rain-On-Snow Events in the Western Cascade Range of Oregon and Washington

By Marijke van Heeswijk, John S. Kimball*, and Danny Marks

*Bioresearch Engineering Department, Oregon State University, Corvallis, Oregon, currently with School of Forestry, University of Montana, Missoula, Montana

---

U.S. Geological Survey
Water-Resources Investigations Report 95-4219

Prepared in cooperation with

THE COOPERATIVE MONITORING, EVALUATION, AND RESEARCH COMMITTEE of the WASHINGTON STATE TIMBER/FISH/WILDLIFE AGREEMENT and the WASHINGTON STATE DEPARTMENT OF NATURAL RESOURCES

Tacoma, Washington
1996

FIGURES

CONTENTS

CONVERSION FACTORS AND 'VERTICAL DATUM--Continued

Multiply	By	To obtain
	Energy-flux density	
watt per square meter ($W\ m^{-2}$)	5.285×10^{-3}	British thermal unit per square foot per minute
	Energy-flux density and Temperature	
watt per square meter per kelvin to the fourth power ($W\ m^{-2}\ K^{-4}$)	0.5035×10^{-3}	British thermal unit per square foot per minute per degree Fahrenheit to the fourth power
	Length	
micrometer (pm)	0.03937×10^{-3}	inch
millimeter (mm)	0.03937	inch
centimeter (cm)	0.3937	inch
meter (m)	3.281	foot
	Mass	
kilogram (kg)	2.205	pound
	Mass and Length	
kilogram per meter ($kg\ m^{-1}$)	0.6721	pound per foot
	Mass. Time, and Length	
kilogram per second per square meter ($kg\ s^{-1}\ m^{-2}$)	0.2048	pound per second per square foot
	Pressure	
pascal (Pa)	0.1450×10^{-3}	pound per square inch
	Rate	
millimeter per hour ($mm\ h^{-1}$)	0.03937	inch per hour
meter per second ($m\ s^{-1}$)	2.237	mile per hour

TABLES

CONVERSION FACTORS AND VERTICAL DATUM

Multiply	By	To obtain
Factors for converting SI units to inch-pound units		
	Acceleration	
meter per square second ($m\ s^{-2}$)	3.281	foot per square second
	Density	
kilogram per cubic meter ($kg\ m^{-3}$)	0.06243	pound per cubic foot
	Energy	
joule (J)	9.478×10^{-4}	British thermal unit

CONVERSION FACTORS AND VERTICAL DATUM--Continued

Multiply	By	To obtain
	Specific-heat capacity	
joule per kilogram per kelvin (J kg^{-1} K^{-1})	2.388×10^{-4}	British thermal unit per pound per degree Fahrenheit
	Specific internal energy	
joule per kilogram (J kg^{-1})	4.298×10^{-4}	British thermal unit per pound
	Temperature	
degrees Celsius (°C)	1.8°C+32	degrees Fahrenheit
kelvin (K)	I .8K 459.67	degrees Fahrenheit
	Thermal conductivity	
watt per meter per kelvin (W m^{-1} K^{-1})	0.9629×10^{-2}	British thermal unit per minute per foot per degree Fahrenheit

Sea level: In this report "sea level" refers to the National Geodetic Vertical Datum of 1929 (NGVD of 1929)--a geodetic datum derived from a general adjustment of the first-order level nets of both the United States and Canada, formerly called Sea Level Datum of 1929.

Simulation of Water Available for Runoff in Clearcut Forest Openings During Rain-On-Snow Events in the Western Cascade Range of Oregon and Washington

By Marijke van Heeswijk, John S. Kimball, and Danny Marks

ABSTRACT

Rain-on-snow events are common on mountain slopes within the transient-snow zone of the Pacific Northwest. These events make more water available for runoff than does precipitation alone by melting the snowpack and hy adding a small amount of condensate to the snowpack. In forest openings (such as those resulting from clearcut logging), the amount of snow that accumulates and the turbulent-energy input to the snowpack are greater than below forest stands. Both factors are believed to contribute to a greeter amount of water available for runoff during rain-on-snow events in forest openings than forest stands. Because increased water available for runoff may lead to increased downstream flooding and erosion, knowledge of the amount of snowmelt that can occur during rain on snow and the processes that control snowmelt in forest openings is useful when making land-use decisions.

Snow accumulation and melt were simulated for clearcut conditions only, using an energy-balance approach that accounts for the most important energy and mass exchanges between a snowpack and its environment. Meteorological measurements provided the input for the simulations. Snow accumulation and melt were not simulated in forest stands because interception of precipitation processes are too complex to simulate with a numerical model without making simplifying assumptions. Such a model, however, would need to be extensively tested against representative observations, which were not available for this study.

Snowmelt simulated during three mill-on-snow events (measured in a previous study in a clearcut in the transient-snow zone of the H.J. Andrew Experimental Forest in Oregon) demonstrated that melt generation is most sensitive to turbulent-energy exchanges between the air and the snowpack surface. As a result, the most important climate variable that controls snowmelt is wind speed. Air temperature, however, is a significant variable also. 'The wind speeds were light, with a maximum of 3.3 meters per second during one event and average wind speeds for all three events ranging from I .7 to 2.1 meters per second. For observed and estimated conditions, the average simulated snowmelt ranged from 0.2 to 0.8 millimeter liquid water per hour, and turbulent-energy exchange provided 51 percent of the energy that led to snowmelt during the largest of the three rain-on-snow events. When wind speeds were multiplied by a factor of 4, the simulated snowmelt ranged from 1.0 lo 2.5 millimeters per hour. Similarly, when wind speeds were multiplied by a factor of 6, the simulated snowmelt ranged from I .6 to 3.7 millimeters per hour. Turbulent-energy exchange provided a dominant 88 and 92 percent of the energy input to the snowpack during the largest rain-on-snow event when average wind speeds were multiplied by factors of 4 and 6, respectively. During the same event, the contribution to melt by the sum of net solar and net thermal radiation (net all-wave radiation) was roughly equal to the contribution of sensible energy carried by the precipitation itself (advective heat).

Estimates of snowmelt resulting from rain on snow for climate conditions other than those observed and estimated in the simulated plot-scale data were expanded by simulating snowmelt for 24-hour presumed rain-on-snow events extracted from the reconstructed, long-term historical climate records for Cedar Lake and Snoqualmie Pass National Weather Service stations in Washington State. The selected events exceeded 75 millimeters of precipitation in 24 hours. When clearcut conditions were assumed to he identical to those at the H.J. Andrew Experimental Forest site and a ripe snowpack that never completely melted was assumed to be available, simulated 24-hour snowmelt ranged from 4.2 to 47.0 millimeters (0.2 to 2.0 millimeters per hour) for low wind speeds (1.5 meters per second) and from 10.3 to 178.8 millimeters (0.4 to 7.5 millimeters per hour) for high wind speeds (8.2 meters per second). The ranges in melt for a given wind speed resulted from the different combinations of air temperature, dewpoint temperature, and precipitation depth that were characteristic of the synthetic events. The average of the median 24-hour snowmelt at Cedar Lake and Snoqualmie Pass was 15. I millimeters (0.6 millimeters per hour) at low wind speeds and 49.6 millimeters (2.1 millimeters per hour) at high wind speeds. Condensa-

tion could increase water available for runoff by a small percentage of the melt. The climate conditions used to generate the range in melt estimates are representative of the transient-snow zone of the western Cascade Range of the Pacific Northwest because Cedar Lake and Snoqualmie Pass are located near the bottom and top of the zone, respectively.

Hourly plot-scale data available from previous studies for clearcut, forested, and plantation conditions in the western Pacific Northwest could not be used to simulate snow accumulation and melt over extended periods of time to investigate the effects of different climate and physical conditions. Measurements of snowpack properties were too infrequent; precipitation-density information was absent; and water-available-for-runoff measurements on vegetated plots were not considered representative of larger areas because lysimeters were too small to account for the lateral variability of snow accumulation and melt due to interception processes in the canopy. Lack of representative data for vegetated land precluded the testing of a numerical model that would simulate precipitation-interception processes in the forest canopy. Even for the plot-scale simulations that were done, basic data had to be estimated, and as a result, the three plot-scale rain-on-snow events, as well as the 24-hour events, could be considered synthetic.

To ensure adequate data sets for future studies of climate and physical factors in snowmelt generation during rain on snow, data-collection efforts would include frequent (at least every few days) visits to obtain measurements of snowpack thickness, density, liquid-water content, and temperature and to verify that climate data suitable for use in energy-balance numerical models are being collected. In addition to climate variables such as average hourly wind speed, incoming solar radiation, air temperature, and dewpoint temperature, variables such as incoming thermal radiation, reflected solar radiation, and precipitation density would be measured. Soil temperature would be measured, except at study sites at altitudes where snowpacks remain close to isothermal at 0 degrees Celsius, where those measurements could be optional.

Studies of melt generation during rain on snow on forested land could be designed to account for the lateral variability of snow accumulation and melt that occurs below the vegetative canopy. Plot-scale studies that use small lysimeters to measure water available for runoff are not appropriate for the study of rain on snow in forested settings; instead, a combination of data collection at both the plot and catchment scale could be used. At the plot scale, water available for runoff would need to be measured in a few extremely large lysimeters, or many small ones. At the catchment scale, water available for runoff would have to be computed from streamflow measurements by correcting it for such variables as baseflow, interflow, soil-moisture storage, evapotranspiration, and bank storage. Plot- and catchment-scale data could be analyzed simultaneously, because a nested, duplicate approach is more likely to produce useful results for simulating water available for runoff during rain on snow in forest stands than analysis of either date type alone.

INTRODUCTION

In the Pacific Northwest, rain-on-snow events occur on mountain slopes in the transient-snow zone. This zone occupies an altitude band extending from approximately 300 to 1,000 meters (m) above sea level (Harr, 1986) and is characterized by shallow winter snowpacks that may melt in part or entirely when rain falls during relatively warm winter storms. Accelerated snowmelt resulting from rain on snow adds to the amount of water available for runoff (WAR) and creates an increased potential for downstream flooding and erosion (Harr, 1981).

In forest openings, the amount of snow that accumulates and the turbulent-energy exchange between the air and the snowpack surface are greater than in forest stands (Berris and Harr, 1987). The greater accumulation of snow available for melt and the greater turbulent-energy exchange to melt snow may increase the amount of WAR during rain-on-snow events in forest openings and worsen downstream flooding and erosion by increasing peak flows. These openings may result from wildfire, insect attack. blowdown, and timber harvest. Of these, timber harvest is the only process that can be planned to help mitigate the potential effects of increased WAR during rain on snow. In Oregon and Washington, much of the timber harvest occurs at mid-altitudes of the western Cascade Range in the transient-snow zone.

Background

In 1987, a landmark agreement to balance timber harvesting with the protection of natural and cultural resources was reached in Washington State between the Native American tribes, timber industry, environmental community, and state natural resource agencies. This agreement is known as the 'Timber/Fish/Wildlife (TFW) agreement. As pert of the agreement, cooperators in TFW have developed analysis methods to estimate the cumulative effects of timber harvest on watershed hydrology, geomorphology, erosion, wildlife habitat, and

human-made structures (Washington Forest Practices Board, 1994). Refinement of the analysis methods is a continuing effort.

Estimation of the cumulative effects of timber harvest on a watershed prior to harvesting can he used to help minimize environmental damage. An important part of this process is knowing how much WAR may he expected during rain-on-snow events after timber harvest, because if increased amounts of water are available, hillslope erosion could he accelerated and peak flows could he higher. Increased flows could in turn accelerate hank erosion, change the character of the streambed, change water quality, and increase downstream flooding. Knowledge of the amount of snowmelt that may he generated in forest openings during rain on snow for different storm conditions improves the ability to estimate the cumulative effects of timber harvest on a watershed. To obtain this knowledge, the U.S. Geological Survey (USGS) began an invcstigation in 1990 in cooperation with the Cooperative Monitoring, Evaluation, and Research (CMER) Committee of TFW and the Washington State Department of Natural Resources (DNR).

Purpose and Scope

This report presents a conceptual model of snow accumulation and melt processes in forest stands and forest openings and characterizes the amount of snowmelt generated in a typical clearcut forest opening during rain-on-snow events for different storm conditions.

A physically-based, energy-balance snow-accumulation and melt model (Marks, 1988) was used to simulate snowmelt during rain on snow using ten days of hourly observations from a plot-scale study in the transient-snow zone of the western Cascade Range in Oregon. The simulated snowmelt was compared to observed snowmelt to assess the accuracy of the simulations, and a sensitivity analysis was performed to identify important factors in generating snowmelt during rain-on-snow events. The model was then used to simulate snowmelt during rain-on-snow events for hypothetical storm conditions in the western Cascade Range of Washington. Reasonable storm conditions for the transient-snow zone of the western Cascade Range were generated by analyzing synthetic historical climate records believed to be representative of the transient-snow zone. The synthetic climate records were created by combining historical hourly wind-speed data from Seattle-Tacoma International Airport (SeaTac) and Stampede Pass National Weather Service (NWS) stations with historical hourly precipitation and daily air temperature extreme data from transient-snow zone NWS stations Cedar Lake and Snoqualmie Pass. Several assumptions were made to estimate the hourly dewpoint temperature, solar radiation, and diurnal air temperature data for Cedar Lake and Snoqualmie Pass.

Sources of Data

Plot-scale micrometeorological and lysimeter data were provided by R. Dennis Harr, retired from the U.S. Forest Service (USFS). Historical meteorological data for NWS stations were obtained from the National Climatic Data Center of the U.S. Department of Commerce in Asheville, North Carolina, and from EarthInfo Inc.

Acknowledgments

The sharing of the plot-scale data by R. Dennis Harr, retired from the USFS, is gratefully acknowledged Brian A. Connelly, formerly with the University of Washington, and Bengt A. Coffin, USFS, were helpful in providing field notes and clarifying questions related to the data. Arnold J. Hansen, USGS, analyzed and corrected NWS climate data for Washington State. Matthew J. Brunengo, DNR, and Walter F. Megahan, National Council of the Paper Industry for Air and Stream Improvement, Inc. (NCASI), provided helpful review comments to an early draft of the report. Members of the Sediment; Hydrology, and Mass Wasting (SHAMW) Subcommittee of the CMER Committee provided helpful input to the invcstigation at different stages. The following USGS personnel (in alphabetical order) contributed to this report: Steven N. Berris, William R. Bidlake, Robert W. Crist, Richard S. Dinicola, Edwin C. Kennison, David L. Kresch, Rohcrt M. Krimmel, George H. Leavesley, James R. Lylcs. William G. Sikonia, and Stuart A. Tomlinson.

PHYSIOGRAPHY AND CLIMATE

The western Pacific Northwest has a maritime climate, which is modified by the terrain of the region. Mountain ranges act as barriers to the principal paths of moisture inflow in the region (fig. 1). The prevailing direction of travel for storms is from west to east (Miller and others, 1973). Humid air masses generated over the Pacific Ocean rise and lose their moisture on the ocean side of the mountains, creating the wet climate west of the Cascade Range. Rain shadows exist on the lee (eastern) side of the mountains, the most extensive example of which is the semi-arid land of eastern Oregon and Washington.

Mean annual precipitation in the region ranges from less than 300 millimeters (mm) just east of the Cascade Range to more than 3,000 mm per year in higher parts of the Coast and Cascade Ranges and the Olympic Mountains (fig. 2). In general, precipitation reaches a minimum during mid-summer (July and August) and a maximum during late fall and early winter (November through January). East of the Cascade Range, however, a second precipitation maximum may be observed during late spring and early summer (May and June) as well (Owenby and Ezell, 1992).

Mean annual temperatures in the region range from less than 5 to more than 11 degrees Celsius (°C). They are strongly correlated with land altitude: lower temperatures occur at the higher altitudes (fig. 3). Minimum average temperatures are observed during the winter (December through February), and maximum average temperatures are. observed during the summer (July and August) (Owenby and Ezell, 1992).

Generally, average temperatures in the mountains are sufficiently low from October through March for snow to accumulate. It is during these months that rain-on-snow events may occur; they do so most frequently in the transient-snow zone, where average air temperatures fluctuate around freezing and precipitation alternates between rain and snow. Snowpacks in this zone may disappear entirely in between snow accumulation phases. Above and below the transient-snow zone, rain-on-snow events occur less frequently. At low altitudes, snowpacks rarely accumulate because precipitation occurs mostly as rain; at high altitudes, snowpacks accumulate, but heavy rain occurs infrequently (Coffin and Harr, 1992; Brunengo, 1990).

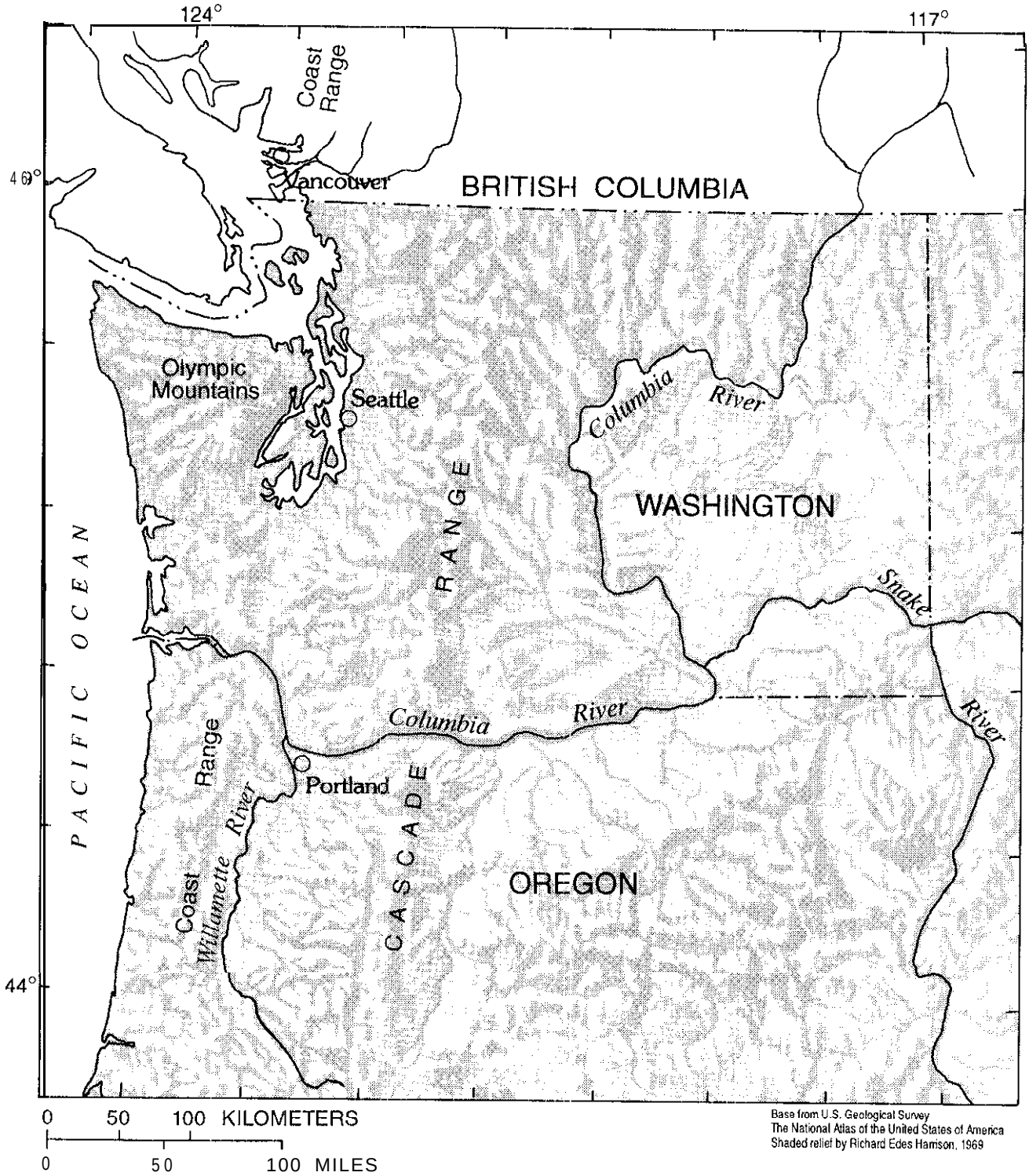

Figure 1.--Generalized physiography of the Pacific Northwest region

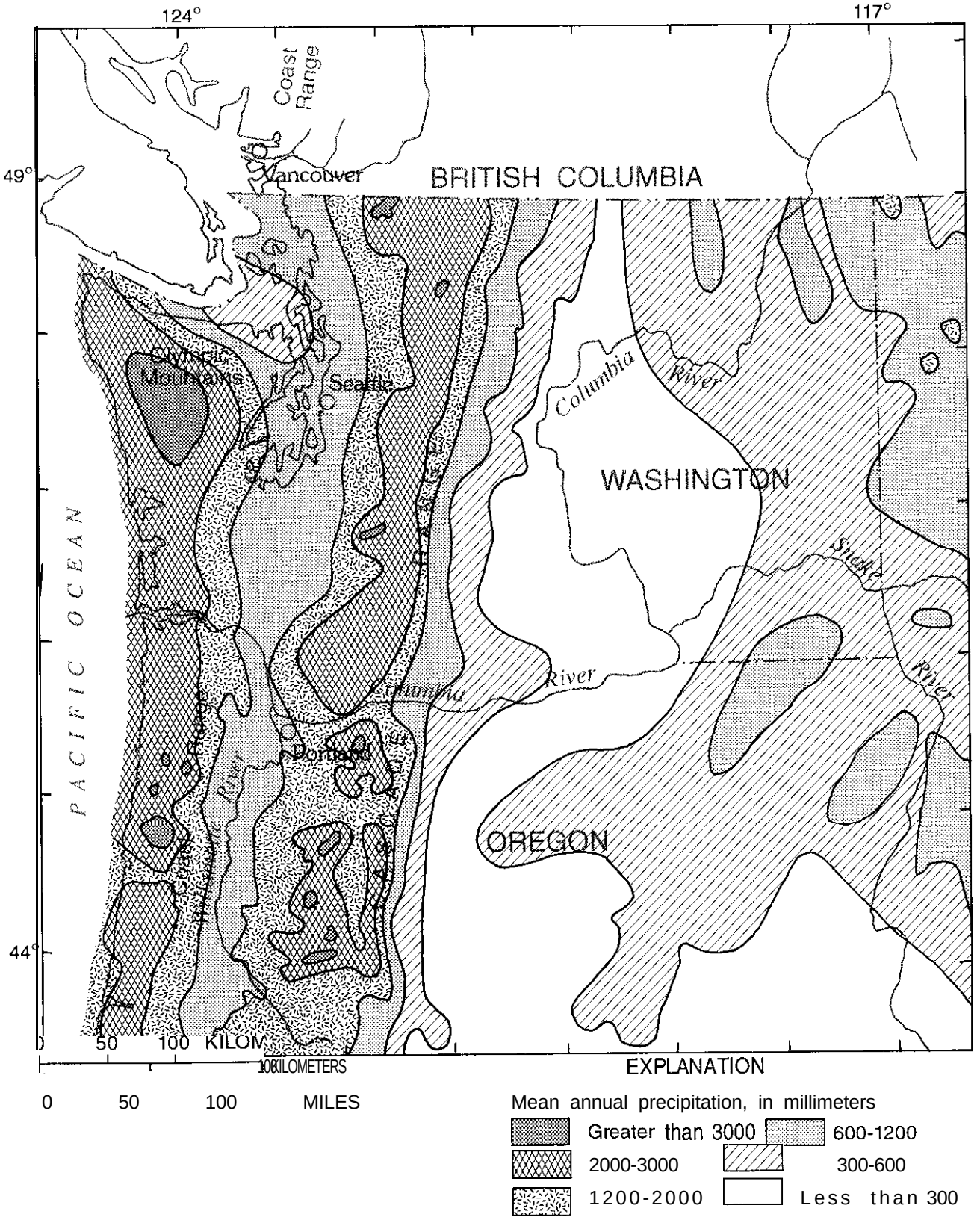

Figure 2.--Mean annual precipitation of the Pacific Northwest region (modified from Pacific Northwest River Basin Commission, 1969).

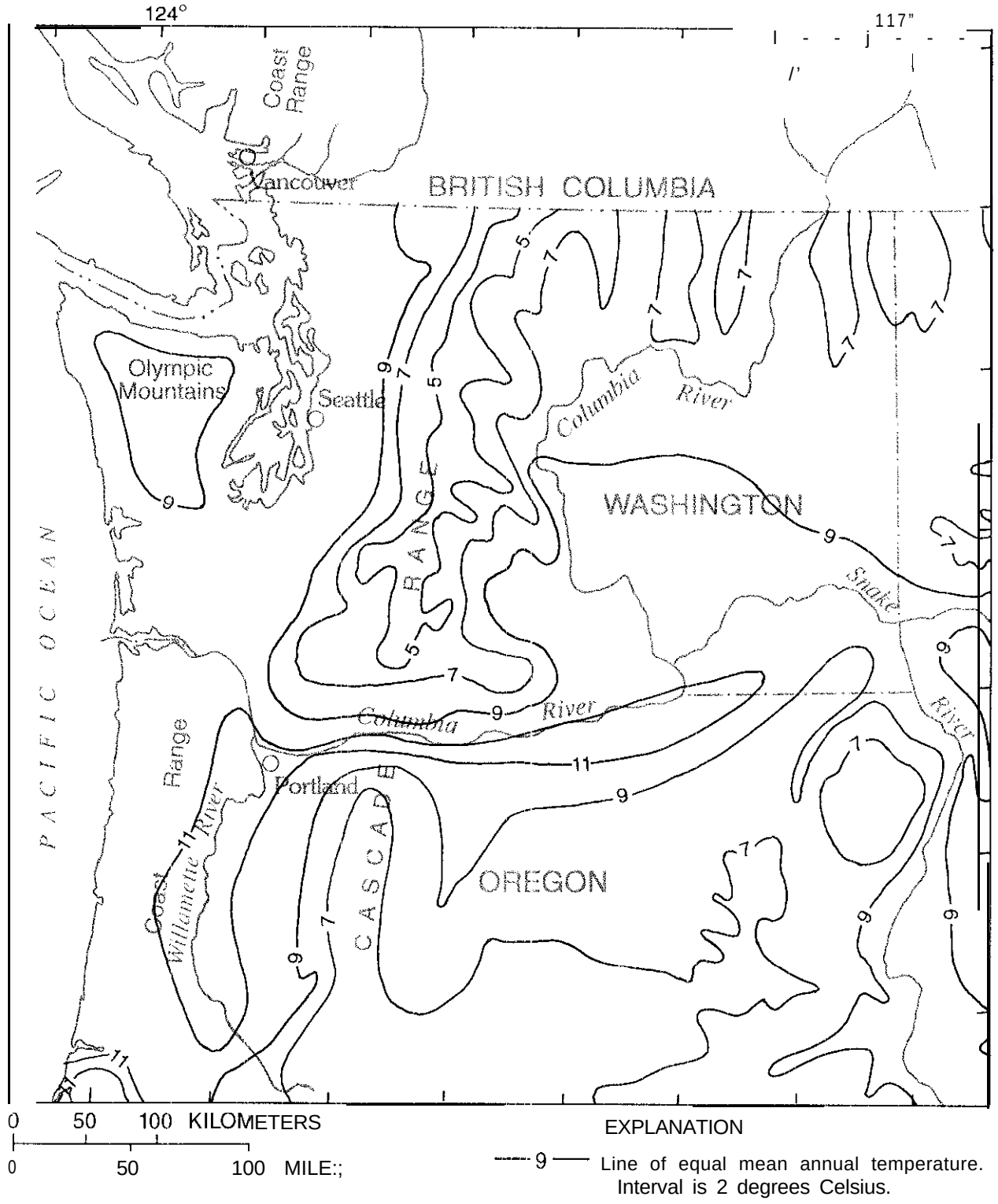

Figure 3.--Mean annual temperature of the Pacific Northwest region, 1931-51, in degrees Celsius (modified from Pacific Northwest River Basin Commission, 1969).

CONCEPTUAL MODEL

A conceptual model of snow accumulation and melt generation in the transient-snow zone is a qualitative description of the important and relevant hydrologic processes. Conceptualization of these processes is useful so that an appropriate numerical model may he selected to simulate them. To facilitate formulation of the conceptual model, a general description of snow accumulation and melt processes is presented here.

Snow Accumulation and Melt Processes

Complex upper- and lower-atmospheric conditions determine the type of precipitation that falls to the ground; no simple prediction can he made on the basis of surface air temperature alone as to whether precipitation will be rain or snow. For instance, snow is frequently observed at air temperatures slightly above freezing. Generally, however, precipitation is in the form of snow when air temperatures are below freezing and in the form of rain when they are above freezing. New-fallen snow may be wet, dry, or a mixture of rain and snow.

Snowpacks accumulate on the ground if precipitation is predominantly in the form of snow, and if snowpack temperatures remain at or below freezing. As a snowpack ages, its density increases due to the compaction and recrystallization of snowflakes into ice crystals. Relatively warm snowpacks may hold liquid water as well, captured in pore spaces between ice crystals. A typical snowpack consists of air, ice crystals at 0°C or below, and, if present, liquid water at 0°C. The amounts of ice and liquid water and their respective temperatures determine the cold content of a snowpack, defined as the amount of energy required to bring the snowpack to a uniform temperature throughout (also referred to as isothermal) at 0°C without phase changes.

Energy Exchanges Between a Snowpack and its Environment

The energy balance of a snowpack is determined by its cold content, phase changes, and the energy gains and losses that affect it. Net energy gains and losses are the result of interactions of the snowpack with the external environment. In response to net energy gains and losses, phase changes may occur within the snowpack that in turn release or absorb energy. If energy is gained by a snowpack, the temperature of ice crystals will increase to a maximum of 0°C, and melting will start if sufficient energy remains. The meltwater will increase the amount of liquid water held by the snowpack until the water-holding capacity of the snowpack has been exceeded; at this point, meltwater will leave the bottom of the snowpack and become WAR. If energy is lost by a snowpack, any liquid water that is present will freeze; once all the liquid water has frozen, the temperature of the ice crystals will decrease if energy loss continues.

A snowpack exchanges energy with the external environment along its top and bottom surfaces (fig. 4). Energy may he gained or lost along the bottom surface by conductive heat transfer between the snowpack and the ground; energy may be gained or lost along the top surface from solar and thermal radiative heat transfer, turbulent sensible and latent heat transfer, and advective heat transfer (U.S. Army Corps of Engineers, 1956). In addition, a small amount of sensible and latent heat may be exchanged between the snowpack surface and the air by conduction. Because air is such a good insulator, however, this amount is to" insignificant to he considered for the purposes of this study.

Conductive heat transfer takes place between the bottom of a snowpack and the ground if a temperature difference exists across the interface. If the snowpack is colder than the ground, energy flows from the ground to the snowpack, and the cold content of the snowpack decreases or some of its ice melts. If the snowpack is warmer than the ground, however, the opposite occurs. The rate at which the energy transfer takes place depends on the thermal properties of the ground and the temperature gradient across the interface (U.S. Army Corps of Engineers, 1956).

Radiative energy may be divided by wavelength into solar and thermal radiation. Solar radiation ranges from visible to near-infrared wavelengths, equivalent to about 0.3 micrometer (μm) to 3 μm (Marks, 1988); radiation in this band-width is also referred to as shortwave radiation. Thermal radiation ranges in wavelengths from about 3.5 μm to 50 μm and is also referred to as longwave radiation. The basic properties of solar and thermal radiation are different; solar radiation may be absorbed and reflected, while thermal radiation may he absorbed and emitted. These different properties are important when considering the radiative energy transfer to and from snowpacks.

During daylight hours, solar radiation is incident on the snowpack surface unless it is obstructed by vegetation, topography, or extreme atmospheric conditions such as heavy cloud cover or precipitation. A fraction of the incident solar radiation is scattered and reflected back into the atmosphere. The amount depends on the wavelengths of

the radiation, the albedo of the snow surface for those wavelengths, and the angle of incidence of the radiation; the latter is a function of the position of the sun in the sky and the snow-surface slope. In general, the albedo of a snow surface decreases as a snowpack ages because the size of ice crystals increases and dust collects on the surface (Marks, 1988). The presence of clouds reduces the amount Of solar radiation that may be incident on the snowpack surface. Net solar radiation is a source of energy to the snowpack.

Thermal radiation is absorbed and emitted by vegetation, snowpacks, clouds, and the atmosphere. Of these, all but the atmosphere absorb and emit thermal radiation as black bodies. Tbis means that they absorb all incident thermal radiation and that they emit the maximum amount possible (that is, the emissivity, defined as the fraction of black-body emission at a given wavelength emitted by a surface. is 1); the higher the temperature of a black body, the greater the emitted thermal radiation. The atmosphere, however, absorbs and emits thermal radiation of spec wavelengths, and may be entirely transparent to other wavelengths. The higher the air temperature and wat vapor content of the atmosphere. tbe larger the amoun thermal radiation that is absorbed and emitted (U.S. A Corps of Engineers, 1956). The net thermal radiation t from the snowpack depends on the complex interactio among the snowpack, vegetation, clouds, and atmosph

Because the surface of a snowpack cannot be war than 0°C, there is an upper limit to the amount of ener that may be lost from a snowpack through thermal rad tion. When no vegetation is nearby and skies are clear colder than the snow surface, there will be a net loss o thermal radiation from the snowpack. When it is clou however, the temperature difference between the base tbe clouds and the snowpack surface determines whet there is a net loss or gain of thermal energy. If the clo temperature is greater than the snowpack surface temp tore, as for rainclouds, there will be a net gain. If vege

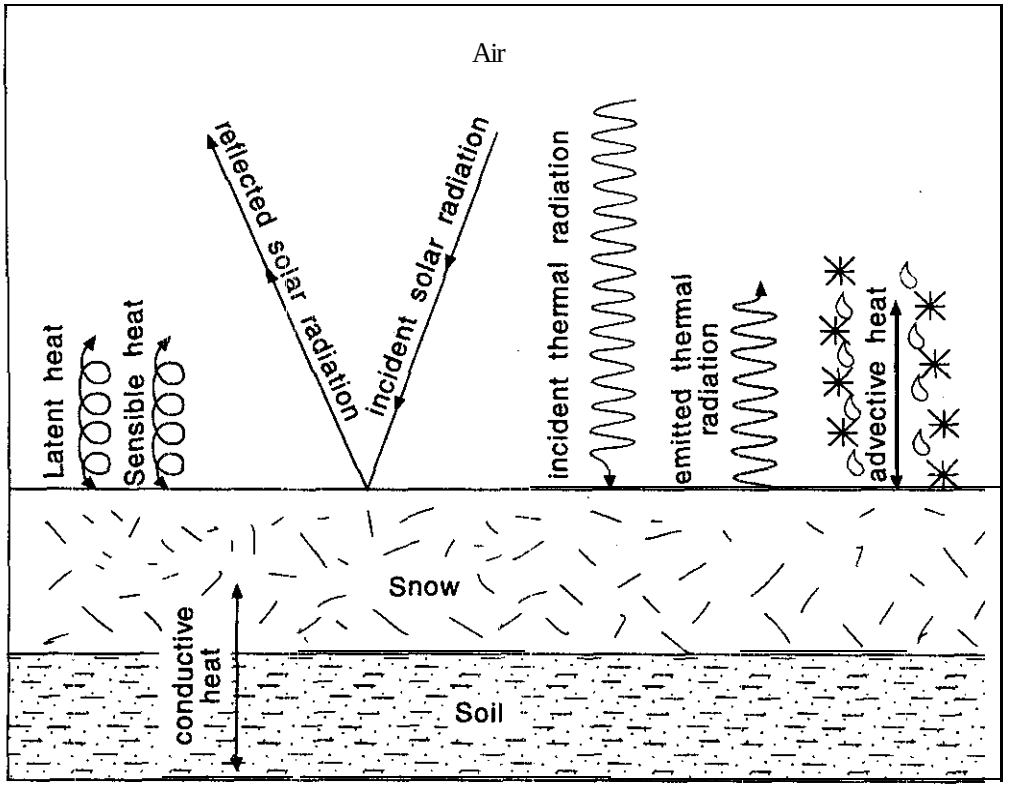

Figure 4.--Energy exchanges between a snowpack and its environment. Arrows indicate the possible directions of energy transfer.

tion is present, the interactions are more complex; in addition to thermal radiation exchange between the snowpack surface and the clouds, the exchange occurs between the clouds and vegetation and between the vegetation and snowpack as well. The temperature differences between the radiating bodies, their emissivities, and the size of their surface areas determine the net amount and direction of thermal radiation transfer to or from the snowpack (U.S. Army corps of Engineers, 1956).

Both sensible and latent heat are conveyed to and from the snowpack by physical transfer in turbulent air currents near the snow surface.. Sensible heat is energy contained in a substance as indicated by its temperature, while latent heat is energy released or absorbed during a phase change. Turbulent sensible heat exchange occurs by transfer of heat between the snowpack surface and the turbulent air currents near the surface. Turbulent latent heat exchange occurs between a snowpack surface and the air immediately above it when liquid water or ice at the snowpack surface evaporates or sublimates, respectively, to add water vapor to the turbulent air currents near the snowpack surface or when water vapor in the air condenses or freezes onto the snowpack surface. The rates and directions of sensible and latent energy transfers depend on the temperature and vapor-pressure gradients *between the* snowpack surface and the air, respectively, as well as on the amount of turbulence, which is a function of wind speed.

Turbulent transfer may add or remove energy from a snowpack. If no wind is present over a snowpack, turbulent heat exchange cannot occur. If wind is present and the temperature of the air is greater than the temperature of the snowpack surface, the snowpack gains sensible heat; if the air temperature is lower, the snowpack loses sensible heat. If wind is present and the vapor pressure of the air is greater than the vapor pressure at the snowpack surface, moisture in the air condenses on the snowpack surface, thereby releasing latent energy and adding mass to the snowpack. The condensed vapor may remain liquid or freeze to the snowpack surface, depending on the cold content of the snowpack. If it freezes, additional energy is released to the snowpack. If wind is present and the vapor pressure of the air is smaller than the vapor pressure of the snowpack surface, liquid water in the snowpack may evaporate, and ice crystals in the snowpack may sublimate; these phase changes remove energy from the snowpack.

Advective heat transfer refers to energy that is carried to and from the snowpack by mass transfer in the form of precipitation. When precipitation falls on a snowpack, not only is its mass added to that of the snowpack, but its thermal energy content *is* added to the overall heat content of the snowpack as well. The energy content of precipitation depends on its phase and temperature. For example, if precipitation falls as snow at a temperature below that of the snowpack, the snow-water equivalent (defined as the depth of liquid water that would result from melting a snowpack with no water loss) and the cold content of the snowpack (or relative amount of ice in the ice-water mixture) will both increase. If precipitation occurs in the form of rain, energy will be supplied to the snowpack because the rain is wanner than the snowpack. Rain on snow may increase the snow-water equivalent of the snowpack in the form of liquid water, or it may freeze and torn into ice. If the water-holding capacity of the snowpack is exceeded, liquid water will leave the bottom of the snowpack and become WAR.

Interception of Precipitation

Precipitation that falls in areas covered by vegetation is partly intercepted by branches and leaves. Some of the intercepted precipitation may be lost to the atmosphere through evaporation and sublimation. while the remainder stays in the canopy and eventually falls through to the ground. How much precipitation is intercepted depends on the vegetation species, its age, the canopy surface area, and the kind of precipitation (Zinke, 1967; Leonard, 1967). The maximum amount of intercepted precipitation a tree or bosh can hold is referred to as the interception storage capacity. Because of snow's lower density, storage capacities for snow exceed those for rain.

Intercepted snow may be blown down by the wind or slide to lower branches and the ground as the load of accumulated snow becomes too heavy and branches bend down (Schmidt and Pomeroy, 1990); intercepted rain may drip to lower branches and the ground. In addition to being removed mechanically, intercepted snow can also melt and thus assume the properties of intercepted rain by dripping to lower branches and the ground.

Intercepted snow may be distributed through a canopy in an infinite *number* of ways. Patches of snow may be present near the top, center, and bottom of the canopy, and the sizes and shapes of patches may vary widely as well. Intercepted snow has an unpredictable surface area that is determined by its depositional and melt history and the number, size, and orientation of branches and leaves on which it has accumulated. The surface area and location of intercepted snow affect the external energy exchange between *it* and the environment.

A patch of intercepted snow will melt if enough energy is supplied to bring its temperature to 0°C and sufficient energy remain:; for ice crystals to melt. The external energy exchanges that may occur between a patch of intercepted snow and the environment are the same as those between a snowpack on the ground and the environment, except that conductive energy transfer between a snowpack and the ground is replaced by conductive cncrgy transfer between intercepted snow and vegetation. Accounting for all possible energy pathways between intcrccptcd snow and the environment, however, is more complicated than for a snowpack because of the unpredictable shapes, sizes, and locations of patches of intercepted snow.

The net thermal radiation that acts on a patch of intercepted snow depends on the amount emitted by the snow itself and on the amount received from emitting black bodies that are inside its sphere of influence, defined as that part of the external cnvironmcnt that may affect a particular patch of intercepted snow. For example, one patch of intercepted snow may receive thermal radiation from the clouds and nearby vegetation; another patch may be entirely shielded from the clouds and receive thermal radiation from nearby vegetation alone; a third patch may exchange thermal radiation with other patches of snow and the snowpack on the ground. The sphere of influence is different for each patch of intercepted snow (fig. 5).

Patches of intercepted snow wilt also have spheres of influence with respect. to solar radiation; the spheres are different from those of thermal radiation, but similar in concept. The amount of solar radiation that may potentially reach intercepted snow is the same as for a snowpack in an unvegetated area. Patches of intercepted snow, however, may he shielded from solar radiation by nearby leaves and branches, and they may receive indirect solar radiation that has reflected off other patches of snow. As for snowpacks that have accumulated on the ground, the amount of solar radiation that is reflected back from intercepted snow depends on the albedo of the snow surface and the angle of incidence of the radiation.

Advective energy exchanges may also take place between intercepted snow and the environment; the exchange process is the same as that described earlier for the snowpack, hut quantifying it is more difficult. Precipitation in the form of rain or snow may fall directly onto a patch of intercepted snow, or it may first be intercepted before it drips or slides down onto another patch of intercepted snow. Whether the precipitation will increase or decrease the cold content or ice fraction of the patch of intercepted snow depends on the temperature, phase, and snow-water equivalent of the added precipitation. If water that is added to a snowpatch consists of drip that is recent snowmelt, its temperature is probably close to 0°C. If, however, the added water consists of snowmelt or rain that has been in the canopy for some time, its temperature may be equal to the ambient air temperature. The direction and amount of net advective energy exchange between all intercepted snow in a canopy and the environment is a function of the interception processes described.

Turbulent heat exchange takes place when sensible and latent heat arc transferred by the wind between the air and intcrccptcd snow. The greater the wind speed, the greater the quantity of available heat that may be exchanged. Wind-speed measurements in adjacent open and forested areas show that winds are reduced as a function of canopy density. As a result, wind reduction is not uniform throughout the canopy; the mid-canopy level, where canopy surface area is the largest, has the greatest reduction in wind speed (Gary, 1975). Wind speeds in treetops are similar to those of unvegetated areas. The net turbulent energy that is exchanged between intercepted snow patches and the environment depends on the wind speed surrounding the patch, the size of the temperature and vapor-pressure gradients between the patch and the surrounding air. and the aerodynamic characteristics of the patch.

In general, the size or rate of the energy exchange between a patch of intercepted snow and its environment is a function of the size of the surface area of the patch as welt. For example, the greater the surface area of a patch, the greater the net solar radiation it may receive and the more likely that new precipitation or drip wilt fall on the patch. Greater precipitation or drip onto the patch means that, for a given temperature of the precipitation or drip, the total advective heat transfer to or from the patch is greater. Energy-exchange proccsscs such as turbulent-, conductive-, and thermal-heat transfer are in part controtted by the vapor-pressure difference between the patch and the air (for latent heat) or by the temperature difference between the patch and that part of the environment with which the exchange takes place (air for sensible heat, vegetation for conductive heat, and clouds, vegetation, and the atmosphere for thermal heat). For these exchange processes, the greater the surface area of the patch, the greater the energy transfer that takes place.

The same energy-exchange processes that take place between intercepted snow and the environment also take place between intercepted rain and the environment. For example, intercepted rain may gain cncrgy from solar radiation, lose mass and latent cncrgy as a result of evaporation, and gain or lose energy from or to the surrounding air and vegetation by conduction, thermal radiation, and sen-

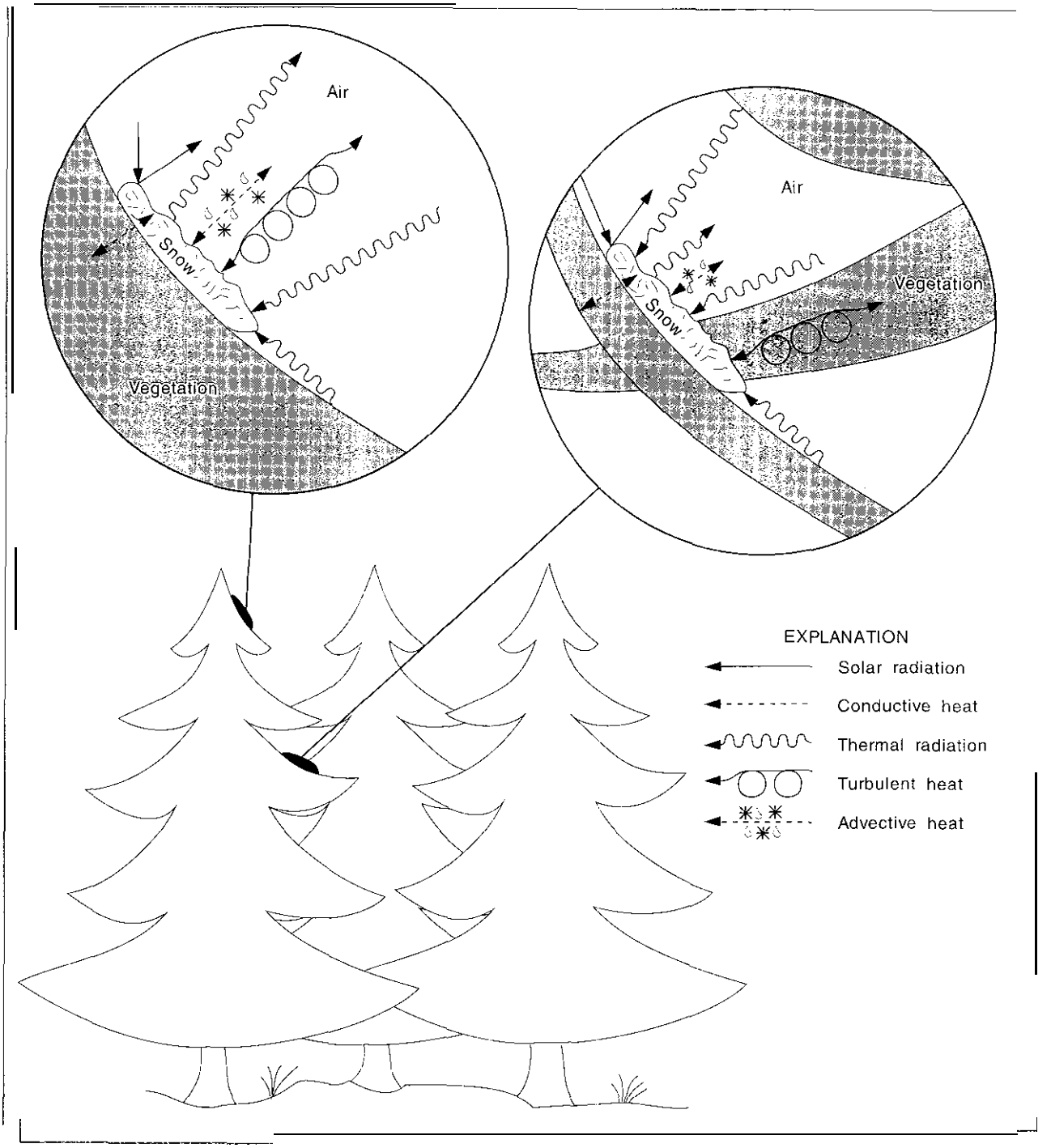

Figure B.--Energy exchanges between intercepted snow and its environment. Arrows indicate the possible directions of energy transfer.

sible heat exchange. Intercepted rain will freeze if enough energy is removed to drop its temperature below 0°C. Because interception storage is smaller for rain than snow, the net energy exchange between intercepted rain and the environment is smaller for identical environmental conditions.

The ultimate disposition of intercepted water is determined by the complex interactions of the canopy structure, antecedent conditions of intercepted water, mechanical unloading of the canopy, the type and condition of new precipitation, and the energy exchange processes that take place between intercepted water and the environment. Water that falls through the canopy will change the mass balance and thermal condition of a snowpack that may be present on the ground. How this snowpack may be affected depends on the phase, quantity, temperature, timing, and distribution of water that falls to the ground.

Once throughfall has reached the snowpack, it is subject to the energy exchange processes that take place between snow on the ground and the environment and that were described in the previous section. In general, the relative sizes of the various energy transfers below a forest canopy differ from those in an unvegetated area because the environmental conditions are different. For example, wind speeds below the forest canopy are reduced compared to unvegetated areas, resulting in decreased turbulent heat exchanges. In addition, incoming solar radiation is diminished below vegetation, net thermal radiation is altered by its presence, and advective heat transfer is different because it is determined by the condition of the throughfall rather than that of direct precipitation.

Interception of precipitation and snow accumulation and melt below a forest canopy were not simulated as part of this study. As demonstrated by the description of the conceptual model above, the large degree of unpredictability of interception processes precludes generating a numerical model without greatly simplifying the conceptual model. Schmidt and Troendle (1992) came to the same conclusion. Simulations using a numerical model that would incorporate simplifications, however, should he extensively tested against representative observations of lysimeter outflow and snowpack conditions for different forested conditions to verify the model. Currently available plot-scale data, however, are insufficient to thoroughly test simplified models, as demonstrated by Wigmosta and others (1993), who tried to test their energy-balance model of interception of precipitation with available data from the transient-snow zone in the Pacific Northwest.

To thoroughly test a simplified model of interception processes, a statistically significant number of data sets that include frequent (at least every few days) measurements of snowpack thickness, density, and liquid-water content and hourly lysimeter outflow measurements that are representative of an entire forested plot should he used. The latter may he achieved by installing many large snow lysimeters below a forest canopy to capture the lateral variability of snow accumulation and melt resulting from interception processes. The data currently (1995) available for the transient-snow zone include relatively infrequent snowpack-condition measurements during a few winters and lysimeter outflows that were usually measured by too few small lysimeters-about two square meters (m^2) each; in cases where more than one smell lysimeter was used, the available measurements indicate that the lateral variability of lysimeter outflow is significant.

Snow Accumulation and Melt in the Transient-Snow Zone

In the transient-snow zone of the Pacific Northwest, snowpacks that are relatively thin, near freezing, and have a high liquid-water content accumulate in both forest openings and below forest canopies during the winter. Generally, snowpacks that form below forest canopies are thinner and denser than in the forest openings, and they have a higher liquid-water content (Berris and Harr, 1987). Snowpacks in this zone are transient in nature because their ripened state readily leads to snowmelt even when the net energy input to the snowpack increases by only a small amount. Examples of conditions that create increased energy input are rain-on-snow events and atmospheric warming not accompanied by precipitation.

During a rain-on-snow event, increases in sensible, latent, thermal radiative, and advective heat transfers may take place from the environment to the snowpack. Rain-on-snow events arc accompanied by an increase in air temperature, creating a source of energy for sensible heat transfer. In addition, the relative humidity of air reaches 100 percent, causing condensation of water vapor onto the snowpack surface that releases latent heat and adds mass to the snowpack (relative humidity is defined as the ratio of the amount of moisture in a given space of air to the amount the space could contain if saturated). Turbulent sensible and latent heat transfer take place only if wind is present. In the western Cascade Range, warm winter rainstorms are commonly accompanied by an increase in wind speed (Harr, 1981), so turbulent heat inputs to the snowpacks are usually significant. The energy contained in precipitation itself is added to the

snowpack as advective heat transfer. During storms, cloud cover is at a maximum, leading to an increased energy input to the snowpack from thermal radiation and a decreased input from solar radiation (Male and Granger, 1981). The increase in thermal radiation is usually more important than the decrease in solar radiation, however (Berris, 1984).

A snowpack that has accumulated below a forest canopy is subject to energy inputs in different relative amounts from a snowpack in a forest opening. Increased air temperatures during general atmospheric warming and rain-on-snow events warm the vegetation, which emits more thermal radiation as a result. The net thermal radiation input to the snowpack, however, is determined by the combined effects of canopy shielding of thermal radiation from clouds, the increased thermal radiation from vegetation, and the vapor content of the air. Depending on the conditions, thermal radiation may be higher, lower, or the same below a forest canopy and in a forest opening. If atmospheric warming is accompanied by increased wind (as it usually is during rain-on-snow events), the increased turbulent heat input to the snowpack will be smaller on the forest floor than in the forest opening because the wind speed is reduced by the air resistance of the vegetation.

Increased energy available during atmospheric warming may melt all or part of the snow held in storage by the forest canopy. When this intercepted snow melts during a rain-on-snow event, the initial amounts of liquid water that fall onto the snowpack below may be greater than in the forest opening; when the intercepted snow melts during a general atmospheric warming without precipitation, rain-like conditions may he present in the forest even though it is not raining (Berris, 1984). The latter situation contributes to the presence of thinner, denser, and wetter snowpacks below vegetation.

The dominant energy exchanges that affect a snowpack in the transient-snow zone take place between the snowpack surface and the air; by contrast, conductive heat transfer, which is a small energy component, takes place between the snowpack bottom and the ground. Measurements by Berris (1984) showed that whenever snow is on the ground, the temperature of the soil immediately below the snow is usually close to 0°C. During prolonged, exceptionally cold weather, soil temperatures may be significantly lower, but those weather conditions are unusual in the transient-snow zone of the Pacific Northwest. Snow acts as an insulator, and when it is absent from the ground, soil temperatures may reach more extreme values. However, because temperature differences between soils and snowpacks are small in the transient-snow zone, little conductive heat transfer takes place along the bottom of snowpacks.

The amount and timing of runoff from a snowpack are determined by the thickness, temperature, density, and liquid-water content of a snowpack prior to a melt event and the amount of energy and mass that is provided to the snowpack during the event. If sufficient energy is available, a thick snowpack will generate more WAR than a thin snowpack because the thick snowpack will continue to supply snowmelt after the thin snowpack would have melted completely. If the cold content of a snowpack is high, more energy is needed to bring it to 0°C, which may delay melting. During a melt event, snowmelt becomes part of WAR once the liquid-water content of the snowpack has been exceeded. In the transient-snow zone, snowpacks have a high liquid-water content and are near freezing, and, as a result, little delay occurs between the start of melt generation and runoff. During a rain-on-snow event, WAR includes water from the rain itself as well as water from snowmelt. Once generated, WAR becomes available for evapotranspiration, infiltration into the soil, or (once the soil is saturated or frozen) surface runoff-the same pathways available to ordinary rainfall.

SIMULATION OF SNOWMELT

Data available for simulation of snow accumulation and melt consist of plot-scale data collected in the H.J. Andrew Experimental Forest in Oregon and in the Canyon Creek and Finney Creek watersheds in the northern Cascade Range of Washington (fig. 6). These data consist of occasional snowpack thickness, density, and liquid-water-content information, and hourly meteorological and lysimeter outflow measurements. Because lysimeters measure liquid water that drains from the bottom of a snowpack before some of it infiltrates into the soil or becomes surface. runoff, lysimeter outflow is a measure of WAR. The collection seasons span winters from 1982 through 1986 and from 1988 through 1991. The data were collected by R. Dennis Harr (retired from the USFS) and several of his students at Oregon State University and the University of Washington (Berris, 1984; Berris and Harr, 1987; Coffin and Harr, 1992). Measurement sites were below the canopy of old-growth forests and plantations and in neighboring clearcut forest openings. These data, together with plot-scale data collected in the Jamieson Creek Experimental Watershed in the western Coast Range of British Columbia (Beaudry and Golding, 1983) (fig. 6), are the most complete measurements available of plot-scale snow accumulation and melt in the

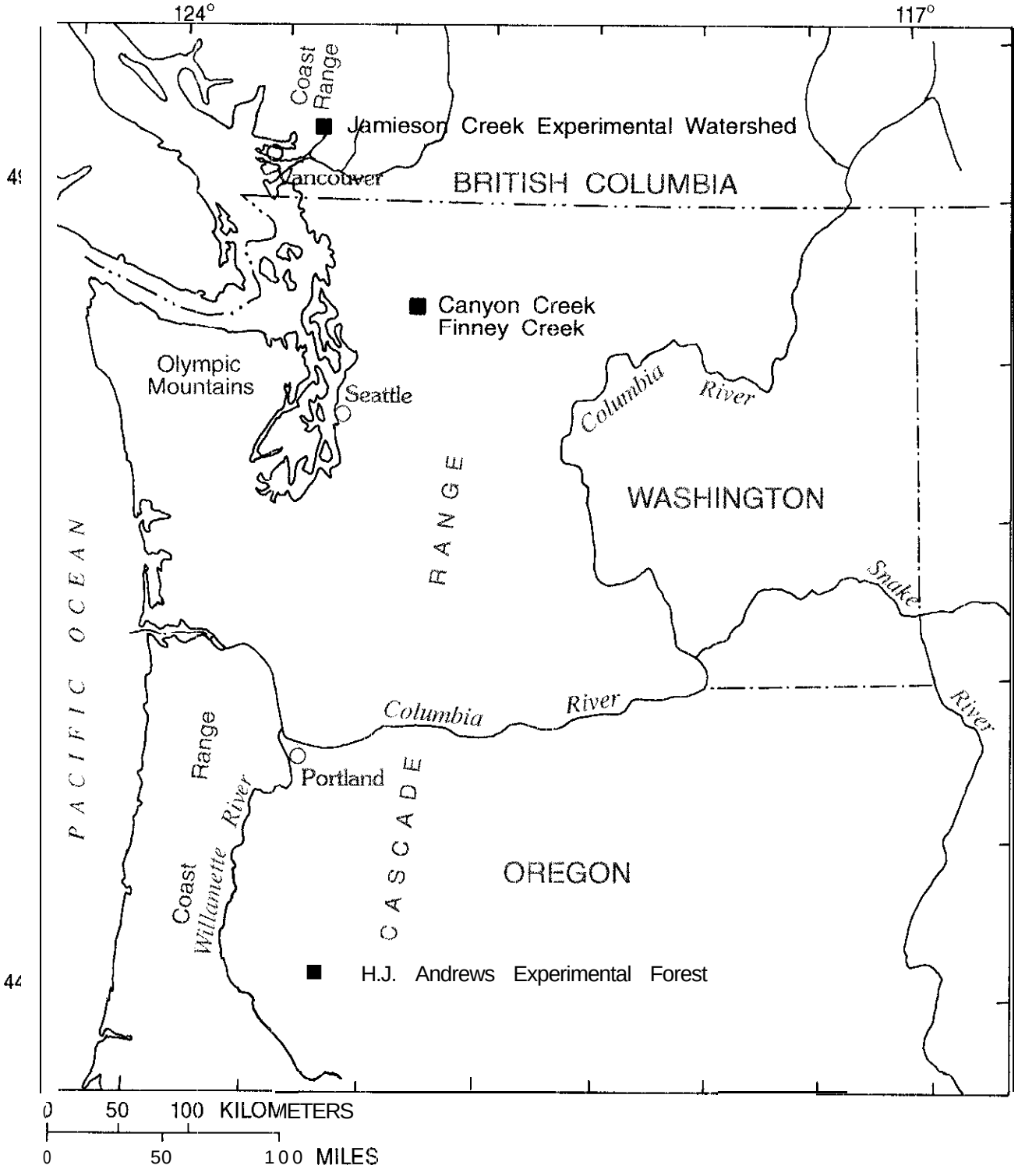

Figure S.--Locations of the plot-scale measurements in the transient-snow zone of the Pacific Northwest.

transient snow zone of the Pacific Northwest. In spite of this, however, most of the data could not be used for simulation purposes, as explained later in this report.

The numerical model selected to perform snow accumulation and melt simulations was a point-scale, energy-balance snowmelt model developed by Marks (1988). This model accounts for the most important energy and mass exchanges between a snowpack and its environment, though it cannot simulate interception processes. Marks' model has previously been used to verify snow accumulation and melt for deep, cold snowpack conditions in the Sierra Nevada (Marks, 1988; Marks and Dozier, 1992).

In an attempt to verify that this model accurately simulates accumulation and melt for shallow, warm snowpacks, simulations were performed for a subset of the available clearcut plot-scale data. Specifically, hourly snow accumulation and melt were simulated continuously from February 10 through 14, 1984, and from February 27 through March 3, 1984, for the clearcut plot of the H.J. Andrew Experimental Forest. These time periods included one large and two small rain-on-snow events. Simulated WAR was compared with observed values. Only a subset of the clearcut data was used because the available data were incomplete and at times lacked quality for use in an energy-balance model. In spite of this, the approach showed that the model behaved as expected based on theoretical considerations. The forested and plantation data were not used because, as explained previously, no validated numerical model to simulate interception processes currently exists. Even if they could be simulated, comparisons of model-generated WAR with measured WAR would have limited meaning: the WAR measured by small lysimeters is not representative of the actual WAR in an entire forested plot because the snow accumulations and melt below the canopy vary laterally.

Even though the lack of complete and reliable data precluded meaningful comparison of observed and simulated WAR during the selected time periods, there is value in using the model to determine the sensitivity of WAR generation to various combinations of atmospheric and antecedent snowpack conditions in forest openings. The model performed well for the Sierra Nevada study (Marks, 1988; Marks and Dozier, 1992), and WAR computed for the clearcut plot as part of the present study appeared reasonable. However, because reliable observations were not available for comparison with the simulation results for shallow, warm snowpacks, the results of the sensitivity analysis should be used with caution.

Description of the Numerical Model

Marks' model is a point-scale, energy-balance model that uses meteorological data as input to simulate the accumulation and melt of snowpacks. The model is similar to the snowmelt model of Anderson (1976) and Morris (1982, 1986), except that in Marks' version the input requirements and snowpack representation have been simplified and the computation of radiative energy has been improved (Marks, 1988).

Marks' model assumes that a snowpack consists of two layers that each have a uniform temperature, density, and liquid-water content. External energy exchanges take place by conductive and diffusive heat transfer between the bottom layer and the ground and by turbulent, radiative, and advective heat transfers between the top layer and the air. Internal energy exchange takes place by conductive and diffusive heat transfer between the top and bottom layers of the snowpack. The thickness of the top layer (also referred to as the snowpack surface) is specified by the user and should equal the depth to which solar radiation penetrates the snowpack. The thickness of the bottom layer is equal to the remainder of the snowpack. If the total thickness of the snowpack is less than the specified thickness of the top layer, the entire snowpack is assumed to consist of the top layer with a thickness equal to that of the total snowpack.

Marks (1988) allows for an increase in the snowpack mass as a result of water added by condensation, frost, and precipitation and for a decrease due to evaporation, sublimation, and melt followed by runoff. Runoff takes place when the threshold liquid-water-holding capacity of the snowpack has been exceeded. Condensation, frost formation, evaporation, and sublimation may take place along the snowpack/air and the snowpack/soil interfaces. The snowpack density is adjusted in response to the type and density of precipitation that is added to the snowpack and in response to melting of snow or freezing of liquid water within the snowpack. Changes in snowpack density because of compaction of air space in the snowpack are not simulated. Marks' model tracks both the energy and mass contents of the snowpack.

According to Marks' model, the energy balance of a snowpack may be expressed as

$$\mathrm{AQ} = R_n + H + L_v E + G + M \,, \qquad (1)$$

where

ΔQ = change in snowpack energy in watts per square meter ($W\ m^{-2}$),

R_n = radiative energy flux ($W\ m^{-2}$),

H = sensible energy flux ($W\ m^{-2}$),

L_vE = latent energy flux ($W\ m^{-2}$); it is the product of L_v, the latent heat of vaporization or condensation in joules per kilogram ($\approx 2.5 \times 10^6$ J kg-'), and E, the mass that condenses onto or evaporates from the snowpack surface in kilograms per second per square meter ($kg\ s^{-1}\ m^{-2}$),

G = conductive and diffusive energy flux ($W\ m^{-2}$),

M = advective energy flux ($W\ m^{-2}$).

Energy transfer to the snowpack is defined as positive, and energy transfer from the snowpack is defined as negative. When the change in snowpack energy, AQ , is negative, liquid water that may be present in the snowpack will freeze, releasing latent energy in the process. If AQ is still negative after all liquid water has frozen, the temperature of the ice crystals in the snowpack will drop. However, if AQ is positive, the temperature of the ice crystals will rise to a maximum value of 0°C, at which point snowmelt starts if AQ remains positive.

Net all-wave radiative energy, R_n, is {computed in Marks' model according to

$$R_n = R_{n,sol} + I_{lw} - \varepsilon_s \sigma T_{s,0}^4 \quad , \tag{2}$$

where

$R_{n,sol}$ = net solar radiation ($W\ m^{-2}$),

I_{lw} = thermal radiation received by the snowpack from the sky, vegetation, and neighboring topography ($W\ m^{-2}$),

ε_s = emissivity of the snow surface (dimensionless) (assumed equal to 0.99 in the model),

σ = Stefan-Boltzmann constant in watts per square meter per kelvin to the fourth power ($5.6697 \times 10^{-8}\ W\ m^{-2}\ K^{-4}$),

$T_{s,0}$ = temperature of the snowpack surface in kelvin (K).

Net solar radiation, $R_{n,sol}$, is the difference between incident and reflected solar radiation. Reflected solar radiation is a function of the snow surface albedo; albedo is a function of the time since the last snowfall, the angle of incidence of the radialion, and the wavelengths contained in the radiation. The difference between net all-wave radiative energy and net solar radiation is the net thermal radiation, $I_{lw} - \varepsilon_s \sigma T_{s,0}^4$. The thermal radiation received by the snowpack, I_{lw}, may be measured, or it may he estimated as a function of air temperature, cloud cover, vegetation. and topography. The thermal radiation emitted by the snowpack, $\varepsilon_s \sigma T_{s,0}^4$, is calculated as a function of the temperature of the top layer of the snowpack, which is estimated by the model.

Turbulent heat transfer equals the sum of sensible and latent heat transfer. Latent heat transfer takes place if liquid water evaporates or ice suhlimates, or if liquid water condenses or frost forms on the snowpack. Latent energy transfer is accompanied by a gain or loss of mass to or from the snowpack, respectively. Sensible heat transfer from the air to the snowpack, H, is calculated hy the model according to

$$H = \rho\, C_p K_H (T_a - T_{s,0}) \tag{3}$$

and latent heat transfer from the air to the snowpack, L_vE, is calculated according to

$$L_vE = \rho K_W L_v (q_a - q_{s,0}) \quad , \tag{4}$$

where variables not defined previously are

ρ density "fair in kilograms per cubic meter ($kg\ m^{-3}$),

C_p = specific beat of dry air at constant pressure in joules per kilogram per kelvin ($1005\ J\ kg^{-1}K^{-1}$),

K_H = hulk transfer coefficient for heat in meters per second ($m\ s^{-1}$),

T_a = temperature of the air (K),

K_W = hulk transfer coefficient for water vapor ($m\ s^{-1}$),

q_a = specific humidity of the air (dimensionless).

$q_{s,0}$ = specific humidity of the snow surface (dimensionless).

All variables in equations 3 and 4 can be readily measured, except for the transfer coefficients, K_H and K_W, which depend on wind speed and surface roughness. To approximate these coefficients by known or measured variables and parameters, Marks (1988) adapted methods suggested by Brutsaert (1982) and thereby changed equations 3 and 4 into

$$H = \frac{\left(T_a - T_{s,0}\right) a_h\, k\, u^* \rho\, C_p}{ln\left[\frac{z_T - d_0}{z_0}\right] - \Psi_{sh}\left[\frac{z_T}{L}\right]} \qquad (5)$$

for sensible heat, and

$$L_v E = \frac{(q_a - q_{s,0})\, a_e\, k\, u^* \rho}{ln\left[\frac{z_q - d_0}{z_0}\right] - \Psi_{sv}\left[\frac{z_q}{L}\right]} L_v \qquad (6)$$

for latent heat, respectively,

where variables not defined previously are

a_h = ratio of the eddy diffusivity and viscosity for heat (dimensionless) [a value of 1.0 was suggested by Brutsaert (1982)],

k = von Kármán's constant (dimensionless) (≈ 0.40),

z_T = air temperature measurement height above the snow surface (m),

d_0 = zero-plane displacement height (m) [Brutsaert (1982) suggested $d_0 = (2/3)\, 7.35 z_0$],

z_0 = surface roughness length(m) [for snow, it ranges from 0.0001 to 0.005 m (Brutsaert, 1982)],

a_e = ratio of the eddy diffusivity and viscosity for water vapor (dimensionless) [a value of 1.0 was suggested by Brutsaert (1982)],

z_q = humidity measurement height above the snow surface (m),

z_u = wind-speed measurement height above the snow surface (m) and

L, Ψ_{sm}, Ψ_{sh}, and Ψ_{sv} are more complicated expressions, L is defined as the Obukhov stability length

$$L = \frac{u^{*3} \rho}{k\, g\left[\frac{H}{T_a C_p} + 0.61E\right]} \qquad (7)$$

in meters, and u^* as the friction velocity

$$u^* = \frac{u\, k}{ln\left[\frac{z_u - d_0}{z_0}\right] - \Psi_{sm}\left[\frac{z_u}{L}\right]} \qquad (8)$$

in meters per second,

where

g = acceleration of gravity in meters per square second (9.80616 m s^{-2}),

u = wind speed (m s^{-1}).

The y-functions, Ψ_{sm} for mass, Ψ_{sh} for heat, and Ψ_{sv} for water vapor, are for stable conditions

$$\left(\zeta = \frac{z_u}{L} > 0\right),$$

$$\Psi_{sm}(\zeta) = \Psi_{sv}(\zeta) = \Psi_{sh}(\zeta)$$

$$= \begin{bmatrix} -\beta_s \zeta & 0 < \zeta \le 1 \\ -\beta_s & \zeta > 1 \end{bmatrix}, \qquad (9)$$

for the choice of constant $\beta_s = 5$ and for unstable conditions $\left(\zeta = \frac{z_u}{L} < 0\right)$

$$\Psi_{sm} = 2ln\left[\frac{1+x}{2}\right] + ln\left[\frac{1+x^2}{2}\right] - 2\arctan(x) + \frac{\pi}{2}, \qquad (10)$$

and

$$\psi_{sh}(\zeta) = \psi_{sv}(\zeta) = 2\ln\left[\frac{1+x^2}{2}\right] \quad , \qquad (11)$$

where

$$x = (1-\beta_u\zeta)^{1/4} \qquad (12)$$

for the choice of constant $\beta_u = 16$

The magnitude of sensible heat transfer is mainly determined by the wind speed, u, and the temperature difference between the air and the surface of the snowpack, $T_a - T_{s,0}$ The magnitude of latent heat transfer is chiefly determined by the wind speed and the specific humidity difference between the air and the surface of the snowpack, $q_a\ q_{s,0}$ Specific humidity is defined as the mass of water vapor per unit mass of moist air, and it is approximately proportional to the vapor pressure divided by the total pressure of the air (Linsley and others, 1975).

When latent heat transfer is computed to be negative, mass is assumed lost from the snowpack surface by either sublimation or evaporation. It is assumed that if liquid water is present in the snowpack, water and ice are removed from the snowpack at a ratio of 0.882, which is equal to the ratio of the latent heat of evaporation and sublimation. When latent heat is computed to be positive, mass has been added to the snowpack surface by either condensation or frost formation. Except during rain-on-snow events, mass is added as liquid water if air temperatures are above freezing and as ice otherwise. During rain-on-snow events, Marks assumes that 50 percent of the mass added by convection condenses as liquid water and 50 percent condenses as ice.

Mass transfer due to phase changes takes place at the bottom surface of the snowpack as well if a vapor pressure gradient exists between the soil and the bottom of the snowpack. In the transient-snow zone of the Pacific Northwest. this gradient is close to zero, and only small amounts of mass transfer take place. Marks' model accounts for the latent energy changes in the snowpack that result from the phase changes along the bottom as pert of the conductive and diffusive heat transfer between the ground and the snowpack, G, which is estimated by

$$G = \frac{2K_{es,l}K_{eg}(T_g - T_{s,l})}{K_{eg}z_{s,l} + K_{es,l}z_g} \quad , \qquad (13)$$

where

$K_{es,l}$ = effective thermal conductivity of the bottom snow layer in watts per meter per kelvin (W $m^{-1}K^{-1}$),

K_{eg} = effective thermal conductivity of the soil layer (W $m^{-1}K^{-1}$),

T_g = temperature of the soil layer (K),

$T_{s,l}$ = temperature of the bottom snow layer(K),

$z_{s,l}$ = thickness of the bottom snow layer (m),

z_g = thickness of the soil layer (m).

The magnitude of conductive heat transfer depends on the temperature differonce between the bottom layer of the snowpack and the soil. In the transient-snow zone, this difference is small, so conductive heat transfer is a minor source of energy to the snowpack. The effective thermal conductivities are calculated by the model and take into account diffusive and latent heat transfers in addition to pure conductive heat transfer.

Advective heat transfer, M, is calculated according to

$$M = \frac{C_{p\_pp}\rho_{pp}z_{pp\_u}[T_{pp} - T_{s,0}]}{t_{step}} \quad , \qquad (14)$$

where variables not defined previously arc

C_{p_pp} = specific heat of precipitation (J $kg^{-1}K^{-1}$),

ρ_{pp} = density of precipitation (kg m^{-3}),

z_{pp_u} = precipitation depth (not adjusted for snow-water equivalent) (m),

T_{pp} = average temperature of precipitation (K),

t_{step} = snowmelt model time step in hours (h),

and z_{pp_u} may bc expressed in snow-water equivalent according to

$$z_{pp} = z_{pp\_u}\rho_{pp} \quad , \qquad (15)$$

where

z_{pp} = snow-water equivalent precipitation depth (mm).

In the remainder of this report, precipitation depth refers to z_{pp}, the snow-water equivalent precipitation depth. When precipitation is rain, z_{pp} equals z_{pp_u} and when it is snow, z_{pp} is less then z_{pp_u} Marks' model assumes that precipitation has the temperature of the air at the time it falls. (If available, it may be assumed that precipitation temperature equals the dewpoint temperature.) Precipitation is assumed to be rain if the air temperature is greater than or equal to a user-specified value, and it is assumed to be snow if the air temperature is less than this value. The density of precipitation has to be provided. During each model time step, the precipitation is assumed to be either rain or snow; mixed rain-and-snow precipitation is not simulated. Precipitation adds mass to the snowpack, and it changes the energy content of the snowpack if a difference exists between the average snowpack and precipitation temperatures. If precipitation is snow, the ratio of solid to liquid water in the snowpack increases; if the precipitation is rain, this ratio decreases until the liquid-water holding capacity of the snowpack has been exceeded, unless a sufficient temperature deficit exists in the snowpack to freeze the rainwater.

To run the model, input of air temperature, precipitation depth and density, wind speed, vapor pressure, net solar radiation, soil temperature, and incident thermal radiation arc required, at a minimum, for each time step. In addition, model parameters such as measurement height above the ground of air temperature, wind speed, and vapor pressure, and snowpack properties at the start of the simulation have to be provided. Model output that can be used to compare the simulations to observations consists of snowmelt, WAR, and snowpack properties such as thickness and density. Other variables are available for output as well. Because Marks' model is physically based, parameters are not adjusted during model runs to improve the match between observed and simulated variables.

Available Data

Meteorological and snow-lysimeter outflow (WAR) data were collected at 21 sites in the western Cascade Range of Oregon and Washington; seven of these sites were located in clearcut forest openings and 14 in mature forests and plantations. One set of three plots (clearcut, forest, and plantation) was located in the H.J. Andrew Experimental Forest in Oregon, and three sets of three plots (clearcut, forest, and plantation at low, medium, and high altitudes) were each located near Canyon and Finney Creeks in the northern Cascade Range of Washington (fig. 6) (Berris, 1984; Coffin and Harr, 1992). Data collection spanned winters from 1982 through 1986 at the H.J. Andrew Experimental Forest and from 1988 through 1991 at Canyon and Finney Creek watersheds.

Although these data sets are the most complete rain-on-snow information available, they were not collected for use as input to an energy-balance, snow accumulation and melt model. As a result, the available data are not of sufficient quality for modeling purposes, and most were rejected for use in the present study.

Data Quality

In general, the available data consisted of hourly air temperature, precipitation, wind speed, dewpoint temperature> solar radiation, and WAR. Snowpack thickness and density information was collected whenever the sites were visited, usually several times each winter. Soil temperature and liquid-water content data were collected at the H.J. Andrews Experimental Forest, and incident thermal radiation was not measured at any of the sites. Precipitation-density information was not measured either, but time-lapse photography was available for the H.J. Andrews Experimental Forest sites to help determine whether precipitation was rain or snow.

Unfortunately, not all the available data were of sufficient quality to meet the input requirements of the numerical model. To accurately simulate snow accumulation and melt, Marks' model requires, at a minimum, accurate measurements of air temperature, precipitation depth and density, wind speed, vapor pressure, net solar radiation, incident thermal radiation, and soil temperature for each time step. To compare model-generated output with conditions in the field, reliable and representative data regarding WAR and snowpack conditions such as snowpack thickness, density, and liquid-water content are needed.

Accurate measurements of WAR, climate, precipitation, and snowpack properties are difficult to obtain in the field under any circumstances, but especially if instruments are unattended for long periods of time, as was the case in the H.J. Andrew Experimental Forest and Canyon and Finney Creek watershed studies. Under those circumstances, solar radiation measurements are prone to error

during rain-on-snow events because of the likelihood of sensor obstructions (Stanhill, 1992). Precipitation gages and lysimeter drain pipes can become clogged, resulting in an underestimate of both depth of precipitation and WAR.

In addition to instrument error, physical displacement of both precipitation and WAR away from instruments contributes to erroneous measurements. Precipitation catch deficiencies occur when wind blows precipitation away from the gage; the catch deficiency increases for increased wind speeds and decreased precipitation densitics. Precipitation falling as snow or as a rain-snow mixture is easily displaced by winds because of the high surface area and low density of the snow (McKay, 1970; McKay and Gray, 1981). These characteristics make it difficult to measure precipitation with rain gages even when sheltering devices are used (Allis and others, 1963; Goodison and others, 1981). The high cohesion of snowfall under near-zero air temperatures increases the likelihood of rain-gage bridging under moderate, to heavy snowfall, which also contributes to catch deficiencies.

The energy-halancc model requires precipitation-density information to properly simulate snowpack characteristics, such as snow depth, density, and liquid-water content. During periods of rainfall, precipitation densities can he easily estimated. When snow or a rain-snow mixture occurs, however, precipitation densities become exceedingly difficult to estimate without combined snowboard and rain-gage information (Goodison and others. 1981; Marks, 1988). 'This information war not collected as part of the field studies.

Incident thermal radiation is a required input to an energy-balance model, hut it was not measured as part of the available data. Thermal radiation is rarely measured in the field, and it is difficult to estimate because it is a function of cloud cover, vapor pressure, and terrain conditions, including vegetation and topography (Male and Granger, 1981; Marks and Dozier, 1979).

Wind speed is an important input variable of the energy-balance snow accumulation and melt model. It is possible to obtain accurate measurements of wind speed in the field, but care must be taken in selecting the proper combination of instruments and recording devices that are sensitive enough to capture the characteristic range of wind speeds at the measurement site. Wind speeds recorded during rain-on-snow events as part of the available data were low, with a maximum recorded hourly average of 5.3 $m\ s^{-1}$ (Coffin and Harr, 1992). Anemometers that were used to measure wind speed were relatively insensitive in the range of the observed values.

Information regarding the snowpack density and liquid-water content is important to set the thermal and mass properties of the snowpack at the start of each simulation. In addition, frequent measurements of these variables are needed to verify the accuracy of snowpack-property simulations. As part of the available rain-on-snow data, snowpack density and liquid-water content were measured only several times each winter. These variables are extremely difficult to measure without sensitive instrumentation (Colbeck, 1978), which was not used to obtain the available rain-on-snow date. Under conditions of active snowmelt (as during rain on snow), however, snowpack density and liquid-water content can be estimated with reasonable accuracy (Marks. 1988).

WAR measurements from a snowpack provide an important means for verifying the accuracy of simulations from an accumulation and melt model. These measurements were collected as part of the available data by small lysimeters, point measurements that may not have been representative for a larger area. The spatial heterogeneity of precipitation and snowcover propertics, the presence of ice lenses. and the lateral movement of melt water within the snowpack, as well as altered snowcover properties and snow-soil interactions from the lysimeter itself, cannot he accurately measured by small lysimeters (R.C. Kattelmann, University of California, Santa Barbara, oral commun., 1993; Conway and Benedict, 1994).

In summary, because most of the available rain-on-snow data were not adequate for the requirements of the numerical model, only a subset of the available data was used to simulate WAR in a forest opening in the transient-snow zone of the western Cascade Range.

Data Used in Simulations

Data for two 5-day time periods during the 1983-84 winter in a clearcut forest opening of the H.J. Andrew Experimental Forest that included some of the best available data were selected for snow accumulation and melt simulations using Marks' (1988) model (fig. 7). Those time periods included three rain-on-snow events (A, B, and C in fig. 7), but only the first of these (A, from 0000 February 12 through 1000 February 13) was previously identified as a rain-on-snow event. It represents the largest rain-on-snow event (the event with the most precipitation) on record for the 1983.84 winter (Berris, 1984; Bcrris and Harr, 198'7). The other two events (B, from 1300 through 1700 February 28, and C, from 1700 February 29 through 1100 March 1) are technically rain-on-snow events, but

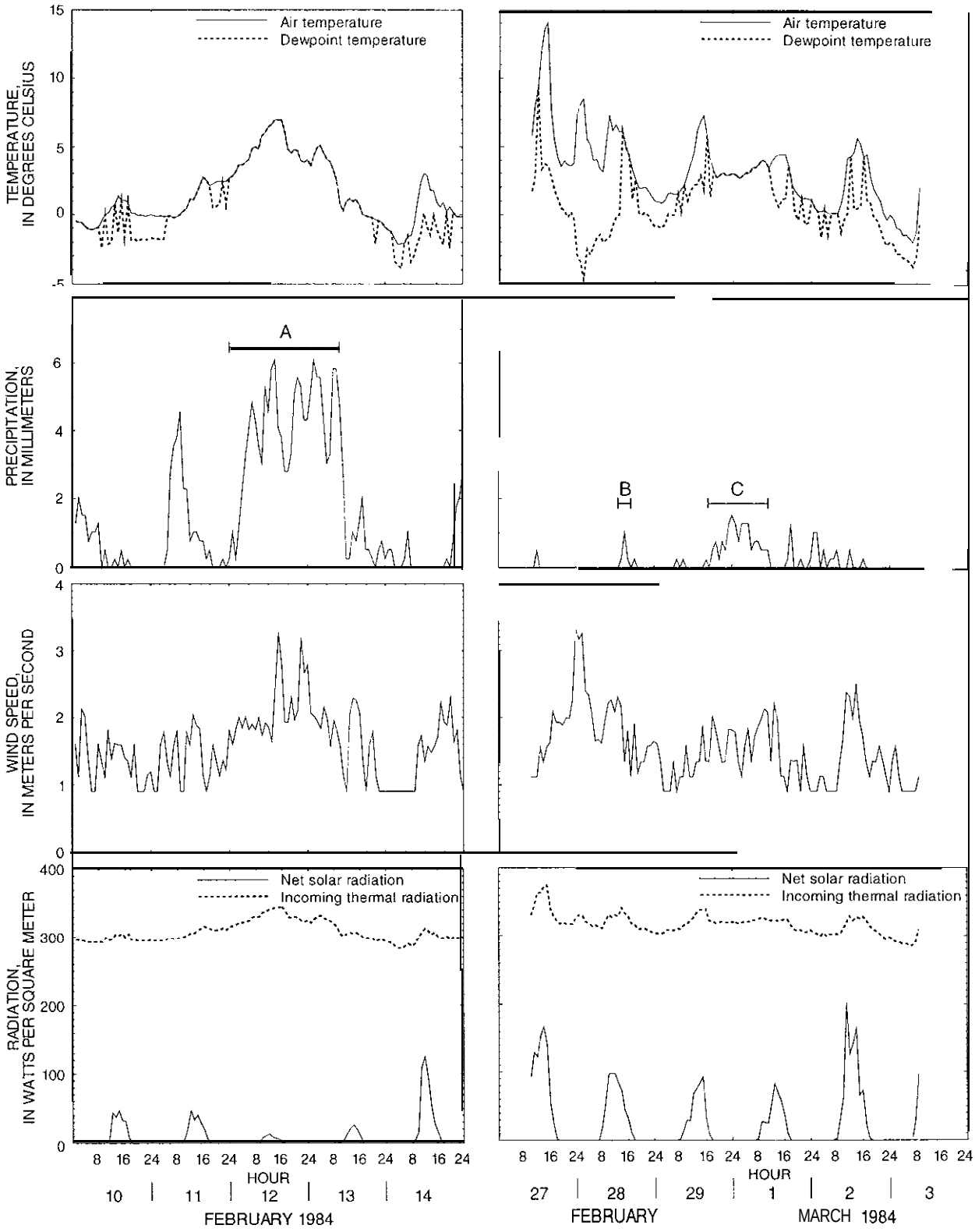

Figure 7.--Measured and estimated values of air temperature, dewpoint temperature, precipitation, wind speed, incoming thermal radiation, and net solar radiation for simulated clearcut data. A, B, and C denote rain-on-snow events discussed in the text.

the rainfall during those periods was so small that they were not noted as such by Berris (1984) and Berris and Harr (1987). Simulation of the small rain-on-snow events in addition to the larger event, however, provides insight into the processes responsible for producing additional WAR during rain on snow.

The site characteristics and data-collection effort were described by Berris (1984) and Berris and Harr (1987) and are repeated here. All climate and WAR data were collected on an hourly basis, and snowpack property information was collected periodically.

The study area was located within a 22-hectare clearcut at 900 m altitude in the McRae Creek drainage within the H.J. Andrew Experimental Forest (fig. 8). The site was logged in 1981 and broadcast burned in 1982. The plot faces in a south-southwest direction, toward the predominant direction of winter winds. An old-growth forest consisting of Douglas fir and western hemlock trees ranging in height from 30-60 m is located approximately 40 m northwest of the plot. Instruments were located on nearly level ground, but surrounding slope gradients approached 80 percent. Annual precipitation at the site averages 2,340 mm; precipitation reaches a maximum during late fall and early winter (November through January). Winter months are usually mild, with air temperatures ranging between -12°C and 12°C during January, the coldest month.

Air temperatures at the site were measured at a height of 1.5 m above the ground with shielded thermistors. Because this type of instrument is accurate, these measurements were considered reliable. Air temperatures during the three rain-on-snow events remained above freezing, averaging approximately 4.1°C (table 1).

Dewpoint temperatures were measured at the same height above the ground as air temperatures with lithium-chloride dewpoint hygrometers, and they averaged 2.1°C during the three rain-on-snow events. However, dewpoint temperatures were assumed to be equal to air temperatures whenever precipitation occurred. This is equivalent to assuming that the relative humidity of air is 100 percent during precipitation, and this assumption increased the simulated WAR by a minor amount. Adjusted dewpoint temperatures averaged 4.0°C during the three rain-on-snow events (table 1). Marks' model requires the input of vapor pressure as a measure of humidity of the air instead of dewpoint temperature, so vapor pressures were computed from the dewpoint and air temperatures according to expressions summarized by Brutsaert (1982, p. 42).

Precipitation was measured with a heated tipping-bucket rain gage and four storage rain gages. As discussed previously, those data are subject to catch deficiencies of unknown amounts, although those deficiencies are probably smaller during rainfall than during snowfall. Precipitation-density information was not available, but 15-minute interval photographs were available to distinguish precipitation types. The three events exhibited light to moderate rainfall intensities over durations of a few hours to two days. Rainfall intensities for the largest event (A) averaged approximately 4.0 millimeters per hour (mm h^{-1}) and peaked at 6.1 mm h^{-1}. Rainfall intensities for event B averaged approximately 0.3 mm h^{-1}, with peak intensities less than 1.0 mm h^{-1} over a brief 5-hour duration. The rainfall intensity increased for event C, averaging 0.8 mm h^{-1}, with a peak intensity of 1.5 mm h^{-1} (table 1).

Wind speed in the clearcut was measured at a height of 1.5 m above the ground with a Weathertronics three-cup, low-threshold anemometer. The anemometer's threshold of accuracy is approximately 0.9 m s^{-1}, but it was found to be most reliable at wind speeds from 3-10 m s^{-1}. Unfortunately, the anemometer was relatively insensitive to wind conditions prevailing at the site, where speeds rarely exceeded 2 m s^{-1}. The instrument frequently recorded hourly wind speeds of 0 m s^{-1}, which was highly improbable even under calm conditions, since the site was located in a cleared area on an exposed mountain slope. A factor of 0.9 m s^{-1} was added to measured wind-speed data to adjust for instrument threshold error. The adjusted wind speeds were light, with a maximum of 3.3 m s^{-1} during event A and average wind speeds for all three events ranging from 1.7 to 2.1 m s^{-1} (table 1).

Incident solar radiation was measured with a LI-COR pyranometer calibrated for cloudy conditions. Net solar radiation at the study plot was computed by subtracting estimated reflected solar radiation from the incident solar radiation according to

$$R_{n,sol} = (1 - \alpha) I_{sol} , \qquad (16)$$

where

α = albedo (dimensionless),

I_{sol} = incident solar radiation (W m^{-2}).

Reflected solar radiation is a function of the solar albedo of the snowpack. Measuring the albedo of a snow surface

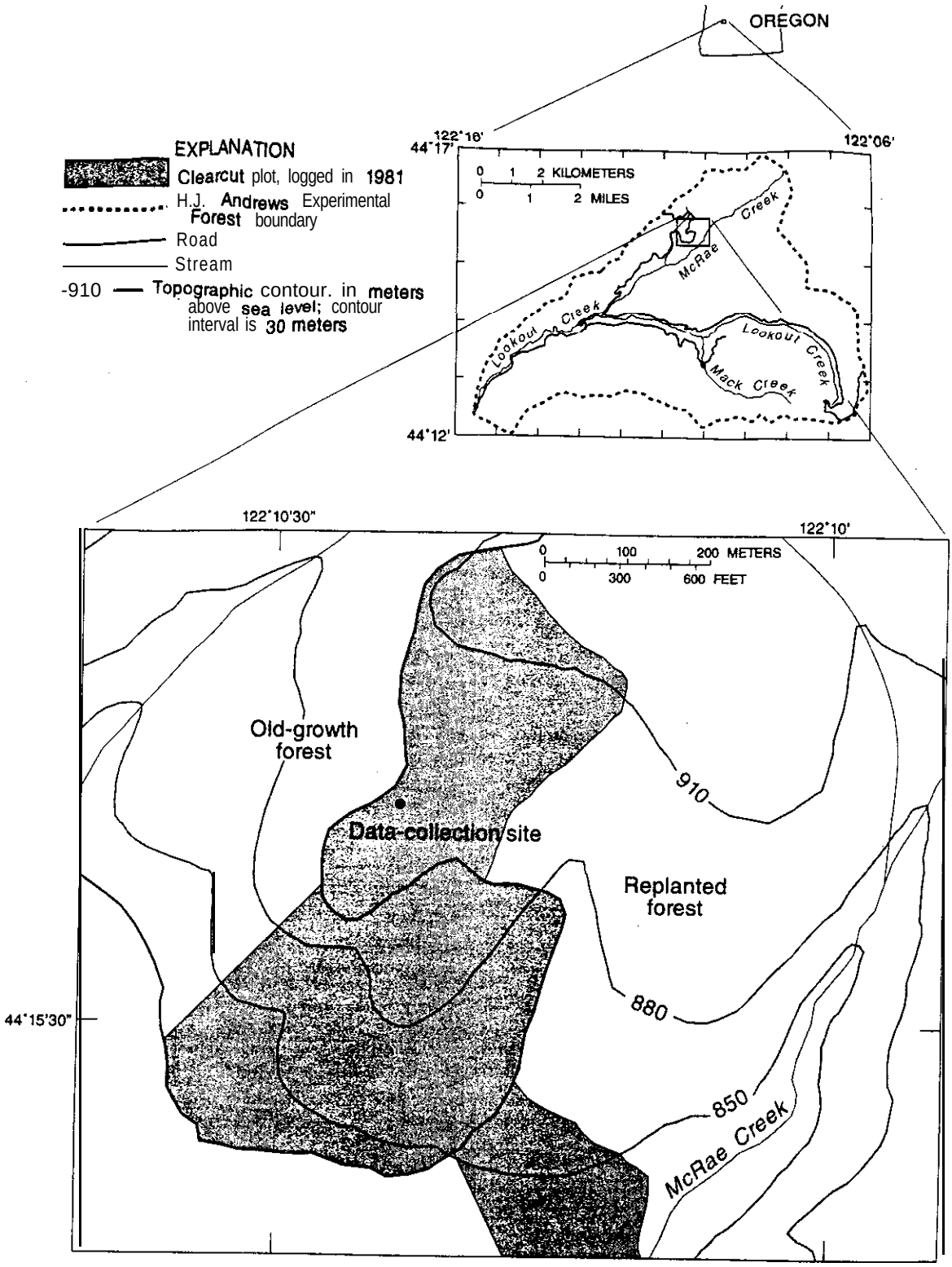

Figure 8.--Location of the clearcut plot and data-collection site in the H.J. Andrews Experimental Forest, Oregon (modified from Berris, 1984).

Table 1.--*Summary of observed and estimated (*) climate and radiation data during rain-on-snow events A, B, and C*

[°C, degrees Celsius; mm h^{-1}, millimeter per hour; m s^{-1}, meter per second; W m^{-2}, watt per square meter]

Variable type	Minimum	Maximum	Average
Event A (hours)			
Air temperature (“C)	0.9	7.0	4.5
Dewpoint temperature (°C)*	0.9	7.0	4.5
Precipitation (mm h^{-1})	0.3	6.1	4.0
Wind speed (m s^{-1})*	1.6	3.3	2.1
Net solar radiation (W m^{-2})*	0.0	13.4	1.7
Incoming thermal radiation (W m^{-2})*	304.6	344.5	327.9
Event B (5 hours)			
Air temperature (°C)	3.3	6.2	5.0
Dewpoint temperature (°C)*	0.0	6.2	3.3
Precipitation (mm h^{-1})	0.0	I.0	0.3
Wind speed (m s^{-1})*	1.1	2.3	1.8
Net solar radiation (W m^{-2})*	11.4	83.3	4x.5
Incoming thermal radiation (W m^{-2})*	318.1	34~1.1	330. I
Event C (19 hours)			
Air temperature (“C)	2.6	4.1	3.2
Dewpoint temperature (°C)*	1.3	4.0	3.1
Precipitation (mm h^{-1})	0.0	1.5	0.8
Wind speed (m s^{-1})*	1.1	2.1	1.7
Net solar radiation (W m^{-2})*	0.0	28.0	4.7
Incoming thermal radiation (W m^{-2})*	318.0	326.9	321.4

is difficult, even under controlled conditions, and it is not possible at a remote, unattended site (Marks, 1988). Detailed models of radiation transfer over a snow surface show that the spectral albedo of snow is determined by the grain size and by the concentration of absorbing impurities in the near-surface layer (Wiscomhe and Warren, 1980; Warren and Wiscombe, 1980). The snow surface albedo is generally larger in the visible portion of the spectrum (0.28-0.7 pm) and lower in the near-infrared (0.7-2.X μm). The solar albedo, however, is generally expressed as an integration of the reflectances over visible and near-infrared wavelengths and can range from 0.9 to 0.4 depending on snow conditions (Male and Granger, 1981).

The solar albedo at the H.J. Andrews Experimental Forest clearcut plot was estimated from a limited set of measured reflectances made at an alpine site in the Sierra Nevada under spring melt conditions (Marks and others, 1992). This estimation is valid because transient-snow-zone snowpack conditions such as those at the Andrew site are similar to those of an alpine snowpack during spring melt. An estimated solar albedo of 0.7 was derived from an integration of hourly measurements of visible and near-infrared reflectances obtained under cloudy conditions at the alpine site. This value was assumed to be constant throughout the two selected simulation periods of the H.J. Andrew Experimental Forest data.

Net solar radiation during the rain-on-snow events was low, averaging only 18 W m^{-2}, with peak values generally less than 80 W m^{-2} (table 1). The low net solar radiation for went A was probably due to cloudy conditions and a high estimate of snow-cover albedo. The low magnitude of net solar radiation for events B and C was primarily due to the time of day in which these events occurred. Solar radiation, however, is a difficult variable to measure over snow under controlled conditions, and it is virtually impossible to monitor over extended periods of time at remote locations (Marks, 1988; Marks and others, 1992). Therefore, the low magnitude of net solar radiation during event A may also have been due, in part, to instrument error resulting from improper sensor calibration or snow or other obstructions on the sensor.

Incoming thermal radiation was not measured at the study site. Instead, it was estimated from temperature and humidity information using an approach developed by Brutsaert (1975) and later modified by Marks and Dozier (1979) for use in alpine areas. This method accounts for variations in atmospheric emissivity with vapor pressure, view factor, and altitude, and has been found to compare well with measured values during spring snowmelt conditions in the Sierra Nevada. According to this method, incoming thermal radiation, I_{lw} or thermal irradiance, is estimated as

$$I_{lw} = \left(\varepsilon_a \sigma T_a^4\right) V_f + \left(\sigma T_t^4\right)(1 - V_f) \quad , \qquad (17)$$

where

I_{lw} = thermal radiation received by the snowpack from the sky, vegetation, and neighboring topography (W m^{-2}),
ε_a = atmospheric cmissivity (dimensionless),
σ = Stefan-Boltzmann constant (5.6697 x 10^{-8} W m^{-2} K^{-4}),
T_a = air temperature (K),
V_f = thermal view factor (dimensionless),
T, = surrounding-terrain temperature (K);

and the atmospheric emissivity, ε_a, is estimated according to

$$\varepsilon_a = \left(1.24\left(\frac{p_a'}{T_a'}\right)^{1/7}\right)\left(\frac{p_a}{1,013}\right) C_f \quad , \qquad (18)$$

where

p_a' = altitude-corrected vapor pressure in pascals (Pa).
T_a' = altitude-corrected air temperature (K),
p_a = measured vapor pressure (Pa),
C_f = cloud-correction factor (dimensionless).

Cloud cover can significantly increase thermal irradiance over a snow surface because of the large absorption and emissivity of clouds in the thermal portion of the spectrum. Because the measurement plot was characterized by predominantly low cloud cover, clear-sky thermal irradiance estimates were adjusted using a cloud-correction factor, C_f, which represents the ratio between thermal irradiances under clear and cloudy conditions. This factor was derived from thermal irradiance measurements at the same alpine site in the Sierra Nevada used to estimate the solar albedo, and it was estimated to be approximately I .34 (Marks and others, 1992).

Thermal irradiance at a snow surface is a function of radiation from both the sky and the surrounding terrain.

The thermal view factor, V_t, ranges from zero to one and represents the proportion of atmospheric thermal irradiance. The thermal view factor was estimated to be 0.6 based on site observations at the H.J. Andrews Experimental Forest clearcut plot. The remaining portion of thermal irradiance was attributed to surrounding terrain and forest vegetation and was assumed to he a black body at temperature, T_t, equivalent to the measured air temperature, T_a. Estimated thermal irradiance averaged approximately 324 W m^{-2} during rain-on-snow events and exhibited little diurnal variation due to cloudy conditions and low air and dewpoint temperatures (table 1).

WAR was measured by a lysimeter that consisted of a series of eight flat, rectangular, fiberglass-covered wooden pans, 0.25 m^2 in area, scattered throughout the clearcut plot and connected by buried plastic pipe to a tipping bucket gage. The existence of multiple connected pans helped in the collection of more representative WAR data in the clearcut plot, although measurement errors were still suspected, as described previously.

Snowpack depth!;, densities, and liquid-water contents were measured at three different times during the time periods selected for simulation (table 2). As described above, however, the density and liquid-water-content values are suspect because imprecise method:; were used to collect them.

Construction of the Simulation Models

The energy-balance snowmelt model requires initial estimates of several snowpack properties in order to effectively simulate snow accumulation and melt at a point. These estimates were derived from measured snowpack properties when possible, but most had to be estimated hccause of a lack of detailed or accurate measurements.

In the model, all surface energy exchange between the snowpack and the environment takes place in the active, top layer of the snowpack. This layer represents the maximum depth of solar radiation penetration, which is variable and depends on factors such as grain size and solar zenith angle. The depth of the active layer has been found to range from 0.1 to 0.2 m for deep snowpacks under spring melt conditions in the Sierra Nevada (Marks and others, 1992). For the purposes of this investigation, the initial snowpack active layer depth was set equal to 0.1 m (table 3). This choice of active layer depth, however, did not influence model estimates of snowpack properties because measured solar radiation at the site was low and the snowpack profile remained at 0°C and under active melt during rainfall events.

Initial snowpack depths at the start of the February IO and February 27 simulations were assumed to be 0.5 m. Observed snowpack depths on February I 1 and 27 were about half the assumed depths (table 2), but as long as

Table 2.--*Snowpack properties measured in the H.J. Andrews Experimental Forest, Oregon, clearcut during the selected simulation periods (from Berris, 1984; Berris and Harr, 1987)*

Date	Snow depth (millimeter)	Snow-water equivalent (millimeter)	Snow density (kilogram per cubic meter)	Liquid-water content (percent)[1]
02-1 1-84	242	36	150	I.1
02-12-84	67	18	270	x.3
02-27-84	253	67	270	4.0

'Defined as the proportion of the air fraction of the snowpack that is taken up hy liquid water. 'This definition differs from that used by Berris (1984) and Berris and Herr (1987), who defined it as the proportion of the snow-water equivalent that exists as liquid water.

Table 3.--*Initial model conditions and conditions assumed constant throughout the simulation periods*

Variable	Value
Initial conditions	
Active-layer depth of the snowpack	0.1 meter
Snowpack depth	0.5 meter
Active-layer temperature of the snowpack	0 degrees Celsius
Lower-layer temperature of the snowpack	0 degrees Celsius
Liquid-water content of the snowpack'	1.7 percent
Snowpack density	500 kilograms per cubic meter
Height above the snowpack of instruments used to measure air and dewpoint temperatures and wind speed	1.0 meter
Constants	
Maximum liquid-water content of the snowpack'	5 percent
Snow-surface roughness length	0.003 meter
Site elevation	900 meters
Model run time step	1 hour
Soil-temperature measurement depth	0.5 meter

'Liquid-water content is defined as the proportion of the air fraction of the snowpack that is taken up by liquih water,

snow is on the ground during the simulation and in reality, this discrepancy should not significantly affect the amount of melt computed during the rain-on-snow events. Available snow-depth measurements indicated that the snowpack was generally shallow (<0.5 m), existing under average air temperatures of approximately 4°C. Initial temperatures for both the active and lower snowpack layers were therefore assumed to be isothermal at 0°C and capable of producing melt (table 3).

The initial snowpack liquid-water content was assumed to be 1.7 percent, a reasonable value for a" unsaturated snowpack. (Liquid-water content is defined as the proportion of the air fraction of the snowpack that is taken up by liquid water.) The maximum allowable liquid-water content was assumed to be 5 percent (table 3), which is roughly equal to maximum values observed during spring melt in other snowpacks. If the density of the snowpack is 500 kg m^{-3}, this corresponds to a liquid-water holding capacity of about 23 kilograms per meter (kg m^{-1}). The assumed initial and maximum liquid-water content values are substantially lower than those reported by Berris and Harr (1987). Some controversy exists about the liquid-water holding capacity of a snowcover, but the volume of liquid water held by a snowpack is probably relatively small (Colbeck, 1978). In the simulations of snow accumulation and melt, liquid-water saturation was reached within one to two hours following the initiation of rainfall.

Physical properties of a snowpack such as thermal conductivity, snow-water equivalent and air permeability depend strongly on snow density. Snowpack densities have been found to range from 65 kg m^{-3} for new snow to upwards of 650 kg m^{-3} for a ripe snowpack under active melt (Marks and others, 1986; Male and Granger, 1981). Available snowpack densities were calculated by weighing a known volume of snow (table 2). Although this method has been widely used, it is prone to error, especially when a snowpack is shallow (like the snowpack under consideration) or ice lenses are present. Snowpack densities derived by this method during the entire 1983-84 winter in the clearcut ranged from 140 to 430 kg m^{-3} and averaged

Table 4.--*Summary of model-input variables and variable assumptions*

[°C, degrees Celsius; K, degrees kelvin; W m^{-2}, watt per square meter; m, meter; kg m^{-3}, kilogram per cubic meter; *Pa,* pascal; m s^{-1}, *meter per* second]

Input variable	Assumption
Air temperature (K)	None, observed values used
Dewpoint temperature (K)	Dewpoint temperatures are assumed to be equal to air temperatures when precipitation occurs (i.e., the relative humidity is assumed to be 100 percent)
Incoming thermal radiation (W m^{-2})	Computed as a function of observed air and dewpoint temperatures using equations 17 and 18
Net solar radiation (W m^{-2})	Computed from observed incoming solar radiation using equation 16 and by assuming an albedo of 0.7
Precipitation depth (m)	None, observed values used
Precipitation temperature (K)	Equal to dewpoint temperature
Precipitation type	Rain if precipitation temperature is greater than or equal to 0°C; snow or rain-snow mixture if precipitation temperature is less than 0°C
Precipitation density (kg m^{-3})	1,000 kg m^{-3} if precipitation temperature is greater than or equal to 0°C; 700 kg m^{-3} if precipitation temperature is less than 0°C and greater than -3°C; 350 kg m^{-3} ilprecipitation temperature is less than or equal to -3°C.
Soil temperature (K)	Constant at 273.16 K
vapor pressure (Pa)	Computed from observed air and adjusted dewpoint temperatures
Wind speed (m s^{-1})	Increased by 0.9 m s^{-1} over measured values

280 kg m^{-3} (Berris and Harr, 1987). The average snowpack density measured during the largest rain-on-snow event that winter was 210 kg m^{-3}. These values were judged to be substantially lower than expected for melt conditions. As a result, reported snowpack densities for the selected simulation periods were ignored, and a density of 500 kg m^{-3} was used to represent initial snowpack conditions (table 3). To test this assumption, snowpack-profile density measurements were conducted near the H.J. Andrew Experimental Forest site during February 1994, under similar snow and climate: conditions. The measurement technique used has more precise volume and weight control (for example, Elder and others, 1991) than that used by Berris and Hat-r. Snowpack densities of approximately 490 kg m^{-3} were measured, which seemed to support the assumption of a higher snowpack density than reported by Berris and Harr (1987).

The snow-surface roughness length (z_0) is used in the calculation of convective energy transfer. Over snow, which is fairly smooth, z_0 ranges from 0.0001 to 0.005 tn. If vegetation and local terrain features have to be considered, however, the value can bc much higher. The snow-surface roughness parameter was set to a constant 0.003 m for the model runs (table 3), as a typical value of z_0. Because the model runs were restricted to relatively short time periods with a complete snow cover, the assumption of a constant roughness value was valid.

Input variables required by the model at each time step to calculate the snowpack energy balance are net solar and incoming thermal radiation, air temperature, vapor pressure, and wind speed (table 4). These variables were measured or estimated, as described previously.

Input variables required at each time step to calculate the snowpack thermal and mass properties are the precipitation type, depth, temperature, and density. Precipitation depths were measured; precipitation type, temperature, and density were not measured, however, and had to he estimated. Precipitation temperatures were assumed to be equal to dewpoint temperatures, and the type and density were approximated on the basis of its assumed temperature. Precipitation was assumed to be rain if the dewpoint temperature was greater than or equal to 0°C and to be either snow or a rain-snow mixture if the dewpoint temperature was less than 0°C. Rainfall densities were assumed to he 1,000 kg m^{-3}. Precipitation densities were assumed to he 700 kg m^{-3} for dewpoint temperatures between 0°C and -3°C (a rain-snow mixture) and 350 kg m^{-3} when dewpoint temperatures were equal to or less than -3-C (snow only; table 4).

To simulate the conductive and diffusive heat transfer between the snowpack and the ground, the temperature of the soil and the effective thermal conductivities of the bottom snow layer and the soil arc needed. Measured soil temperatures were close to 0°C, and they were assumed constant at 0°C for the duration of the simulations. Effective thermal conductivities of the bottom snow layer and the soil were computed by the model (Marks, 1988).

The energy-balance model computes WAR (equivalent to measured lysimeter outflow), snowmelt, snowpack properties such as depth, snow-water equivalent, liquid-water content, and temperature, and the size of individual energy terms during each time step. The simulated WAR, melt, evaporation, and the relative contribution of individual energy sources to generate snowmelt were variables used in this study (table 5).

Table 5.--*Summary* **of model-output** *variables used in this study*

[W m^{-2}, watt per square meter; mm, millimeter]

Mass-halancc information:
Evaporation (mm)
Melt (mm)
Water available for runoff (WAR) (mm)
Energy-balance information:
Advective heat (W m^{-2})
Conductive and diffusive heat (W m^{-2})
Latent heat (W m^{-2})
Net all-wave radiation (W m^{-2})
Sensible heat (W m^{-2})

Sources of Differences Between Observed and Simulated Snowmelt

Roth the ability of mathematical models to accurately represent hydrologic processes and the reliability of measurements used as input to the models introduce error in the simulation results. Any time the physical world is represented by a mathematical model, simplifications and assumptions about the real system introduce error and limit the predicting ability of the model. However, a mathematical model is useful to understand the relative importance of various processes that influence the prediction and thus to improve the understanding of the real world.

Initial snowpack properties were assumed for the simulations because they were not reliably known. For this reason alone, simulated snowpack properties cannot be compared with observed values. The timing and general pattern of simulated WAR, however, can be compared with observed values to the extent that the observations can be trusted. WAR is defined as the amount of liquid water that leaves the bottom of the snowpack after the liquid-water holding capacity of the snowpack has been exceeded. The source of liquid water is precipitation, condensation, and melt. Provided that all required hourly model inputs are known exactly during the simulation, then if the initial (assumed) snow-water equivalent of the snowpack is too small, the simulated snowpack may melt entirely before the end of an event, resulting in an under-simulation of WAR. The assumption of an initial snow-water equivalent of the snowpack that is too large, however, is expected to have little effect on the simulated WAR during an event, unless this results in a snowpack being available for melt at a time when the real snowpack has already disappeared. If the assumed initial liquid-water content of a snowpack is too low or if the assumed maximum value is too high, some or all of the liquid water may remain tied up in the snowpack during simulations instead of becoming simulated WAR. Error in simulated WAR is due not only to possible incorrect initial conditions, however, because error is also introduced by hourly model inputs that may be incorrect or because the model is not suitable.

The reliability of measured variables that are input to the energy-balance model varies depending on the variable type. Observed hourly precipitation is frequently lower than the true amount of precipitation because of catch deficiencies that increase as wind speed increases; catch deficiencies are more severe for snow than for rain. According to Larson and Peck (1974), when wind speeds reach 4.5 m s^{-1}, the catch deficiency is about 12 percent for rain in a shielded or unshielded gage, 27 percent for snow in a shielded gage, and 47 percent for snow in an unshielded gage. For the data used in this study, none of the precipitation gages was shielded. Inaccurate precipitation measurements contribute significantly to error in simulated snowpack properties and lysimeter outflow. These errors are compounded by the lack of knowledge of precipitation type, composition, density, and temperature.

For modeling purposes, the precipitation type is arbitrarily decided with respect to a threshold temperature, which remains constant for the length of the simulation. Whenever the determination of rain versus snow is incorrect, however, the simulation of the snowpack mass and thermal properties and thus WAR are affected. For example, if precipitation is assumed to be snow when in fact it is predominantly rain, the simulated snowpack thickness will be too great, and precipitation that should be contributing to simulated WAR is instead tied up in the snowpack. The extra thickness of the snowpack results in more WAR at a later time when snowmelt conditions occur. If precipitation is assumed to be rain when it is predominantly snow, the simulated snowpack thickness will be too small, and precipitation that should be contributing to the snowpack thickness instead is part of the simulated WAR. The determination of precipitation type can have a significant effect on the accuracy of simulated WAR. During rain on snow, however, dewpoint temperatures are generally sufficiently high so the precipitation type is not in doubt.

Errors in the estimation of snowfall densities and rain-snow proportions substantially affect model-simulated snowpack density, liquid-water storage, melt, and snow accumulation. However, focusing on relatively short time periods (5 days) with documented rain-on-snow events minimizes cumulative model error in simulated mass and thermal snowpack properties. It is likely that the estimation errors of precipitation properties are especially significant during snowfall or mixed rain-and-snow precipitation. The accuracies of model-simulated snow accumulation and melt are therefore likely to decrease over longer time periods without adequate precipitation information.

Errors in simulated snowpack properties as a result of net all-wave radiation can be significant. Those errors would mostly result from errors in the estimation of incoming thermal radiation rather than from errors in the computed emitted thermal or net solar radiation. Incoming thermal radiation is estimated as a function of air temperature, the degree of cloudiness, vegetation, and topography. Air temperature is well known, but estimating the degree of cloudiness and the effects of vegetation

and topography is difficult without measurements. Errors due to thermal radiation emitted by the snowpack arc small during melt conditions because the temperature of the snowpack surface remains near 0°C. Errors due to the estimation of net solar radiation should be minimal during rain-on-snow events of interest (those with a high precipitation) because extreme cloudiness reduces net solar radiation to a minor source of energy to the snowpack.

Wind speed is an important variable to determine the amount of turbulent-energy exchange between the air and the snowpack. As described previously, wind-speed measurements were hampered by the high anemometer threshold compared to the predominant wind speeds observed at the site. In an attempt to compensate for instrument threshold error, wind speeds were adjusted by adding a factor of 0.9 $m\ s^{-1}$ to actual measurements. In spite of these adjustments, however, it is likely that wind measurement error contributes significantly to observed differences between simulated and measured snowpack runoff.

Simulation Results

Simulated and observed WAR compare reasonably well for rain-on-snow events A, B, and C (fig. 9). The reason for this, however, is that a large component of WAR is precipitation itself. To better assess the quality of the simulation, it is useful either to compare the simulated melt (defined as the amount of water generated from melted ice in the snowpack) and the difference between observed WAR and precipitation in the form of rain (defined in this report as excess runoff) or to compare the simulated and observed excess runoff (fig 9. and table 6).

Table 6.--*Simulated und observed water available for runoff (WAR), water available for runoff minus rain (excess runoff), melt, and ratios between simulated and observed values for rain-on-snow events A, B, C, and the entire simulation period*

Variable type	Simulated (millimeter)	Observed (millimeter)	Simulated divided by observed
	Event A (35 hours)		
WAR	154.1	185.0	0.83
WAR minus rain (excess runoff)	13.1	44.0	0.30
Melt	21.1	‘44.0	0.48
	Event B (5 hours)		
WAR	5.8	7.0	0.83
WAR minus rain (excess runoff)	4.3	5.5	0.78
Melt	4.1	‘5.5	0.75
	Event C (19 hours)		
WAR	19.4	30.8	0.63
WAR minus rain (excess runoff)	4.4	15.8	0.28
Melt	4.2	‘15.8	0.27
	Total simulated period (240 hours)		
WAR	204.0	278.5	0.73
WAR minus rain (excess runoff)	13.3	X7.8	0.15
Melt	80.4	‘87.8	0.92

‘Values are assumed equal to WAR minus rain because they arc not measured. Melt is similar to WAR minus rain, except that it does not include effects from evapotranspiration, condensation, and liquid-water storage in the snowpack (see text).

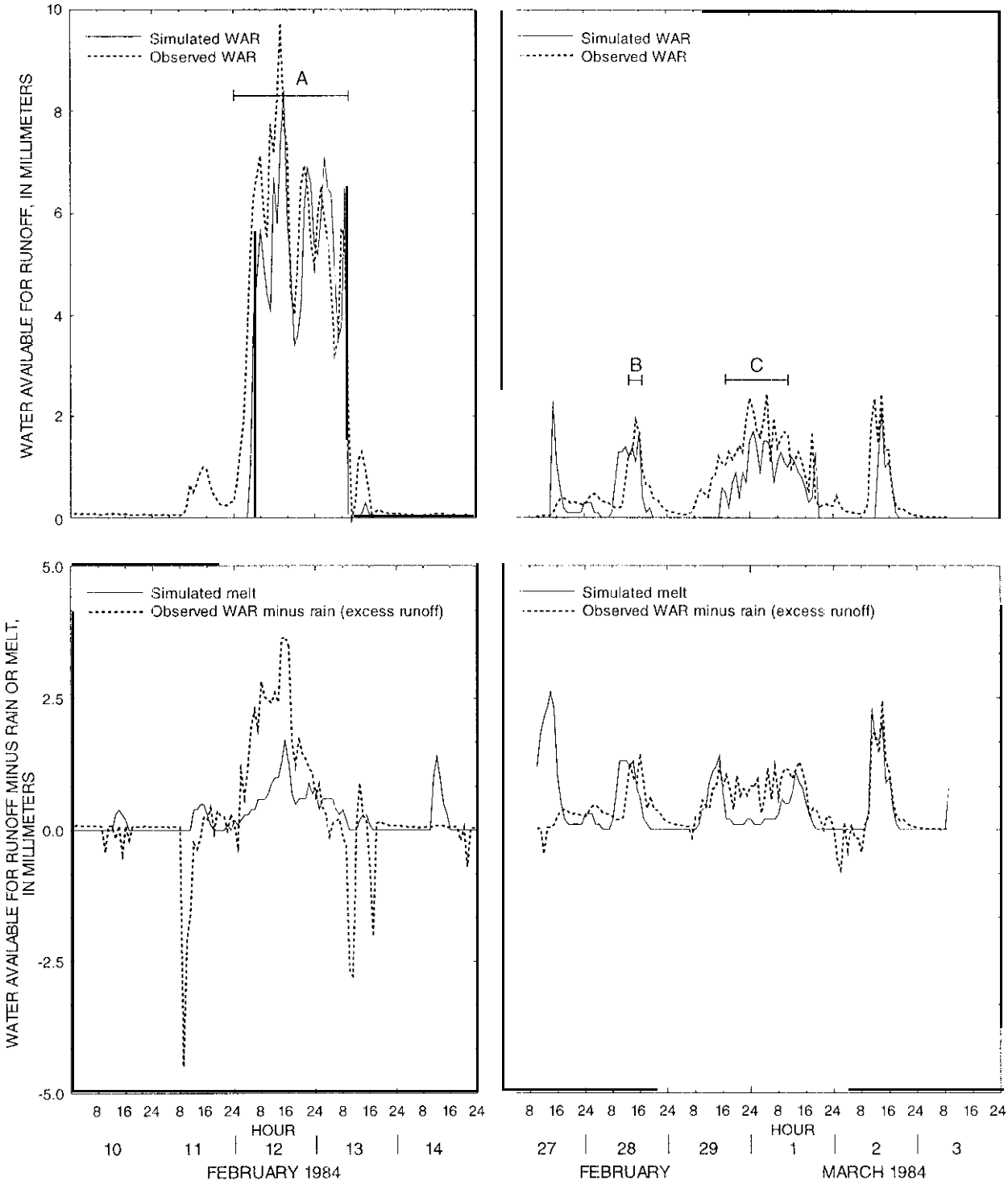

Figure B.--Simulated and observed water available for runoff (WAR), simulated melt, and observed water available for runoff minus rain (excess runoff). A, B, and C denote rain-on-snow events discussed in the text.

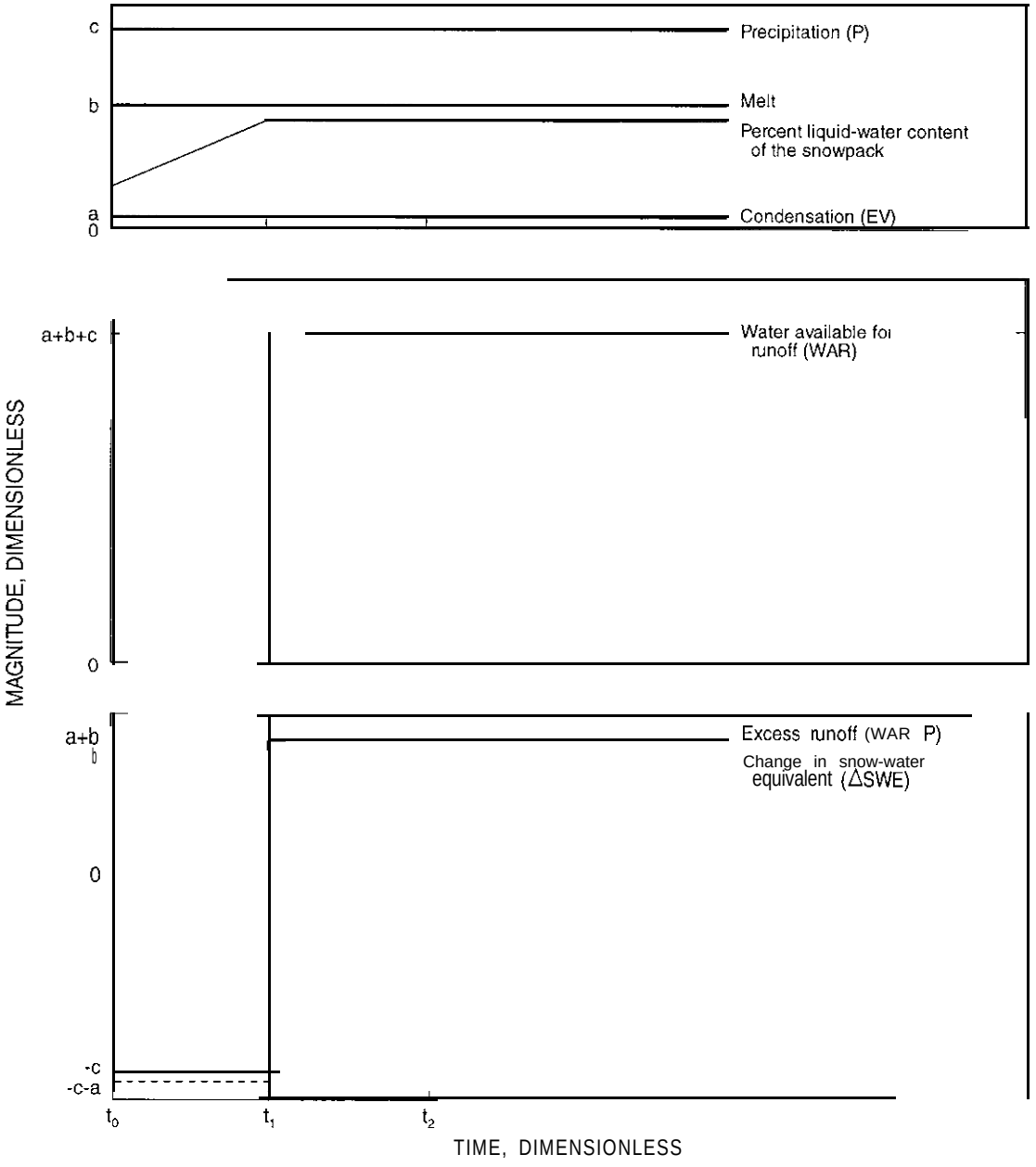

Figure 10.--Schematic magnitude and timing of water available for runoff (WAR), water available for runoff minus precipitation (excess runoff), and change in snow-water equivalent and their relation to melt, precipitation, condensation, and percent liquid-water content of the snowpack during rain-on-snow events. Time=t_1 represents the time at which the unsaturated snowpack has reached liquid-water saturation.

The difference between WAR and precipitation, P, may he expressed as

$$WAR - P = EV + \Delta SWE \quad , \qquad (19)$$

where variables not previously defined arc

EV = evaporation or condensation (mm),

ΔSWE = change in snow-water equivalent (mm).

A positive value of EV is defined as the addition of mass to the snowpack (that is, condensation), and a positive value of ΔSWE is defined as a decrease in the snow-water equivalent. During rain on snow, condensation usually only accounts for a small fraction of the mass balance of a snowpack. For the simulation periods, El' was zero at all times except for one hour, when it was 0.1 mm. This condensation represents less than 0.8 percent of the total decrease in snow-water equivalent (ΔSWE) simulated during the same time period As will he demonstrated later in the report, condensation can be more significant for climate conditions different from those ohserved during the simulation periods. Even then, however, condensation represents only a small fraction of the total water balance.

Both observed and simulated excess runoff ($WAR - P$ in equation 19) can be either negative or positive. Excess runoff for a given hour is negative when it is raining but the liquid-water holding capacity of the snowpack has not been reached (time $< t_1$ in fig. 10). During such hours, the snow-water equivalent of the snowpack increases. Excess runoff becomes positive once the liquid-water holding capacity of the snowpack has been reached. The snow-water equivalent of the snowpack will begin to decrease at that time. (For simplicity, melt and the change in snow-water equivalent after saturation have been assumed to be the same in fig. 10. I" reality. the change in snow-water equivalent would be slightly larger than the melt, hecausc liquid water that was held in storage by the melted portion of the snowpack also runs off.) The total excess runoff could be negative for an entire event if the available liquid-water holding capacity of the snowpack is greater than the sum of precipitation and melt. However, during large rain-on-snow events in the transient-snow zone, the total excess runoff will usually be positive hecausc snowpacks will already he near saturation at the start of an event and prccipitatio" and melt will quickly saturate rhc snowpack.

The magnitude of excess runoff depends on the amount of liquid water that the snowpack can store, hut the magnitude of melt is essentially independent from this. This also means that melt is independent from the assumed initial liquid-water content of the simulated snowpack, and melt could he considered as the maximum amount of runoff that can occur during a rain-on-snow event. Treating melt as such, however, ignores condensate and liquid water that is held in storage by the melted portion of the snowpack. Because the ignored sources of liquid water are usually smaller than the available liquid-water holding capacity of the snowpack, melt will usually exceed excess runoff. When it does not exceed excess runoff, the difference between the two variables is small.

At the start of each S-day simulation, the actual liquid-water content of the snowpack was not know", hut for the simulations it was assumed that the snowpack was not fully saturated. However, at the start of each rein-on-snow event within each S-day simulation period, it was presumed that the actual snowpack was fully saturated. Thus, the accuracy of the simulations was assessed by comparing simulated melt and observed excess runoff rather than simulated excess runoff and observed excess runoff. The discussion of the H.J. Andrews Experimental Forest simulations will focus on the comparison of simulated melt and observed excess runoff in the remainder of this report. Simulated excess runoff is also reported, however, to demonstrate how the particular set of assumed antecedent snowpack conditions influenced the amount of simulated excess runoff.

Simulated melt does not match observed excess runoff as closely as do simulated and observed WAR during the rain-on-snow events (fig. 9). This is also illustrated hy the smaller ratios of simulated to observed values for melt compared to those for WAR during the same time periods (table 6). To compute this ratio for simulated and observed melt, it was assumed that observed melt was the same as observed excess runoff because melt was not measured. As stated previously, the reason for the poorer match between simulated and assumed melt compared to simulated and observed WAR is that a large component of WAR is precipitation itself. For events A, B, and C, rain constituted 76, 21, and 49 percent of the observed WAR, respectively. For all three events and the entire simulation periods, the observed excess runoff was greater than either the simulated excess runoff or the melt.

The simulation of the three rain-on-snow events demonstrates that the model is behaving as expected. The timing of simulated melt generally agreed with the timing of observed excess runoff (fig. Y), hut the magnitudes of simulated and observed values agreed poorly (table 6). Not

too much importance can bc placed on this poor match, however, because only two 5-day periods were simulated, and only one of the three rain-on-snow events during that time (event A) was of a significant size. It is difficult to attribute differences in magnitude between simulated and observed values to any single factor. Large differences are most likely due to one or more measurement and estimation errors involving precipitation depth and density, wind speed, radiation, and observed WAR.

The rate of snowmelt is a function of the condition of the snowpack and the energy exchange between the snow surface and the atmosphere, as defined by equation 1. Simulated energy exchanges that took place along the snow surface are summarized below for the entire simulation periods and individual rain-on-snow events (fig. 11 and table 7).

During the events, the simulated snowpack was thermodynamically active and isothermal at 0°C. Light winds, humid conditions and above-freezing air temperatures resulted in a small net transfer of energy to the snowpack

Table 7.--*Simulated melt, simulated water available for runoff (WAR) minus rain (excess runoff), and the relative contribution of energy terms to the simulated melt for different simulation periods*

[mm, millimeter]

Simulation period	Simulated Melt (mm)	WAR minus rain (excess runoff) (mm)	Percent contribution to simulated melt of: Net solar radiation ($R_{n,sol}$)	Net thermal radiation (I_{lw})	Net all-wave radiation (R_n)	Sensible heat (H)	Latent heat (L_vE)	Turbulent heat ($H+L_vE$)	Advective heat (M)
Event A									
0000 02-12-84 through 1000 02-13-84	**21.1**	13.1	**3.1**	**21.3**	**24.4**	**25.1**	**25.4**	50.5	**25.1**
Event B									
1300 02-28-84 through **1700** 02-28-84	**4.1**	**4.3**	**63.9**	**18.6**	**82.5**	**9.2**	**5.9**	**15.1**	**2.4**
Event C									
1700 02-29-84 through 1100 **03-01-84**	**4.2**	**4.4**	**23.1**	**27.3**	**50.4**	18.6	17.1	**35.7**	**14.0**
Total simulation period									
0100 02-10-84 through 2400 02-14-84 and 1000 02-27-84 through 0900 03-03-84	**80.4**	13.3	71.4	**-7.4**	**64.0**	**19.6**	**7.7**	**27.3**	**8.8**

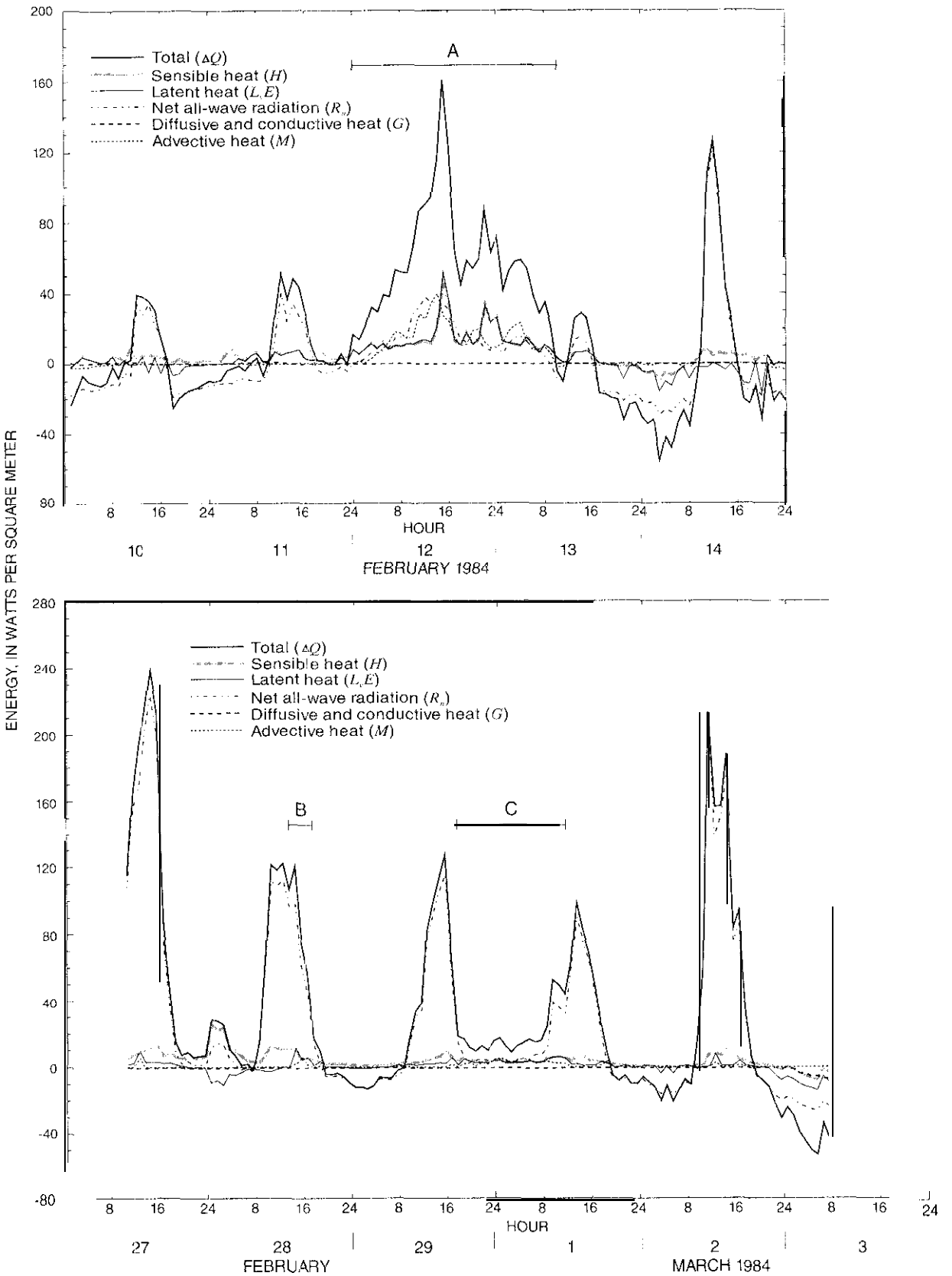

Figure 11.--Simulated energy exchanges along the snowpack surface. A. B, and C denote rain-on-snow events discussed in the text.

and small but fairly continuous rates of melt. Total simulated melt for events A, B, and C, was 21.1, 4.1, and 4.2 mm, respectively; the average rate of melt ranged from 0.2 to 0.8 mm h^{-1}. These rates were generally independent of the intensity and duration of the rainfall. Instead, they were strongly dependent on the sum of the net all-wave radiation and turbulent-energy exchange (sensible and latent heat). Because this sum was typically small, the rate of snowmelt was relatively low. Even so, the sum of net all-wave radiation and turbulent-energy exchange was responsible for a dominant 75, 98, and 86 percent of melt for events A, B, and C, respectively. Turbulent-energy exchange provided 51 percent of the energy that led to snowmelt during the largest of the three events.

The simulated maximum hourly net all-wave radiation was 37.9, 97.7, and 39.0 W m^{-2} for events A, B, and C, respectively, and averaged only 13.7, 62.7, and 10.3 W m^{-2}. The net all-wave radiation was small but positive during the selected events, indicating a net transfer of energy to the snowpack. Thermal radiation emitted by the snowpack was approximately 316 W m^{-2} and was constant during rainfall events because the snowpack surface temperature remained at 0°C. These conditions resulted in low, average hourly, net thermal radiation values of 12.0, 14.1, and 5.6 W m^{-2} for events A; B, and C, respectively. This is equivalent to 87, 23, and 54 percent of the net all-wave radiation for the events.

The contribution of advective heat of precipitation to the total melt during these events increased with the intensity of rainfall. It accounted for 25, 2, and 14 percent of the melt for events A, B, and C, respectively. Except for event A-the only simulated rain-on-snow event previously identified as such (Berris and Harr, 1987)—snowmelt due to advective heat was generally small compared to the sum of net all-wave radiation and turbulent-energy exchanges.

Simulated energy transfer by conduction and diffusion between the soil and the snowpack was insignificantly small. Soil temperatures were assumed to be 0°C, and snowpack temperatures generally remained near O'C during the simulations. The resulting small temperature differences and the low thermal conductivity of snow were responsible for the low energy transfer between the soil and the snowpack. During the rain-on-snow events, rainfall did not freeze within the snowpack because snow temperatures were at 0°C. This resulted in rapid runoff as the liquid-water holding capacity of the snowpack was typically attained within one to two hours following the beginning of rainfall. These results are supported by findings of Conway and Benedict (1994), who monitored rainfall infiltration into a maritime snowpack using a matrix of thermistors.

These simulations show that the model behaved as expected. Traditional calibration (matching simulated and observed WAR and snowpack properties) had no meaning in this case and was not attempted. Instead, the model was used to perform a sensitivity analysis to examine the relative importance of various snowmelt processes during rain on snow.

Sensitivity Analysis

Model inputs of solar radiation, precipitation, air temperature, and wind speed were increased to evaluate the individual effects of each variable on the generation of snowmelt. The two 5-day periods that were previously simulated using observed conditions (also referred to as base conditions) were simulated again with systematically adjusted input variables. At the start of each simulation, snowpack conditions were assumed to be identical to base conditions (table 3).

Net Solar Radiation

Net solar radiation, $R_{n,sol}$, is an important energy source to generate snowmelt under clear-sky conditions, but not usually under rain-on-snow conditions. The estimated net solar radiation during the largest rain-on-snow event (event A) was small because the measured incoming solar radiation was small. The estimated net solar radiation averaged I .7 W m^{-2} for the duration of the event (assuming a solar albedo of 0.7). Although the low value of solar radiation could have resulted from the extreme cloudiness that must have been present during the event, low incoming solar radiation measurements may also have been due, at least in part, to shielding of the sensor by snow or some other obstruction. Hourly net solar radiation values calculated for a less cloudy February day with no precipitation and assuming an identical solar albedo of 0.7 ranged from 0 to 126 W m^{-2} and averaged approximately 15.4 W m^{-2}.

Thcsc values are about nine times larger than the average net solar radiation values for event A. As part of the sensitivity analysis, snowmelt was simulated during event A using an adjusted solar radiation, $R_{n,\,sol.\,adj}$, so that the mean hourly net solar radiation during the event was increased from 1.7 to 15.4 W m^{-2}. All other variables were kept the same.

Snowmelt simulations of event A using the adjusted solar-radiation values increased the total melt during the event by 5.2 mm over base conditions to 26.3 mm (table 8). This represents an increase in snowmelt of 25 percent. The relative contribution of net solar radiation to generating melt increased from 3 to 22 percent, and it reduced the relative contributions of sensible, latent, and advective hear as a result (H, L_vE, and M, respectively).

Precipitation

The three rain-on-snow events selected for simulation provided a wide range of depths of precipitation, from light rainfall (event B, average precipitation 0.3 mm h^{-1}) to heavy rainfall (event A, average precipitation 4.0 mm h^{-1}). Observed precipitation rates were doubled ($z_{pp} \times 2$) for the simulation of events A, B, and C to assess snowmelt responses under a wider range of rainfall conditions. All other variables were kept the same.

Doubled precipitation rates generated total rainfall depths of 280.0, 3.0, and 30.4 mm for events A, B, and C, respectively. This resulted in small increases in simulated melt over base conditions for event B (0.1 mm, or 2 percent) and event C (0.5 mm, or 12 percent; fig. 12 and table 8). The increase was more significant for event A-5.6 mm, or 27 percent over base conditions. The relative contribution of advective heat to snowmelt generation, M, increased hy 60, 92, and 75 percent for events A, B, and C, respectively, to 40, 5, and 25 percent of the total contribution to snowmelt. Even though increased snowmelt occurred, it did not lead to an increase in simulated excess runoff during event C; instead, the liquid-water content of the snowpack increased. Net radiation and turbulent-energy exchange (R_n and $H + L_vE$, respectively) remained the dominant energy sources controlling snowmelt for events B and C. For event A, advective heat became equally important as turbulent heat as a contributor to snowmelt.

The amount of energy imparted to a snowpack by rainfall depends on the amount of precipitation and the temperature difference between the snowpack and precipitation (equation 14). On average, temperature differences between rainfall and a snowpack do not exceed 5°C in a transient-snow zone because the snowpack is usually isothermal at 0°C and the average rainfall temperatures are less than 5°C. This means that 10 mm of rainfall at a temperature of 5°C on a ripe snowpack would impart only enough energy to produce 0.6 mm of snowmelt. This computation illustrates that advection has a minor impact on snowmelt under normal rainfall conditions and hccomes an important factor only during heavy rainfall, as during event A.

Air Temperature

Temperature effects on snowmelt were evaluated hy increasing the measured air temperatures hy 2°C ($T_a + 2$). Vapor pressures and dewpoint temperatures were recomputed by assuming that relative humidities had not changed, which resulted in increased vapor pressures and dcwpoint temperatures. Because the temperature of precipitation was assumed equal to the dewpoint temperature, the temperature of precipitation increased also. Precipitation densities were recomputed using the new precipitation-temperature data, and incoming thermal radiation was recalculated at each time step according to the adjusted air temperatures. Solar radiation, depth of precipitation, and wind speed were kept the same.

With higher air temperatures, simulated snowmelt increased for events A, B, and C by 11.0, 0.8, and 3.6 mm over base conditions, respectively, to 32.1, 4.9, and 7.X mm (fig. 12 and table 8). These increases arc equivalent to increases of 52, 20, and 86 percent over base conditions. The melt increases were due to increases both in incoming thermal radiation and in turbulent heat. Generally, however, the increase in net thermal radiation was twice the increase in turbulent heat. The average net thermal radiation at the snow surface for events A, B, and C, $I_{lw} - \varepsilon_s \sigma T_{s,\,0}^4$, increased by 108, 76, and 188 percent, to 25.0, 24.8, and 16.1 W m^{-2}. Higher air temperature and specific humidity gradients increased the avenge turbulent energy flux to the surface during the events hy 22, 49, and 69 percent for events A, B, and C, respectively, to 34.6, 17. I, and 12.3 W m^{-2}.

The effects of increased temperature and specific humidity gradients on sensible and latent energy exchange were minimized as a result of observed wind speeds that were small during the simulation period. A simultaneous increase in wind speed would have produced a significant increase in snowmelt, as described below. As a result of increased dewpoint temperatures, melt from advective heat, M increased by 70 30, and 64 percent to 9.0, 0.13. and 1.0 mm for events A, B, and C, respectively.

Table *S.--Simulated melt, simulated water available for runoff (WAR) minus rain (excess runoff), and the relative contribution of energy terms to the simulated melt for different model inputs and for different simulation periods*

[mm, millimeter]

Type of input conditions'	Simulated		Percent contribution to simulated melt of						
	Melt (mm)	WAR minus rain (excess runoff) (mm)	Net solar radiation ($R_{n,sol}$)	Net thermal radiation (I_{lw})	Net all-wave radiation (R_n)	Sensible heat (H)	Latent heat (L_vE)	Turbulent heat ($H+L_vE$)	Advective heat (M)
			Event A (hours)						
base	*21.1*	13.1	*3.1*	21.3	*24.4*	*25.1*	*25.4*	*50.5*	*25.1*
$R_{n,sol,adj}$	*26.3*	*18.3*	*22.0*	17.1	*39.1*	*20.2*	*20.4*	*40.6*	*20.2*
$z_{pp} \times 2$	*26.7*	*17.8*	*2.5*	17.0	*19.5*	*20.1*	*20.3*	*40.4*	*40.2*
$T_a + 2$	32.1	36.6	*2.0*	*29.4*	*31.4*	19.5	21.1	*40.6*	*28.0*
$u \times 4$	*87.3*	*88.3*	*0.7*	*5.2*	*5.9*	*55.9*	32.1	*88.0*	*6.1*
$u \times 6$	129.6	134.8	*0.5*	*3.5*	*4.0*	*58.3*	*33.6*	*91.9*	4.1
$T_a + 2, u \times 4$	161.1	177.0	*0.4*	*5.9*	*6.3*	*42.2*	*45.7*	88.1	*5.6*
			Event B (5						
base	4.1	*4.3*	*63.9*	18.6	*82.5*	*9.2*	*5.9*	15.1	*2.4*
$z_{pp} \times 2$	*4.2*	*4.5*	*62.4*	18.2	*80.6*	*9.0*	*5.7*	14.7	*4.6*
$T_a + 2$	*4.9*	*5.3*	*52.2*	*26.7*	*78.9*	10.4	8.0	18.4	*2.7*
$u \times 4$	10.2	10.9	*25.8*	*7.5*	*33.3*	*40.5*	*25.2*	*65.7*	1.0
$u \times 6$	14.5	15.6	*18.0*	*5.3*	*23.3*	*46.6*	*29.4*	*76.0*	*0.7*
$T_a + 2, u \times 4$	*13.3*	14.4	19.6	10.0	*29.6*	*39.6*	*29.9*	*69.5*	1.0
			Event C (19 hours)						
base	*4.2*	*4.4*	23.1	*27.3*	*50.4*	18.6	17.1	*35.7*	14.0
$z_{pp} \times 2$	*4.7*	*4.4*	*20.2*	*24.0*	*44.2*	16.3	*15.0*	31.3	*24.5*
$T_a + 2$	*7.8*	*7.9*	12.5	*42.6*	55.1	*16.3*	16.2	*32.5*	*12.4*
$u \times 4$	19.3	20.8	*5.0*	5.9	10.9	*44.8*	41.3	86.1	*3.0*
$u \times 6$	*29.6*	31.7	*3.3*	*3.8*	7.1	*47.3*	*43.6*	*90.9*	*2.0*
$T_a + 2, u \times 4$	*30.5*	*32.6*	*3.2*	10.8	14.0	41.5	41.4	*82.9*	*3.2*

'As explained in the text, input condition $R_{n,sol,ndj}$ means that the solar radiation is changed with respect to base conditions; $z_{pp} \times 2$ means that the precipitation rates are doubled; $T_a + 2$ means that the air temperatures are increased by 2 degrees Celsius; $u \times 4$ and $u \times 6$ mea" that the wind speeds are multiplied by 4 and 6, respectively; and $T_a + 2, u \times 4$ means that both the air temperatures are increased by 2 degrees Celsius and the wind speeds are multiplied by 4.

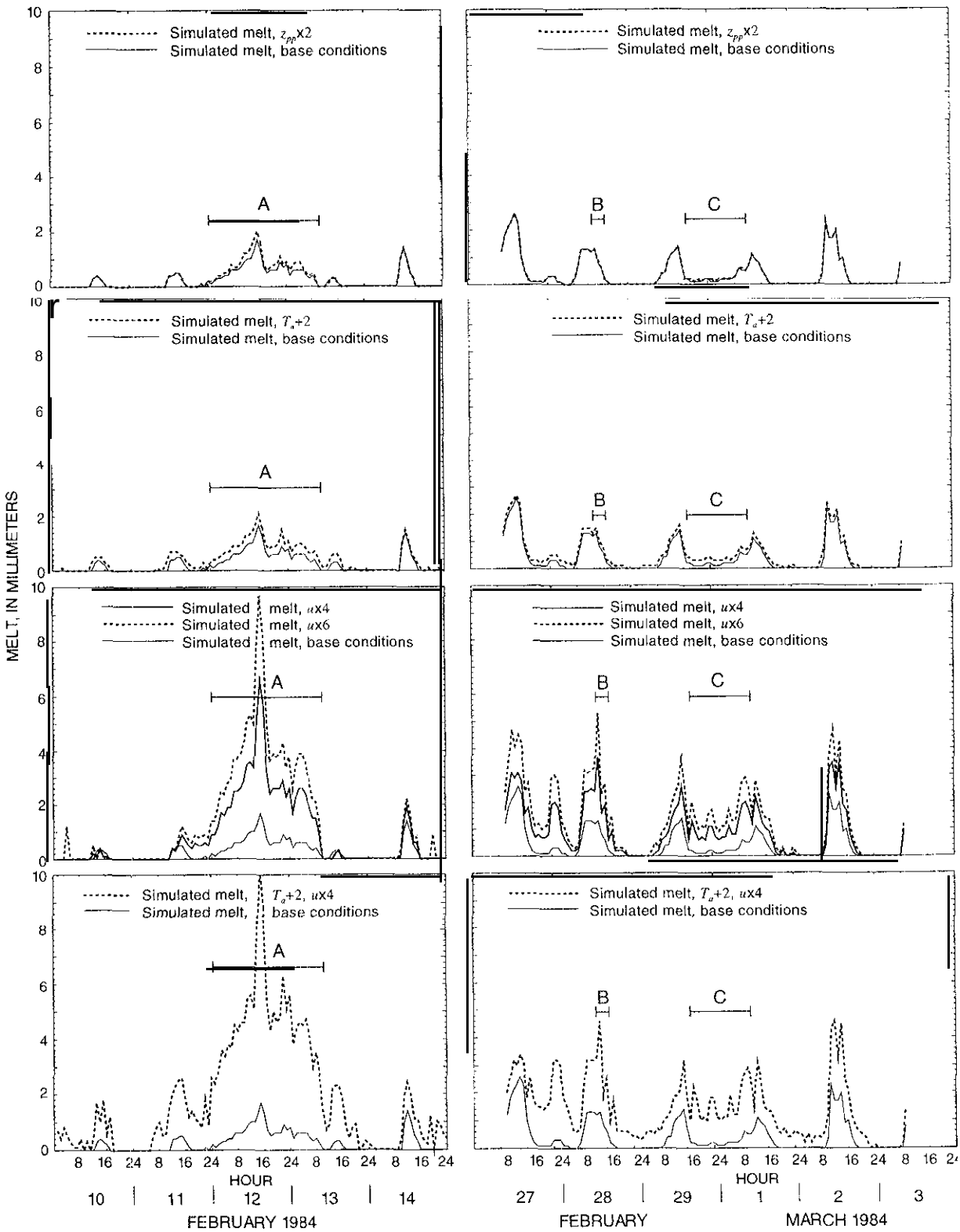

Figure **12.--**Simulated melt for base conditions, increased precipitation (z_{pp}x2), increased air temperature (T_a+2), increased wind speeds (ux4 and ux6), and combined increased air temperatures and wind speeds (T_a+2, ux4). A, B, and C denote rain-on-snow events discussed in the text.

Increased precipitation temperatures significantly enhanced the already significant ability of rainfall to affect snowmelt for event A. For the events with less rain (B and C), the overall effect of advection remained small compared to the sum of net all-wave radiation and turbulent heat exchanges.

Wind Speed

Wind can strongly affect snowmelt processes by regulating the amount of convection over the snow surface and thus the amount of melt occurring from condensation. Wind speeds (adjusted for instrument threshold) were generally low during the simulated rain-on-snow events, averaging from 1.7 to 2.1 m s^{-1}. To determine the effects of wind on melt, wind speeds were multiplied by factors of four and six to evaluate snowmelt processes under moderate and stronger wind conditions. All other variables were kept the same.

Hourly wind speeds multiplied by four ($u \times 4$) resulted in mean wind speeds of 8.4, 7.2, and 6.8 m s^{-1} for events A, B, and C, respectively; hourly wind speeds multiplied by six ($u \times 6$) resulted in mean wind speeds of 12.6, 10.8, and 10.2 m s^{-1}. A four-fold increase in wind speed resulted in an increase in snowmelt of 66.2, 6.1, and 15.1 mm for events A, B, and C, to 87.3, 10.2, and 19.3 mm (2.5, 2.0, and 1.0 mm h^{-1}) (fig. 12 and table 8). This represents an increase of 314, 149, and 360 percent over base conditions for the three events. Enhanced rates of snowmelt were produced by a marked increase in surface convection in which the melt from turbulent heat, $H + L_v E$, increased by 621, 982, and 1,008 percent over base conditions for events A, B, and C. Turbulent heat provided a dominant 88, 66, and X6 percent of the energy input to the snowpack. The sensible heat contributed 64, 62, and 52 percent of the turbulent heat for events A, B, and C. A six-fold increase in wind speeds produced even larger increases in snowmelt over base conditions, resulting in an increase in total melt of 108.5, 10.4, and 25.4 mm for events A, B, and C, to 129.6, 14.5, and 29.6 mm (3.7, 2.9, and 1.6 mm h^{-1}) (fig. 12 and table 8). This represents an increase of 514,254, and 605 percent over base conditions for the three events. The melt contributed by turbulent heat, $H + L_v E$, increased hy 1,018, 1,680, and 1,695 percent for events A, B, and C, respectively. Turbulent heat provided a dominant 92, 76, and 91 percent of the energy input to the snowpack. In response to four- and six-fold increases in wind speed, the amount of condensation onto the snowpack increased by 3.3 and 5.0 mm for event A, by 0.4 and 0.5 mm for event B, and by 0.8 and 1.8 mm for event C over base conditions (table 9). The simulated condensation represents between 3 and 6 percent of the simulated melt.

Table 9.--*Simulated condensation for different model inputs and for different simulation periods*

[N/A; not applicable]

Type of input conditions'	Simulated condensation (millimeter) Event A (35 hours)	Event B (5 hours)	Event C (19 hours)
base	0.1	0.0	0.0
$R_{n,sol,adj}$	0.1	N/A	N/A
$z_{pp} \times 2$	0.1	0.0	0.0
$T_a + 2$	0.2	0.0	0.0
$u \times 4$	3.4	0.4	0.8
$u \times 6$	5.1	0.5	I.8
$T_a + 2, u \times 4$	8.5	0.5	1.7

'As explained in the text, input condition $R_{n,sol,adj}$ means that the solar radiation is changed with respect to base conditions; $z_{pp} \times 2$ means that the precipitation rates are doubled; $T_a + 2$ means that the air temperatures are increased by 2 degrees Celsius; $u \times 4$ and $u \times 6$ mean that the wind speeds are multiplied by 4 and 6, respectively; and $T_a + 2$, $u \times 4$ means that both the air temperatures are increased by 2 degrees Celsius and the wind speeds are multiplied by 4.

Air Temperature and Wind Speed Combined

The combined effects of increased air temperature and wind speed were investigated by simulating the three rain-on-snow events with air temperatures increased by 2°C and wind speeds multiplied by four ($T_a + 2$, $u \times 4$). All other variables were kept the same. This combination resulted in an increase in snowmelt over base conditions of 140.0, 9.2, and 26.3 mm for events A, B, and C, respectively, to 161.1, 13.3, and 30.5 mm (fig. 12 and table 8). This is equivalent to an increase of 664, 224, and 626 percent over bare conditions for events A, B, and C, or an increase of 56, 4, and 11 percent of the total snow-water equivalent assumed at the start of the simulation (which was 250 mm). Melt from turbulent heat, $H + L_v E$, contributed a dominant 88, 70, and 83 percent of the total snowmelt. This represented proportional increases in turbulent-heat induced melt of 1,230, 1,430, and 1,590 percent over base conditions for events A, B, and C. The large response of snowmelt to convection surpassed the increase in snowmelt due to increased net all-wave radiation, R_n, and advective heat, M. Net all-wave radiation accounted for 6, 30, and 14 percent of the total melt under warmer, windier conditions, and advection accounted for 6, 1, and 3 percent of the total snowmelt for events A, B, and C. In response to the combined increase in air temperatures and wind speeds, the amount of condensation onto the snowpack increased by 8.4, 0.5, and 1.7 mm for events A, B, and C over base conditions (table 9). The simulated condensation represents between 4 and 6 percent of the simulated melt.

Discussion of Simulation Results and Sensitivity Analysis

The previous analyses of two 5-day periods of snow accumulation and melt in the H.J. Andrews Experimental Forest demonstrate that Marks' model accurately predicts the timing of snowmelt generation during rain on snow. However, the depth of simulated melt was consistently lower than the depth of observed excess runoff; for the three events, simulated melt ranged from 27 to 75 percent of observed excess runoff. This relatively poor agreement between simulated snowmelt and observed excess runoff was attributed to a lack of reliable data, such as precipitation type, density, and depth, wind speed, incoming thermal radiation, and WAR rather than to shortcomings in Marks' model. Considering the limitations of the available data, the model appeared to perform reasonably well, although the model remains unvalidated for rain-on-snow conditions in a transient-snow zone. In a previous study, Marks' model was shown to perform well when simulating snow accumulation and melt for a deep, cold snow pack in the Sierra Nevada (Marks, 1988; Marks and Dozier, 1992).

The sensitivity of WAR to different climate conditions during rain on snow was evaluated by systematically changing input variables during the two 5-day simulation periods and by computing the resulting changes in simulated snowmelt and energy inputs to the snowpack during three rain-on-snow events. The analysis showed that snowmelt is most sensitive to changes in wind speed and air temperature and less so to changes in depth of precipitation. Wind speed and differences in temperature and specific humidity between the snow surface and the atmosphere determine the degree of turbulent-energy exchange that takes place between the snowpack and the air. During significant rain-on-snow events, turbulent-energy exchange is the dominant energy input to the snowpack responsible for generating melt. Changes in air temperature affect the amount of incoming thermal radiation to the snowpack, which is also an important energy source during rain on snow. Net solar radiation is a minor source of energy during significant rain-on-snow events because extreme cloudiness limits penetration of this radiation. During extreme rain-on-snow conditions (that is, strong winds and high air temperatures), simulations indicated WAR may be greater than precipitation plus snowmelt by up to 6 percent of the snowmelt depth because of condensation of water vapor onto the snowpack.

GENERATION OF LONG-TERM CLIMATE DATA FOR THE WESTERN CASCADE RANGE

To determine the possible range of WAR that may be generated during rain on snow in a typical clearcut forest opening in the transient-snow zone of the western Cascade Range, Marks' model was applied to 24-hour presumed rainstorms extracted from the historical climate data for two NWS stations in Washington. Based on theoretical considerations, WAR is thought to be greater in forest openings than in forest stands; for this reason, the simulated range in WAR for a typical clearcut forest opening can be used for worst-case-scenario planning. The use of Marks' model assumes that the model accurately simulates the magnitude of WAR for the transient-snow zone, even though this could not be validated in this study, as discussed previously. However, because the model is physically based and because it was validated in a study of a deep, cold snowpack in the Sierra Nevada (Marks, 1988; Marks and Dozier, 1992), the assumption was made that it was valid to use the model to simulate possible ranges of WAR in the transient-snow zone of the western Cascade Range.

Data needed for the 24-hour simulations are hourly values of depth of precipitation, air temperature, dewpoint temperature, wind speed, and solar radiation. Such hourly historical meteorological records, however, are available only at First Order NWS stations that are located at altitudes above or below the transient-snow zone in Washington. There are NWS stations located in the transient-snow zone, but they collect only precipitation on an hourly basis (Cooperative Stations). The hourly precipitation time series of two of these in western Washington were corrected and expanded by incorporation of data from other NWS stations in the region. To complete the required data sets at each site, synthetic time series for dewpoint temperature, air temperature, solar radiation, and wind speed were either computed or assumed.

Available Data

Cooperative Stations in the transient-snow zone selected for representative rainstorm analyses are Cedar Lake at an altitude of 476 m--near the bottom of the transient-snow zone--and Snoqualmie Pass at 921 m—near the top of the transient-snow zone (fig. 13). At these sites, hourly depth of precipitation has been recorded since 1953 and 1948, respectively; daily temperature extremes and daily observations of snowpack conditions have been collected from 1931 to the present and from 1931 through 1972, respectively. Of these variables, only the hourly precipitation and daily temperature extremes were used in this study. Snowpack-condition information was not used because it consisted of a daily observation of snow depth only, without a record of the snow density.

To estimate representative rainstorm wind speeds in the western Cascade Range, the hourly historical data sets of two First Order Stations were used. They were Seattle-Tacoma Airport (also referred to as SeaTac), located at an altitude of 122 m, and Stampede Pass, located at 1,207 m (fig. 13). Hourly measurements have been made at these sites since 1948 for variables such as air temperature, dewpoint temperature, depth of precipitation, wind speed, and wind direction; measurement of hourly solar radiation started at SeaTac in December 1951. Cedar Lake and Snoqualmie Pass stations are located roughly along a line between SeaTac and Stampede Pass (fig. 13).

The SeaTac and Stampede Pass data were obtained from the National Climate Data Center in Asheville, North Carolina, and the Cedar Lake, Snoqualmie Pass, and other Cooperative Station network data were obtained on CD-ROM from EarthInfo Inc. The data sets used in this study were based on the period 1948 through 1988 because at the time of this study, this was the period of record compiled by EarthInfo Inc. At all stations, there were periods of time when data were missing and when the sampling interval exceeded one hour.

Generation of Synthetic Data

To create two complete sets of meteorological time series for Cedar Lake and Snoqualmie Pass, hourly air temperature, dewpoint temperature. wind speed, and solar radiation had to be synthesized, and the existing precipitation records had to be corrected and expanded as much as possible. The parts of the record of interest were those hours during which precipitation occurred at either Cedar Lake or Snoqualmie Pass that could have caused melt if snow were on the ground. The majority of rain-on-snow events are known to occur from October through March (the interval defined as winter for the purposes of this study), and, as a result, data for only these months were selected or synthesized from the historical record.

Precipitation

It is common for large data gaps and errors to be present in the historical hourly precipitation record. Reported data may be unrealistic, the sampling interval may have been changed temporarily, and hourly data may be missing entirely for long periods of time, which may or

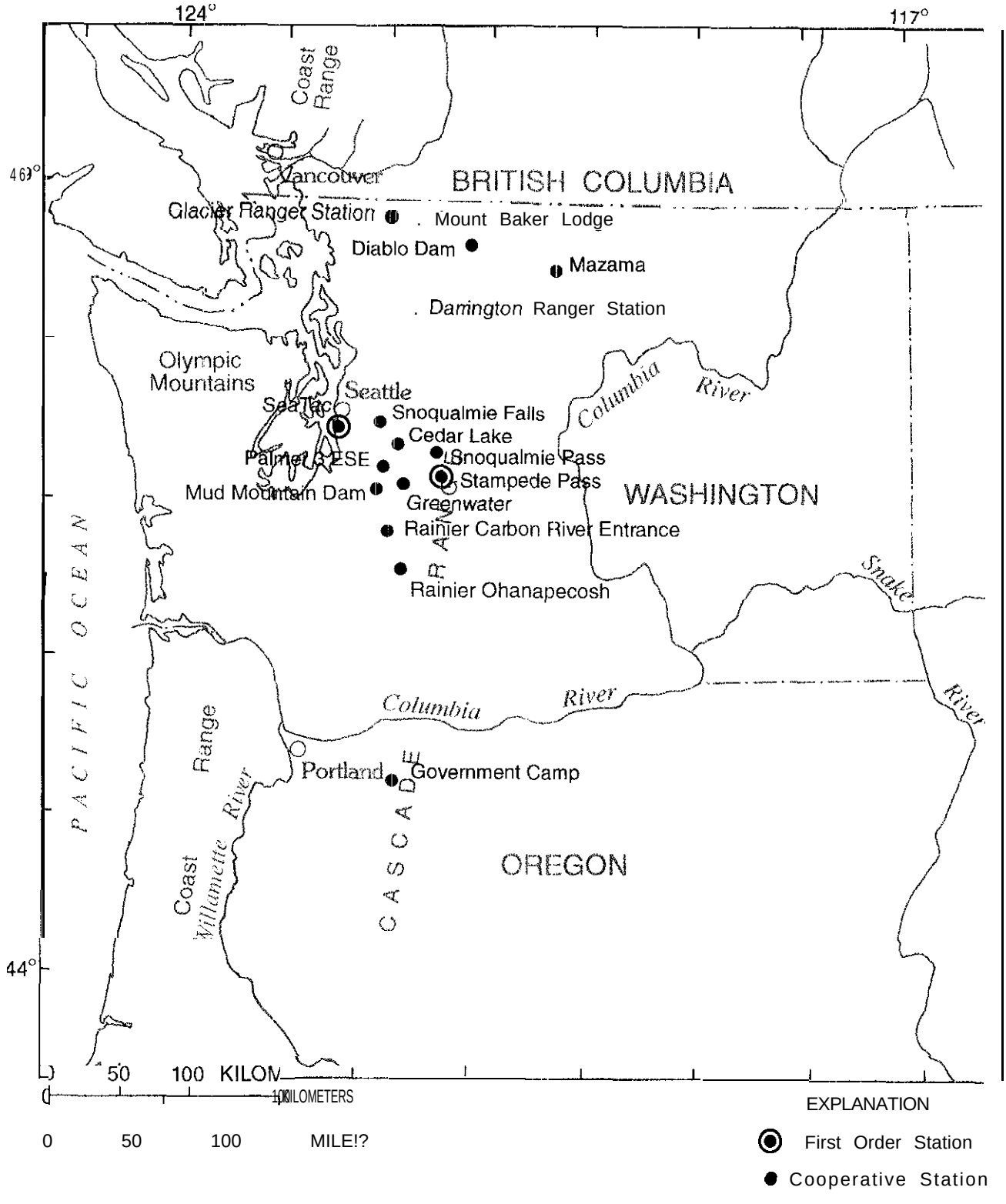

Figure 13.--Locations of National Weather Service stations used to generate synthetic time series for the transient-snow zone.

may not bc followed by a reported cumulative precipitation for the time interval. To create the best and most complete precipitation time series for Cedar Lake and Snoqualmie Pass, error checking was performed to remove unreasonably large values, and missing data were estimated from interpolation among other NWS stations in the region.

Precipitation was considered unreasonably large if the daily total exceeded the 100-year, 24-hour precipitation event at Mount Rainier, the highest point-and the point with the highest precipitation-in the Washington Cascade Range. This value is about 305 mm (Miller and others, 1973). If a daily total exceeded this threshold, the hourly precipitation values reported for that day were assumed to bc missing. Reported hourly precipitation values of zero were thought to be correct part of the time and erroneous at other times. Presumably, these errors were the result of instrument error or catch deficiencies. For the same reasons, reported non-zero values may have been lower than the actual precipitation, although erroneous zero entries were considered to be more likely the result of instrument error. Under-reported precipitation was not corrected, however, because of the difficulty in deciding whether a correction should be applied and how large any correction should be.

The choice of stations used for interpolation of missing hourly precipitation values for Cedar Lake and Snoqualmie Pass was based on correlation coefficients that were computed between the stations to be corrected (the dependent stations, Cedar Lake and Snoqualmie Pass) and other stations in the region (the independent stations). Specifically, correlation coefficients were computed on the basis of hourly precipitation with non-zero values at both stations. (Zero values were excluded from the computations due to the uncertainty of their accuracy.) The entire record was used to compute the correlation coefficients. Stations with the highest correlation coefficients were used to estimate the missing values for Cedar Lake and Snoqualmic Pass except when the stations also had missing values during the same periods; in those cases, stations with progressively lower correlation coefficients were used to estimate the missing values (table 10). Missing data not followed by a cumulative precipitation were not interpolated for more than one week, and missing data that were followed by a cumulative precipitation were not interpolated for more than two weeks.

Interpolation was accomplished by determining the ratio hetwecn the total precipitation of the dependent and independent stations for the entire historical record. During the times that data were missing at the dependent station, reported values at the independent stations were multiplied by these ratios to obtain estimates for the missing values. If a cumulative precipitation was reported at the dependent station, a second correction was applied to the interpolated interval to assure that the estimated total matched the reported total. This sequence of steps was repeated for each of the stations (listed in table 10) until the one-week and two-week interpolation limits were met or until no stations were left for interpolation. Once these precipitation corrections were applied, a possible record of 36 winters for Cedar Lake (1953-88) turned into a record of 30.9 usable winters, and a possible record of 41 winters for Snoqualmie Pass (1948-B) turned into a record of 34.1 usable winters. The precipitation corrections extended the record of usable data by 2.0 percent for Cedar Lake and by 2.3 percent for Snoqualmic Pass.

The only part of the precipitation record that was of interest comprised those hours in which precipitation occurred in the form of rain during the winter. Reported precipitation at Cedar Lake and Snoqualmie Pass, however, was not differentiated between ice, snow, rain, or a mixture of the three. To attempt to differentiate between rain and non-rain precipitation events, it was assumed that all precipitation that occurred when air temperatures were at or above freezing consisted of rain.

Air Temperature

Hourly air temperatures at Cedar Lake and Snoqualmie Pass were estimated from measured daily minimum and maximum air temperatures by fitting a diurnal temperature signal to the data. As with precipitation measurements, daily temperature extreme measurements were also missing for periods of time. To create the best and most complete daily temperature-extreme time series, missing data were obtained from interpolation among NWS stations in the region.

As with the interpolation of the precipitation, the choice of stations used for interpolation of temperature extremes was also based on correlation coefficients that were computed between the stations to be corrected (Cedar Lake and Snoqualmie Pass) and other stations in the region. Specifically, correlation coefficients were computed on the basis of daily minimum or maximum temperatures when those values were recorded at both stations. The entire record was used to compute the correlation coefficients, and missing data were interpolated using stations with progressively lower correlation coefficients (table I I). For Cedar Lake, all missing daily minimum and maximum temperatures could he estimated from one

Table 10.--*National Weather Service stations used to interpolate hourly precipitation data at Cedar Lake and Snoqualmie Pass*

Data type to be interpolated	Correlated station	Station ID	Correlation coefficient	Altitude of correlated station (meter above sea level)
		Cedar Lake		
Hourly precipitation	Palmer 3 ESE	6295	0.886	280
	Snoqualmie Falls	7773	0.790	134
	Snoqualmie Pass	77x I	0.777	921
	Mud Mountain Dam	5704	0.712	399
	Rainier Carbon River Entrance	6892	0.703	530
	Stampede Pass	8009	0.69 I	1,207
	Darrington Ranger station	lYY2	0.665	168
	Greenwater	3357	0.658	527
	Rainier Ohanapecosh	6896	0.655	594
		Snoqualmie s		
Hourly precipitation	Stampede Pass	8009	0.835	I,207
	Rainier Ohanapecosh	6896	0.787	594
	Cedar Lake	1233	0.777	476
	Diablo Dam	2157	0.740	271
	Palmer 3 ESE	6295	0.717	280
	Snoqualmie Falls	7773	0.714	134
	Darrington Ranger Station	1992	0.699	168
	Greenwater	3357	0.692	527
	Rainier Carbon River Entrance	6892	0.667	530
	Glacier Ranger Station	3160	0.662	287
	Mud Mountain Dam	5704	0.598	399
	Mazama	5133	0.53 I	661
	Government Camp	3402	0.527	1,213
	Mount Baker Lodge	5663	0.514	1,265

Table 11.--*National Weather Service stations used to interpolate daily air temperature data at Cedar Lake and Snoqualmie Pass*

Data type to he interpolated	Correlated station	Station ID	Correlation coefficient	Altitude of correlated station (meter above sea level)
		Cedar Lake		
Daily minimum air temperature	Palmer 3 ESE	6295	0.964	2x0
Daily maximum air temperature	Palmer 3 ESE	6295	0.982	2x0
		Snoqualmie Pass		
Daily minimum air temperature	Diablo Dam	2157	0.929	271
	Palmer 3 ESE	6295	0.928	280
Daily maximum air temperature	Stampede Pass	8009	0.95 1	1,207
	Greenwater	3357	0.950	527

independent station (Palmer 3 ESE). The maximum length of time that was interpolated was six months (October 1951 through March 1952 for Snoqualmie Pass).

Interpolation was accomplished by determining an average monthly temperature difference between the daily minima or maxima of the dependent and independent stations. During the times that data were missing at the dependent station, the applicable differences were added to reported values at the independent station to obtain estimates for the missing values. This sequence of steps was repeated for each of the stations (listed in table 11) until all missing data had been estimated. Less than 1 percent of the Cedar Lake temperature extremes had to be estimated to obtain a complete record of 41 winters (1948.88); 18.5 percent of the Snoqualmie Pass temperature extremes had to be estimated to obtain a complete record of 25 winters (1948-72). No extreme temperature measurements were available for Snoqualmie Pass after 1972, and the period from 1973 through 1988 was considered too long to estimate by interpolation.

The corrected daily air temperature record was used to generate hourly air temperatures by fitting a diurnal curve to the data, according to the method proposed by Ca'Zorzi and Dalla Fontana (1986). This method requires that the times of day that the minimum and maximum air temperatures occur be specified. These times are not known for Cedar Lake and Snoquahnie Pass, but they are known for SeaTac and Stampede Pass. The median time at which daily minimum temperatures occurred was 6 a.m. at both SeaTac and Stampede Pass, and the median time at which the daily maximum temperatures occurred was 2 p.m. at SeaTac, and 1 p.m. at Stampede Pass. Based on the observations from SeaTac and Stampede Pass, 6 a.m. and 2 p.m. were selected as the respective times of daily minimum and maximum air temperatures to interpolate the air temperature records at Cedar Lake and Snoqualmie Pass.

The assumption of a diurnal temperature signal with minimum and maximum air temperatures during the early morning and early afternoon, respectively, does introduce some error because it is possible during rain-on-snow events for maximum temperatures to occur at night instead of during the day. This is because a warm, winter storm can move in any time during a 24-hour period. However, minimum air temperatures during synthetic 24-hour storms simulated as part of this study were at or above freezing (as described later in the report), and therefore an erroneous diurnal signal would not change the simulated precipitation type. In addition, because it was assumed that wind speeds were constant during the synthetic 24-hour storms, the 24-hour total turbulent sensible heat exchange between the air and the snowpack was independent of the shape of the diurnal air temperature signal.

Dewpoint Temperature

Hourly dewpoint temperatures at Cedar Lake and Snoqualmie Pass were assumed constant throughout the day and equal to the minimum air temperature observed that day, This assumption assured that the dewpoint temperature did not exceed the air temperature during any hour of the day. The assumption is commonly made when hourly dewpoint measurements are unavailable (for example, Wigmosta and others, 1994). For the NWS data, the assumption effectively meant that the 24-hour average relative humidity ranged from 72 to 94 percent at Cedar Lake and from 69 to 97 percent at Snoqualmie Pass. The average relative humidity of all 24-hour events was 83 percent.

Wind Speed

An attempt was made to estimate hourly wind speed at Cedar Lake and Snoqualmie Pass based on a wind speed correlation between SeaTac and Stampede Pass. This correlation, however, was poor, even if wind speed was grouped by wind direction and only those hours during which precipitation occurred were considered. The wind-direction analysis did show that when precipitation occurred at Cedar Lake or Snoqualmie Pass, wind came chiefly from a southwesterly direction at both SeaTac and Stampede Pass. The only other significant wind direction was from an east-southeasterly direction at Stampede Pass. For calculation of snowmelt during rain on snow, however, it is not the wind direction, but speed that is significant. Because no hourly wind-speed time series could be generated for Cedar Lake and Snoqualmie Pass by interpolation, it was decided to analyze the wind-speed distribution at SeaTac and Stampede Pass to determine the range of wind speeds that could be expected in the western Cascade Range.

The frequency distributions of the average hourly October-through-March wind speed at SeaTac and Stampede Pass from 1945 through 1988 were analyzed. Observed wind speeds ranged up to 24.7 $m\,s^{-1}$ at SeaTac, and up to 47.3 $m\,s^{-1}$ at Stampede Pass. The two largest reported wind speed values at Stampede Pass (one occurrence each of an hourly average of 47.3 and 37.6 $m\,s^{-1}$) were removed from the time series because they were considered unrealistic. Without those two extremes, the Stampede Pass maximum wind speed was 25.2 $m\,s^{-1}$. Wind speeds that were equalled or exceeded 90, 50, and

10 percent of the time were 1.5, 3.6, and '7.7 $m\ s^{-1}$, respectively, at SeaTac (fig. 14), and 1.5, 4.6, and X.7 $m\ s^{-1}$ at Stampede Pass (fig. 15). Based on these frequencies of occurrence, average hourly wind speeds selected as representative for low, medium, and high wind conditions for the western Cascade Range were 1.5, 4.1, and 8.2 $m\ s^{-1}$, respectively.

Solar Radiation

Hourly solar-radiation data were available only at SeaTac, starting in December 1951. Cloud conditions at SeaTac could be significantly different from those at Cedar Lake and Snoqualmie Pass, however, so an estimate of solar radiation was made for those stations without consideration of the SeaTac record. Instead, observed hourly solar radiation measured at the H.J. Andrews Experimental Forest during the 19X3-84 winter was used to estimate solar radiation at Cedar Lake and Snoqualmie Pass.

Because of cloud cover, solar radiation during rainstorms is greatly reduced over clear-sky conditions. In addition, most incoming solar radiation is not absorbed by the snowpack, but instead reflects back into the atmosphere. As a result, solar radiation is a relatively minor source of energy during significant rain-on-snow events. For this reason, it was sufficient to estimate a representative solar radiation trace throughout the day to approximate conditions during precipitation events at Cedar Lake and Snoqualmie Pass. Based on measurements of solar radiation at H.J. Andrews Experimental Forest, a net solar-radiation maximum of 50 $W\ m^{-2}$ at solar noon during a rain-on-snow event was a somewhat high, but realistic estimate. When it was assumed that the sun rose at 6 a.m. and set at 6 p.m. (sunrise and sunset times on March 21 for a horizontal plane at 47.4 degrees North, the latitude of Cedar Lake and Snoqualmie Pass) and that the trace followed half of a sine curve, the average daily value of estimated net solar radiation (17.2 $W\ m^{-2}$) was high for many days during the winter, when in fact days are shorter (by up to four hours). This high estimate of energy from net solar radiation, however, assured that the simulated runoff for 24-hour presumed rain-on-snow events was not underestimated. Underestimation of runoff during the events could result in improper planning for runoff conditions that could occur in the western Cascade Range.

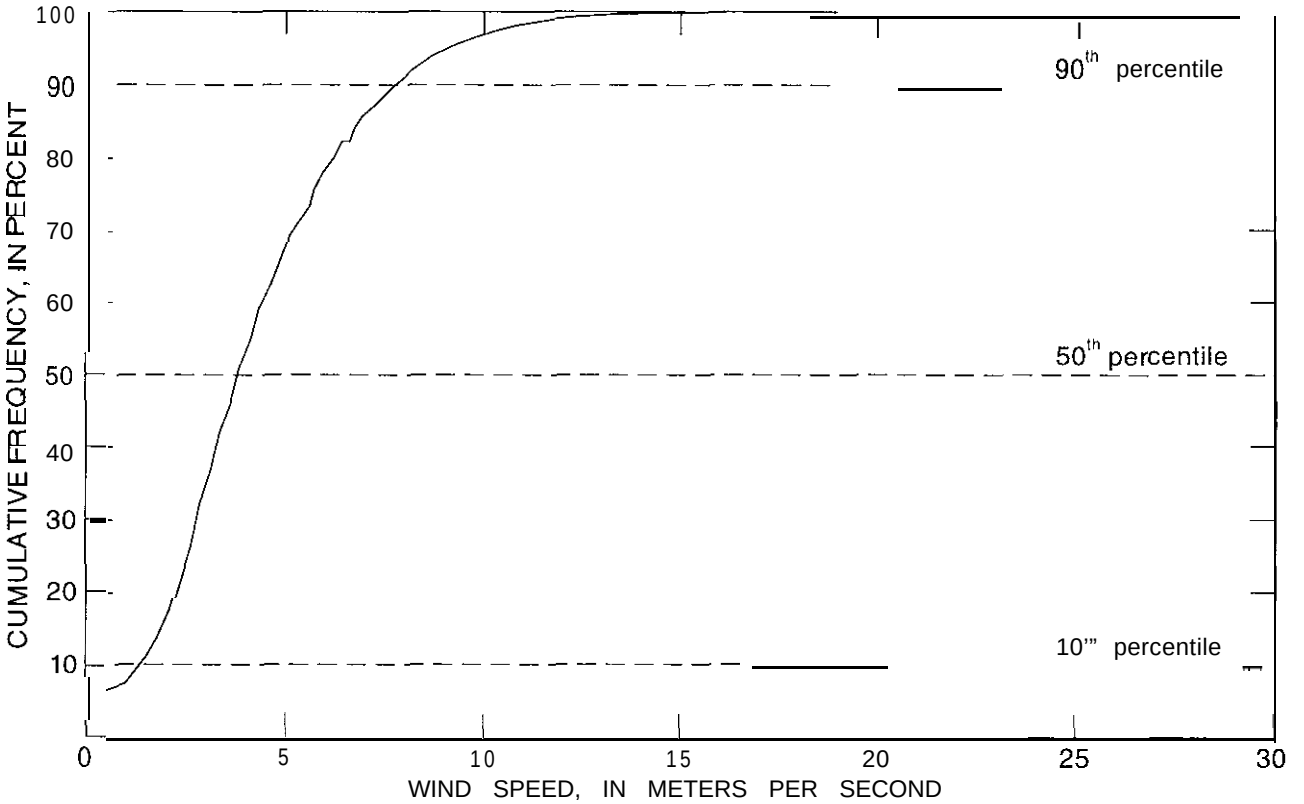

Figure 14.--Cumulative frequency of hourly SeaTac wind speeds

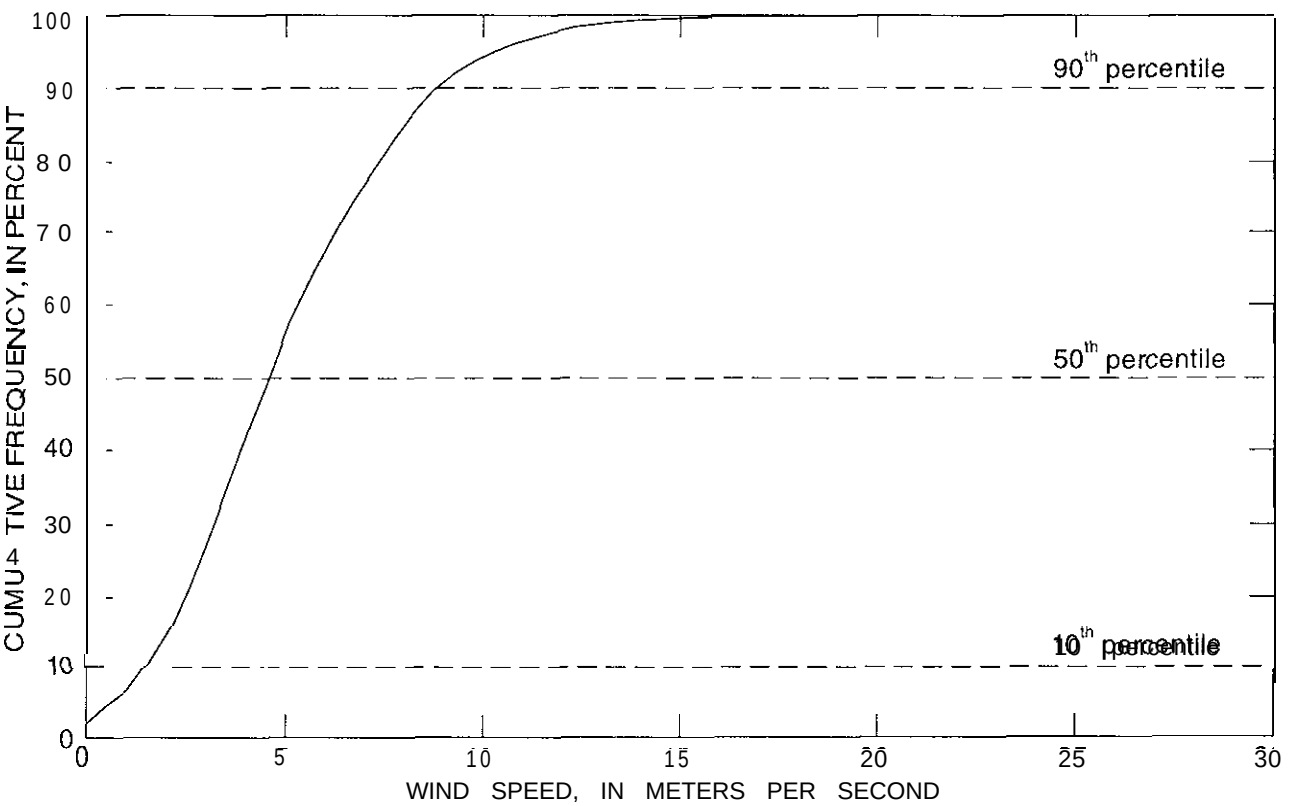

Figure 15.--Cumulative frequency of hourly Stampede Pass wind speeds.

SIMULATION OF SNOWMELT DURING SYNTHETIC RAINSTORMS

'To plan appropriately for potential flooding conditions that could occur during rain on snow, it is important to know what range of rainstorms can he expected during the winter in the western Cascade Range and, when storms occur while snow is on the ground, how much snowmelt can he generated. To answer these questions, the synthetic, long-term climate records at Cedar Lake and Snoqualmie Pass were analyzed to extract 24-hour periods of significant, presumed rainstorms. The amount of snowmelt that would occur in a forest opening if snow were on the ground during each of those 24-hour periods was computed using Marks' snow accumulation and melt model (1988). Worst-case conditions were modeled by assuming that a thick, ripe snowpack was on the ground at the beginning of each 24-hour period.

Synthetic Western Cascade Range Rainstorm Conditions

Presumed rain events that exceeded 75 nun of precipitation during 24 hours were extracted from the synthetic climate records at Ceder Lake and Snoqualmie Pass. This was accomplished by moving a 24-hour window through the time series, one hour at a time, during which the total precipitation was computed. A rain event was assumed to have occurred if the total 24.hour precipitation exceeded 75 mm and if the average air temperature during the event equalled or exceeded 0°C. It was assumed that a rain event had ended when the total 24-hour precipitation of the moving window dropped below 75 mm or when the average 24-hour air temperature dropped to or below freezing. For each event that lasted longer than 24 hours, only the 24-hour period with the highest precipitation was selected. If more than one 24-hour period occurred with the same high precipitation, the 24-hour period with the highest 24-hour average air temperature was selected. Once the 24-hour precipitation maximum had been selected in an cvcnt, the moving window was moved forward by 24 hours to avoid the selection of overlapping, 24-hour precipitation maxima.

An event threshold of 75 mm precipitation per 24 hours was chosen because it represents a medium-sized storm that may generate flooding, depending on the watershed conditions. According to Miller and others (1973), the 75 mm, 24-hour rain storm at the foot of the western Cascade Range has a recurrence interval of five years; this interval decreases at higher altitudes.

Applying these criteria to the synthetic records of Cedar Lake and Snoqualmie Pass resulted in the extraction of 57 qualifying events for Cedar Lake and 19 for Snoqualmie Pass. Even though only the average air temperature of each event had to equal or exceed 0°C, this threshold was met for each hour of the extracted events. The total record during which hourly precipitation, dewpoint temperature, and air temperature were all available was 30.9 winters for Cedar Lake and 20.6 winters for Snoqualmie Pass. Thus, on average, I .8 presumed rainstorms of 24 hours or longer per winter were extracted from the synthetic Cedar Lake record and 0.9 from the Snoqualmie Pass record. It was assumed that these storms were representative of the entire population of rainstorms that may have occurred at Cedar Lake and Snoqualmie Pass and that would have been identified if no data had been missing.

For each simulated event, the 24-hour-average assumed net solar radiation was 17.2 W m^{-2}. Ranges in 24-hour averages for the remainder of the input variables other than wind speed were 0.9 to 11.7°C and 2. I to 7.2°C for air temperature, 0 to 10.0°C and 0 to 6.1°C for dewpoint temperature, and 3.1 to 5.4 mm h^{-1} and 3.2 to 8.2 mm h^{-1} for precipitation at Cedar Lake and Snoqualmie Pass, respectively. Median values of 24-hour averages of the input variables at Cedar Lake and Snoqualmie Pass are 4.8 and 4.2°C for air temperature, I .7 and 1.1°C for dewpoint temperature, and 3.5 and 3.X mm h^{-1} for precipitation. The distribution of average event air temperatures is close to normal, hut the distributions of the average event precipitation and dewpoint temperature are skewed (fig. 16).

Simulation Results

Each synthetic 24-hour storm was simulated using the snow accumulation and melt model for a low, medium, and high constant wind speed Input for each simulation consisted of hourly precipitation, air temperature, vapor pressure (computed from dewpoint and air temperature), solar radiation, and an assumed wind speed. The low, medium, and high wind speeds selected (I .5, 4.1, and 8.2 m s^{-1}) were based on the distribution of observed wind speeds at SeaTac and Stampede Pass. An identical, thick, 0.25 m snow-water-equivalent, ripe snowpack was assumed at the start ofcach simulation. Table 3 lists the specific conditions assumed at the start of each 24-hour simulation and the values for parameters kept constant during the simulation, such as the roughness length and the maximum water saturation of the snowpack. All valucs are identical to those used for the two 5-day period simulations for the H.J. Andrew Experimental Forest.

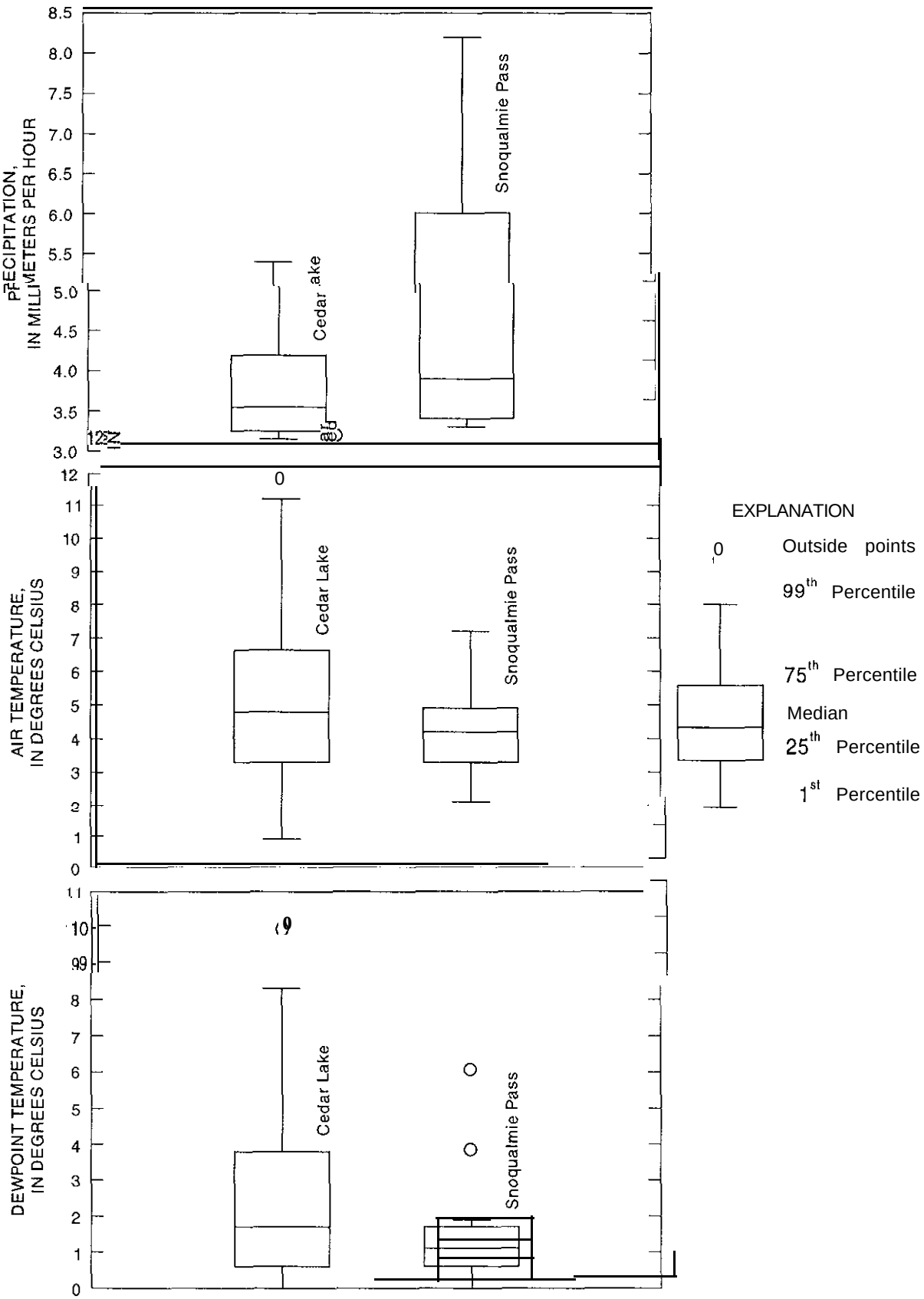

Figure 16.--Average precipitation, air temperature, and dewpoint temperature for 24-hour, presumed rain events at Cedar Lake and Snoqualmie Pass.

The thermal radiation for the hypothetical 24-hour rain events at Cedar Lake and Snoqualmie Pass was computed assuming the same clearcut forest-opening conditions used for the H.J. Andrews Experimental Forest (equations 17 and 18).

Both snowmelt and excess runoff (previously defined as WAR minus precipitation) were simulated for the synthetic rain-on-snow events and compared. with the total rainfall during each event. As discussed previously, simulated melt plus precipitation represents WAR without consideration of condensate as a source of water (sensitivity analyses showed condensation could increase WAR by up to 6 percent of the simulated melt depth during extreme rain-on-snow conditions) and without consideration of changes in liquid-water storage in the snowpack. Simulated excess runoff includes condensate, but it does not include liquid water that was retained by the snowpack to bring it to saturation after the initiation of snowmelt. Estimates of WAR based on both simulated melt and excess runoff are considered, however, because the estimate based on simulated melt represents close to worst-case WAR conditions and the estimate based on simulated excess runoff represents, in effect, WAR for unsaturated initial snowpack conditions.

Simulated WAR for 24-hour rain-on-snow events at Cedar Lake and Snoqualmie Pass was always greater than precipitation alone for all simulated wind speeds if WAR was based on simulated melt (fig. 17 and 18), and it was usually greater if the simulated WAR was based on simulated excess runoff (fig. 19 and 20). WAR based on simulated excess runoff was smaller than precipitation for 26, 11, and 5 percent of the events at Cedar Lake for low-, medium-, and high-wind conditions, respectively, and for 42, 11, and 0 percent of the events at Snoqualmie Pass. When WAR based on simulated excess runoff is smaller than precipitation, excess runoff is negative and part of the precipitation increases the liquid-water content of the snowpack.

At Cedar Lake, a maximum simulated melt plus precipitation of 291.9 mm occurred once assuming a high wind speed of 8.2 $m\ s^{-1}$ (fig. 17). For this particular event, precipitation represented 40 percent of the simulated WAR. The simulated melt plus precipitation for this event assuming a low or medium wind speed was 166.1 and 197.3 mm, respectively. At Snoqualmie Pass, a maximum simulated melt plus precipitation of 253.8 mm occurred once assuming a high wind speed of 8.2 $m\ s^{-1}$ (fig. 18). For this particular event, precipitation represented 78 percent of the simulated WAR. The simulated melt plus precipitation for this event assuming a low or medium wind speed was 218.5 and 230.8 mm, respectively. In general, the increase in WAR over precipitation was largest for high-wind events (fig. 17, 18, 19 and 20).

Comparison of simulated melt and excess runoff shows that melt almost always exceeds excess runoff (fig. 21.22, 23 and 24). This difference decreases for higher wind conditions and at times reverses its sign when excess runoff exceeds melt. If if had been assumed that the snowpack had a higher initial liquid-water content, excess runoff would have been larger and the differences between the two variables would have been smaller. The median value of simulated melt at Cedar Lake ranges from 16.2 mm in 24 hours for low winds to 54.7 mm in 24 hours for high winds. Similarly, the median value at Snoqualmie Pass ranges from 13.9 mm in 24 hours to 44.5 mm in 24 hours (table 12). The median values of simulated excess runoff are consistently lower than simulated melt, by 15 to 64 percent at Cedar Lake and by 24 to 81 percent at Snoqualmie Pass.

Simulated melt ranges from a minimum of 4 to a maximum of 197 percent of precipitation at Cedar Lake; the range is 6 to 117 percent of precipitation at Snoqualmie Pass. Median simulated melt ranges from 18 to 62 percent of precipitation at Cedar Lake and from 12 to 38 percent of precipitation at Snoqualmie Pass (table 12). These results indicate that if a sufficiently thick snowpack is present on the ground during a large rain-on-snow event, melt in forest openings in the transient-snow zone of the western Cascade Range can be almost twice the precipitation alone.

Discussion of Simulation Results

The snowmelt and excess runoff simulated for 24-hour rainstorms, taken from the synthetic records of Cedar Lake and Snoqualmie Pass, give a qualitative indication of the amount of WAR that can be generated in a typical clearcut forest opening during rain on snow in the western Cascade Range if the amount of snow on the ground is not limiting. The assumption of an unlimited amount of snow on the ground may not he realistic, but it does provide for worst-case estimates of WAR. The more extreme the warming conditions during a rain-on-snow event, the higher the altitude will be at which melting occurs. At higher altitudes snowpacks are thicker and they arc less likely to limit the amount of snowmelt that can occur during rain on snow.

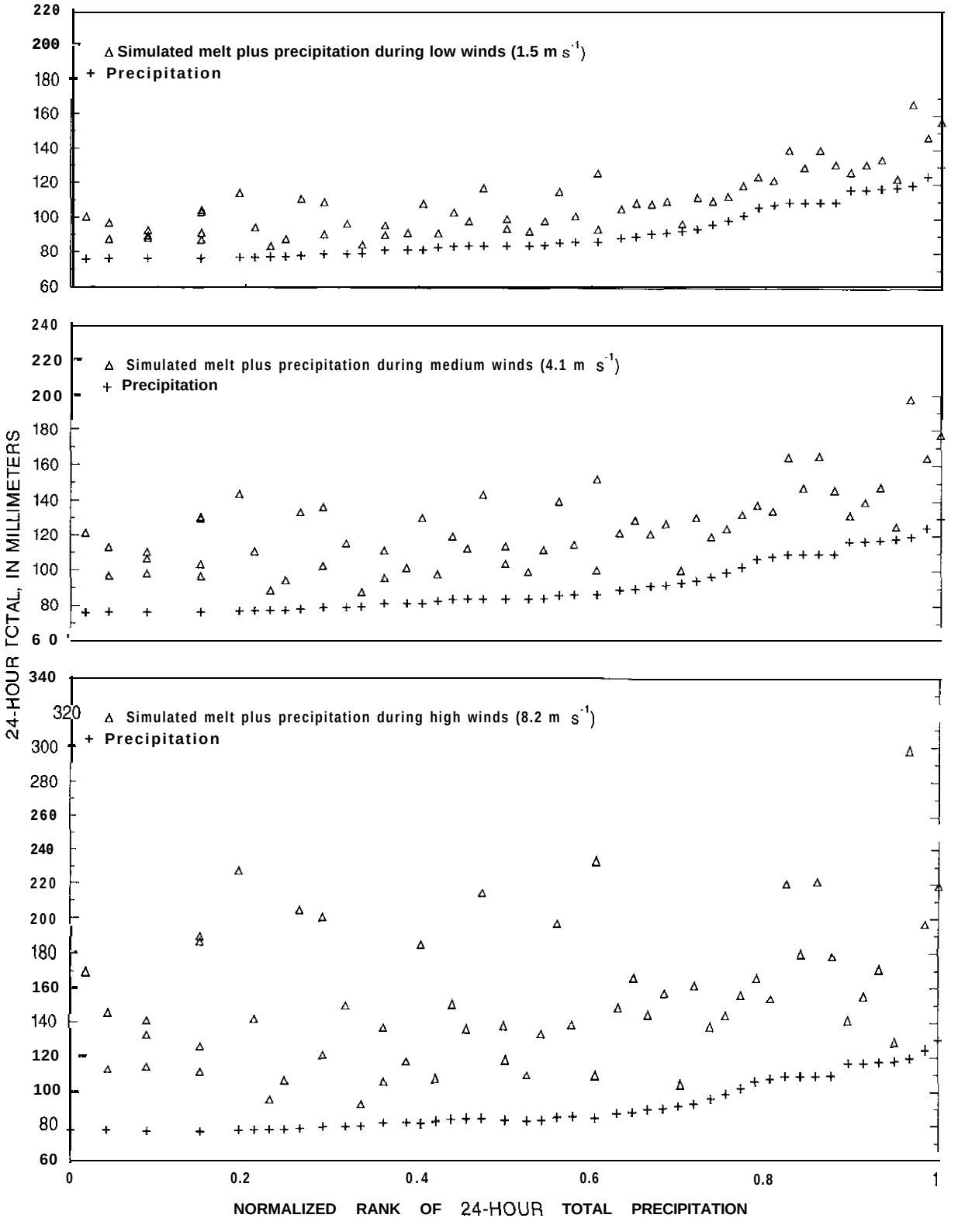

Figure 17.--Cedar Lake, ranked 24-hour total precipitation and simulated melt plus precipitation during each 24-hour event for low-, medium-, and high-wind conditions. Different simulated melt plus precipitation values may occur for events of identical size (and normalized rank) if the air or dewpoint temperatures differ among those events.

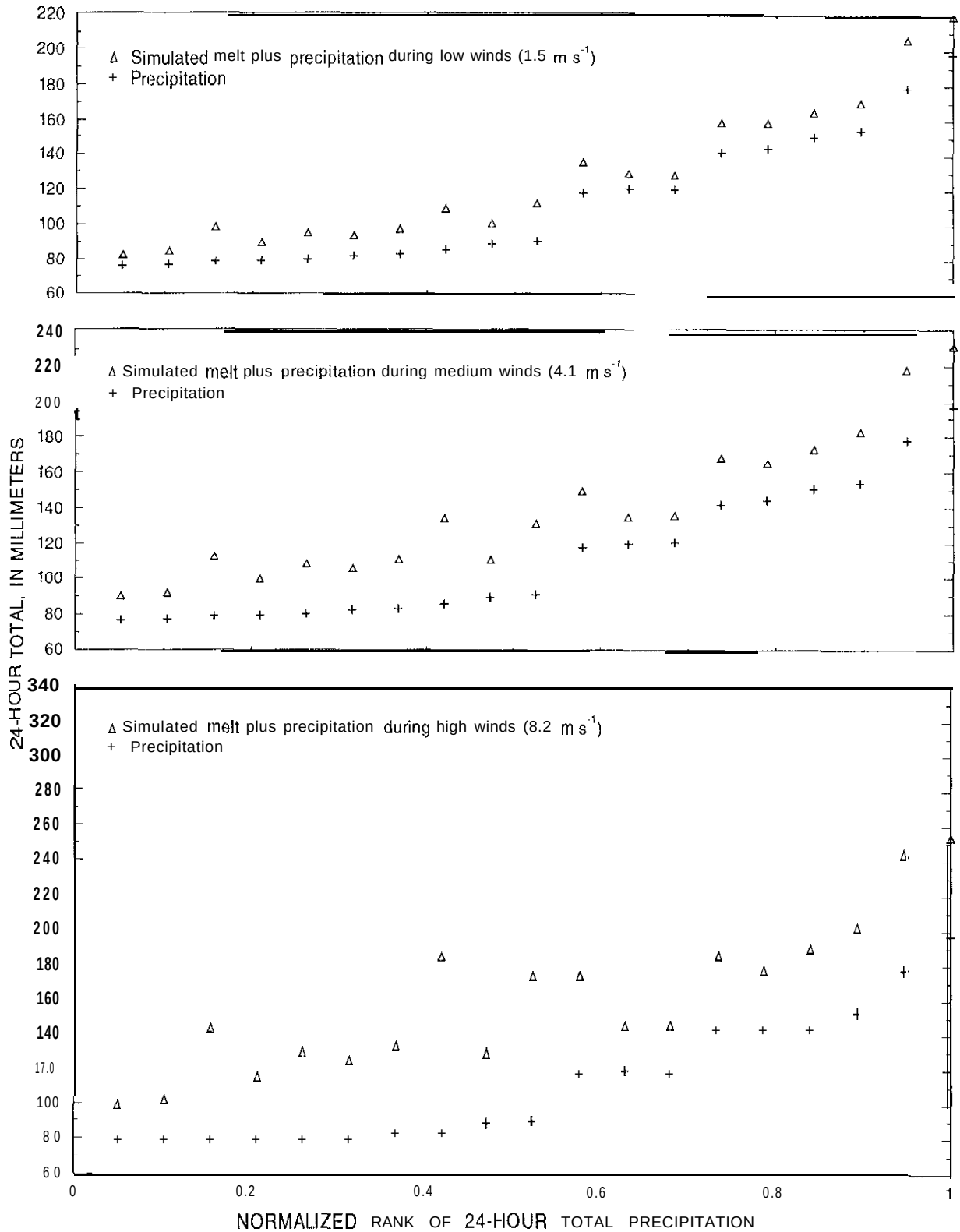

Figure 18.--Snoqualmie Pass, **ranked** 24-hour **total precipitation and simulated melt plus precipitation during each** 24-hour **event for low-, medium-, and high-wind conditions.**

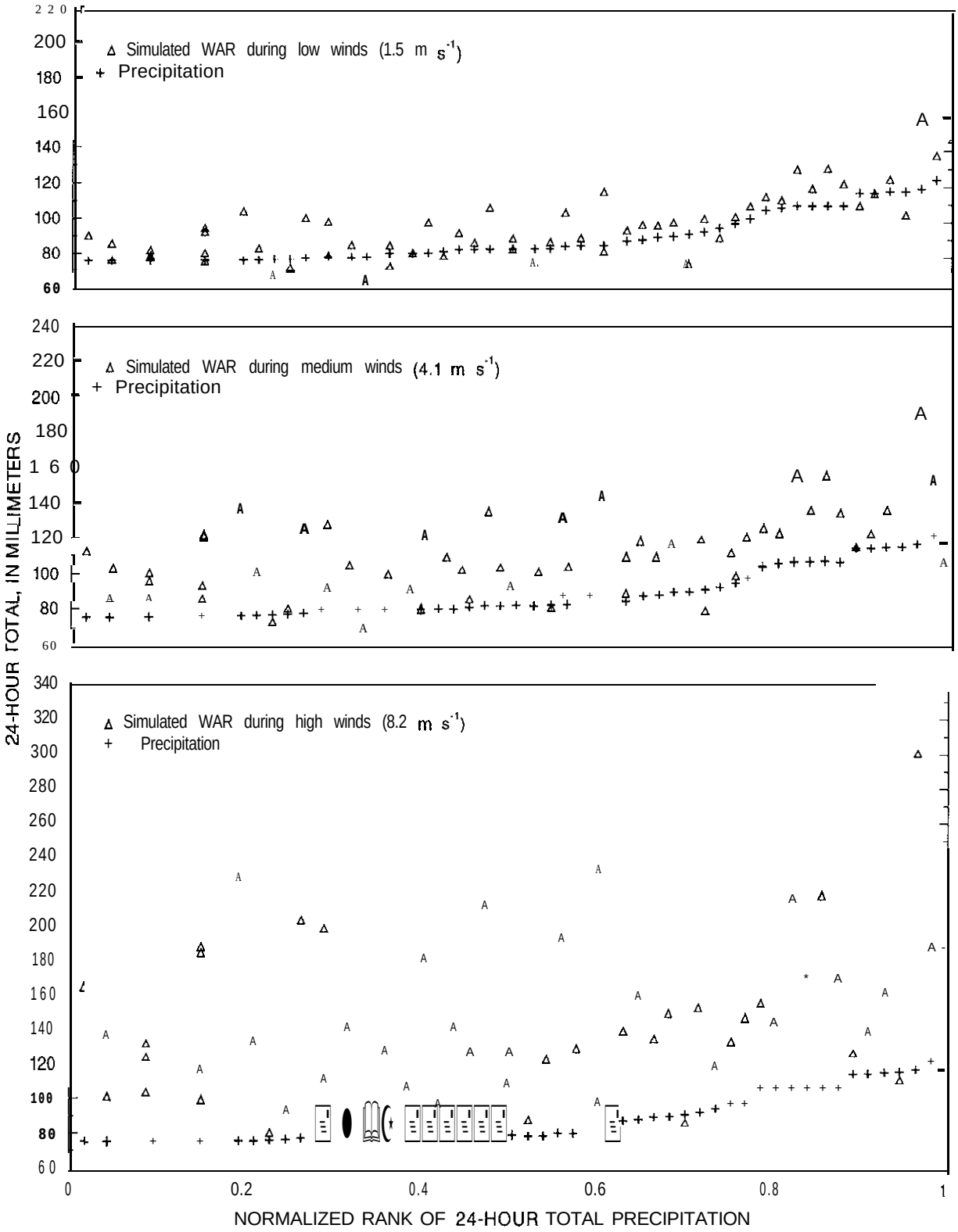

Figure 19.--Cedar Lake, ranked 24-hour total precipitation and simulated water available for runoff (WAR) during each 24-hour event for low-, medium-, and high-wind conditions. Different simulated water available for runoff values may occur for events of identical size (and normalized rank) if the air or dewpoint temperatures differ among those events.

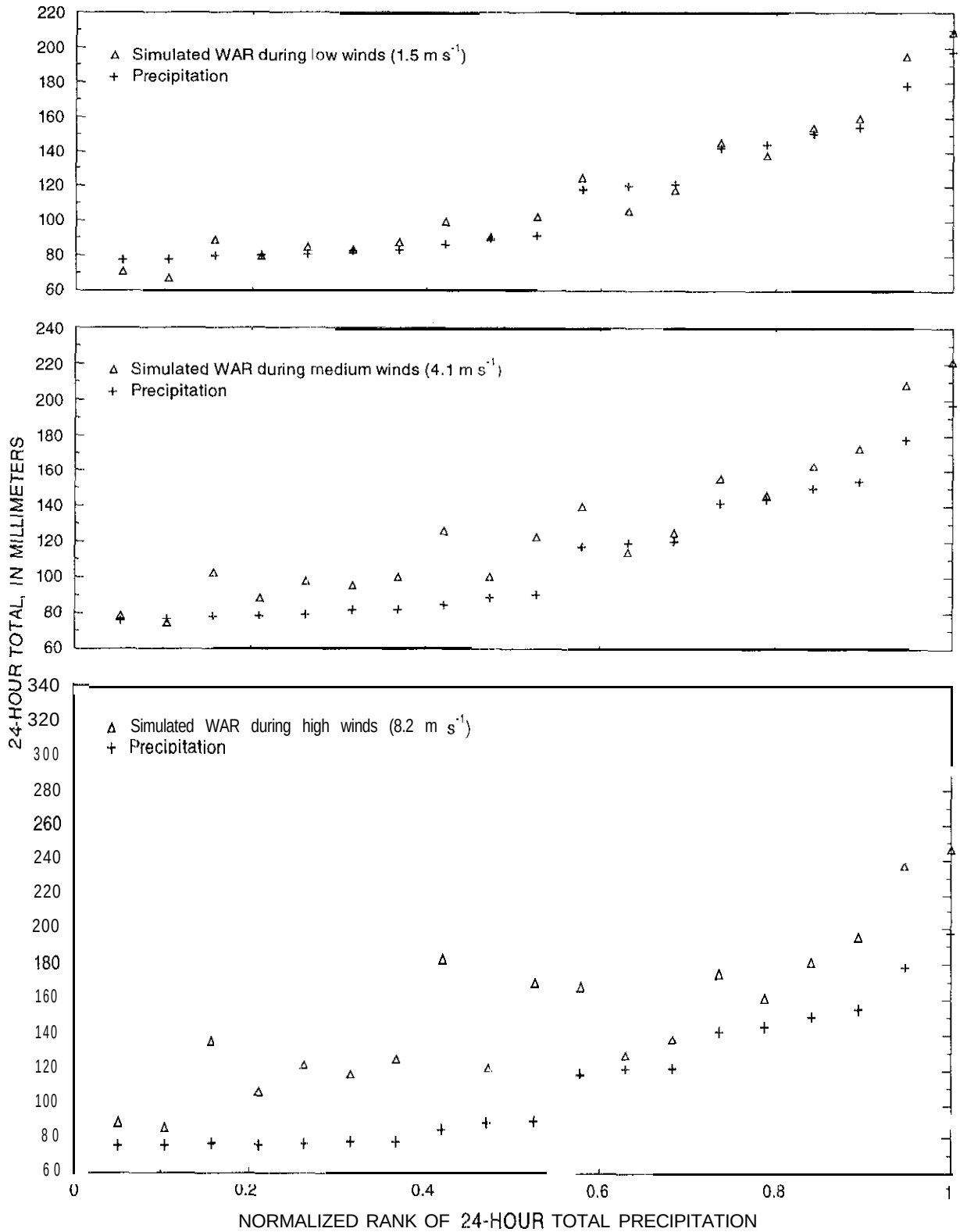

Figure 20.--Snoqualmie Pass, ranked 24-hour total precipitation and simulated water available for runoff (WAR) during each 24-hour event for low-, medium-, and high-wind conditions.

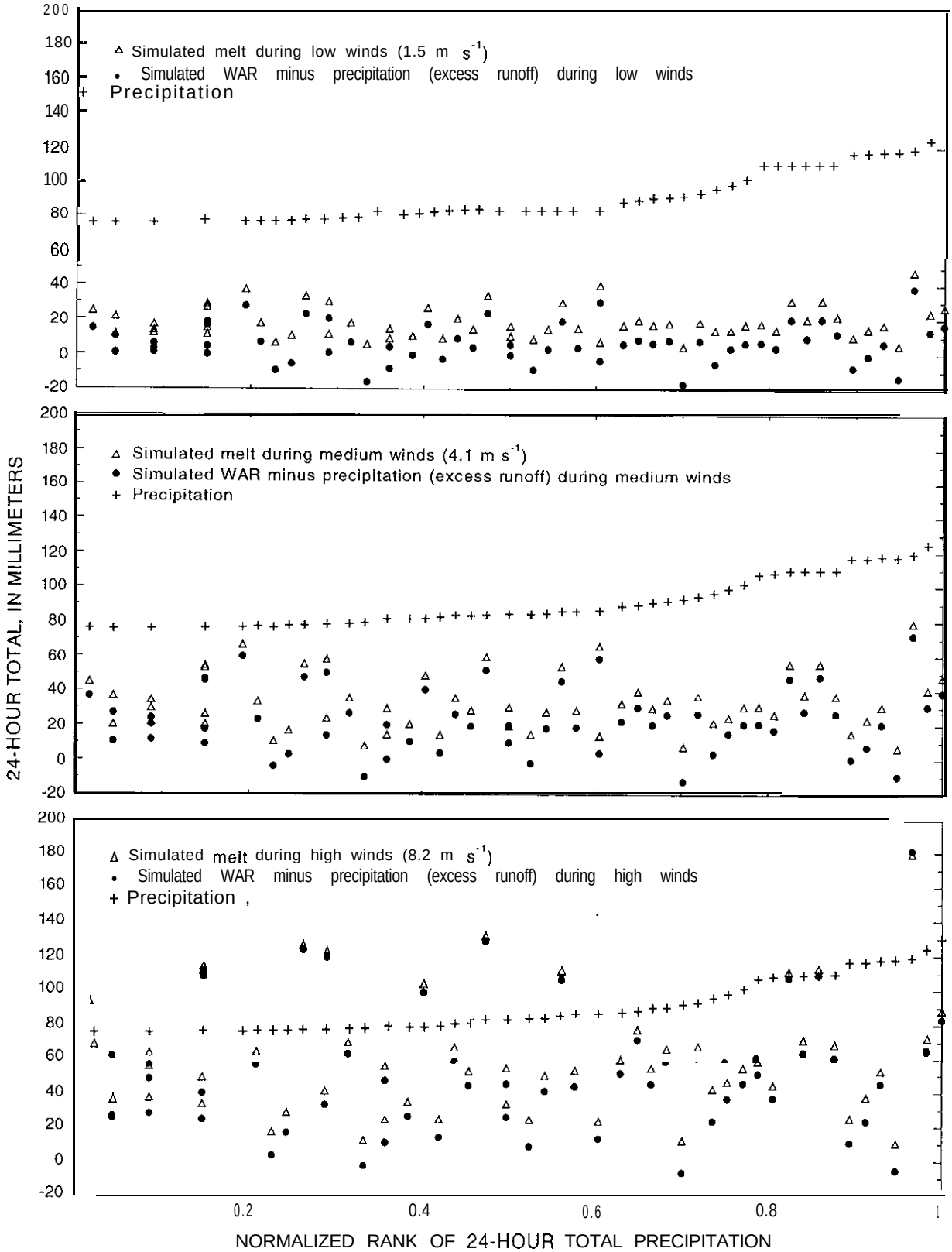

Figure 21.--Cedar Lake, ranked 24-hour total precipitation, simulated melt, and simulated water available for runoff (WAR) minus precipitation (excess runoff) during each 24-hour event for low-, medium-, and high-wind conditions. Different simulated melt and simulated runoff minus precipitation values may occur for events of identical size (and normalized rank) if the air or dewpoint temperatures differ among those events.

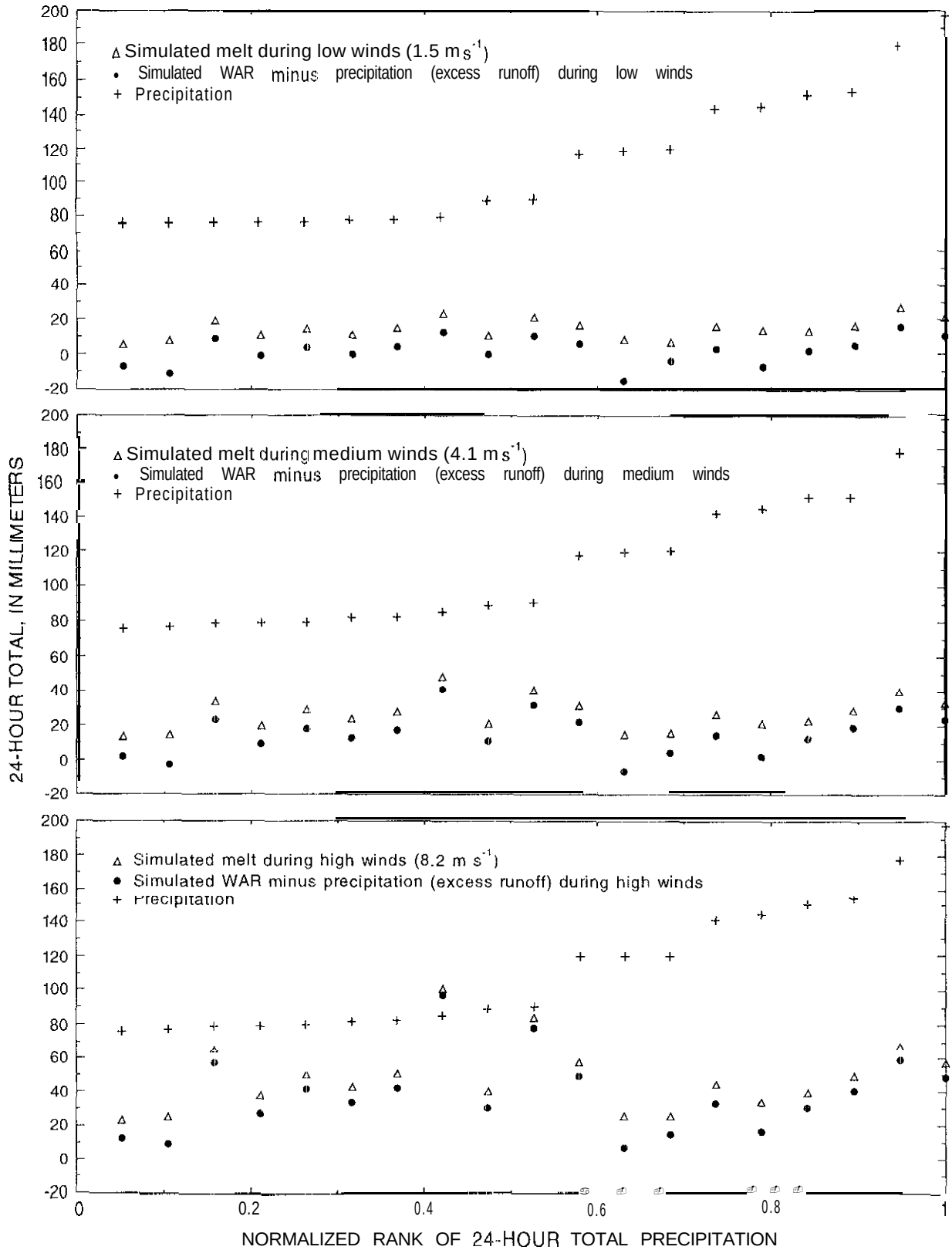

Figure 22.--Snoqualmie Pass, ranked 24-hour total precipitation, simulated melt, and simulated water available for runoff (WAR) minus precipitation (excess runoff) during each 24-hour event for low-, medium-, and high-wind conditions.

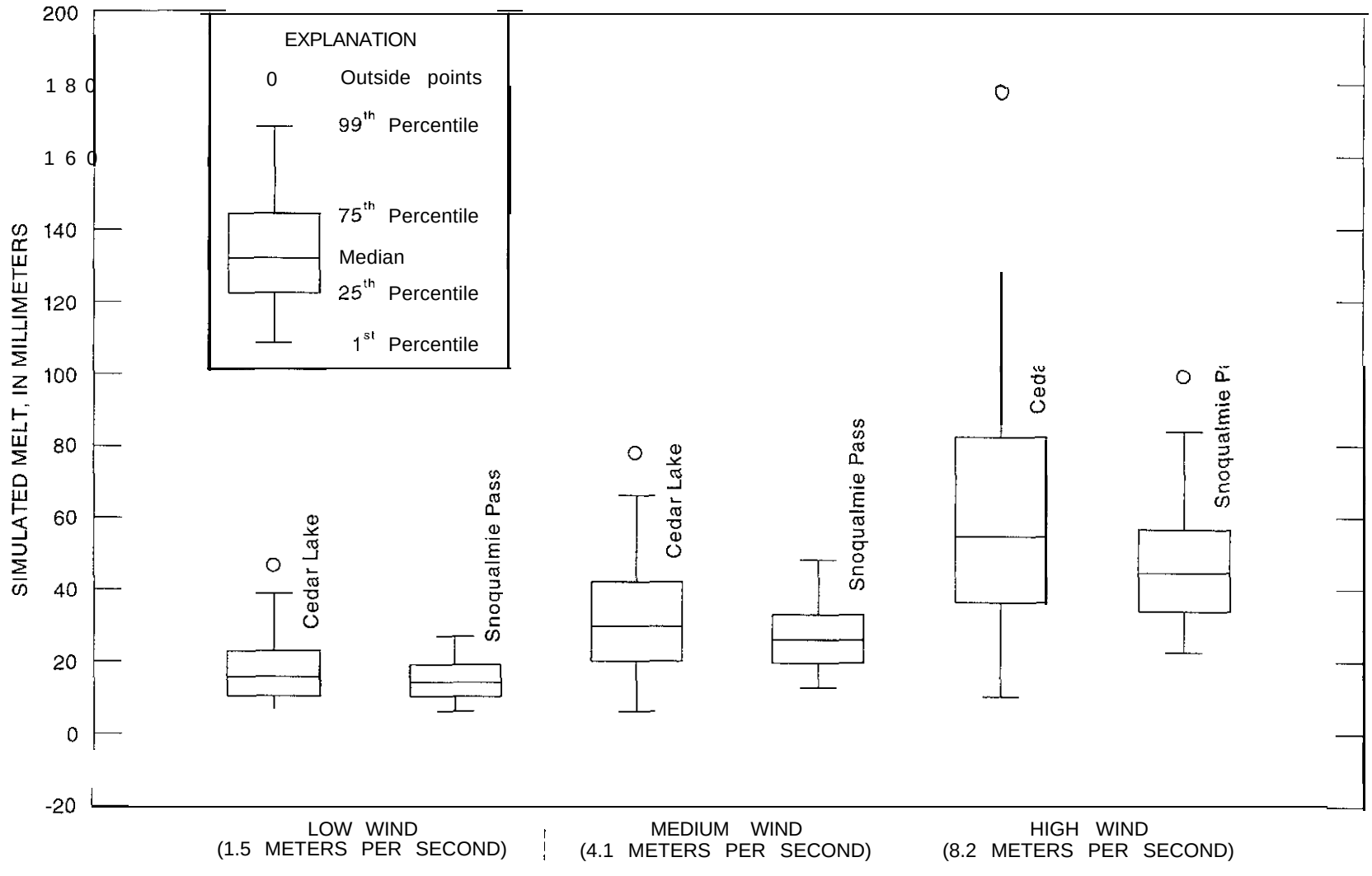

Figure 23.--Simulated melt for 24-hour events at Cedar Lake and Snoqualmie Pass for low-, medium-, and high-wind conditions.

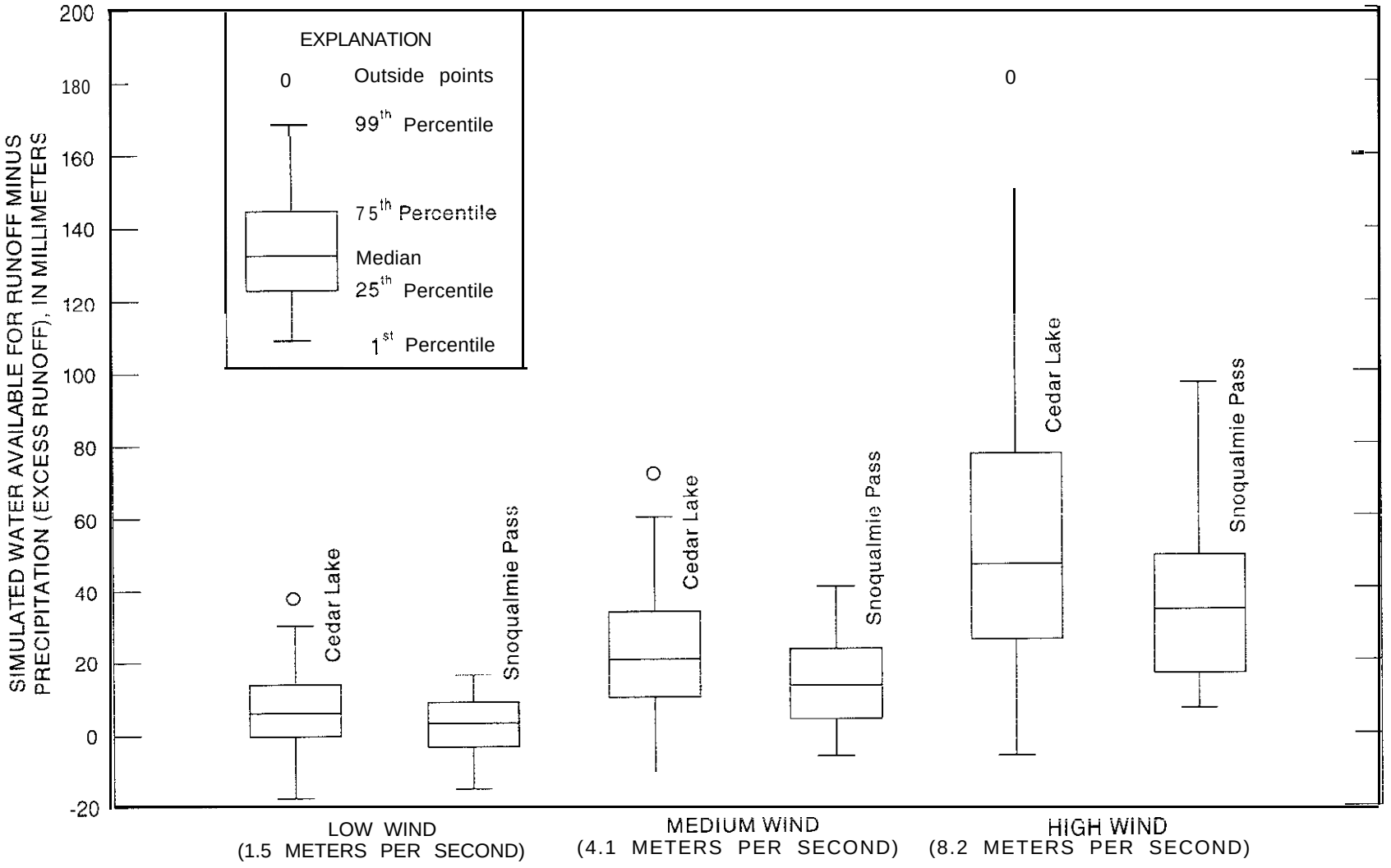

Figure 24.--Simulated water available for runoff minus precipitation (excess runoff) for 24-hour events at Cedar Lake and Snoqualmie Pass for low-, medium-, and high-wind conditions.

Table 12.--*Summary of simulated melt, simulated water available for runoff (WAR) minus precipitation (excess runoff), and simulated melt and water available for runoff minus precipitation as a percent of precipitation for different assumed wind conditions at Cedar Lake and Snoqualmie Pass*

[$m\ s^{-1}$, meter per second; mm, millimeter]

Station	Wind condition	Variable type	Minimum	Maximum	Median
Cedar Lake	LOW (1.5 $m\ s^{-1}$)	Simulated melt (mm)	4.2	47.0	16.2
	Medium (4.1 $m\ s^{-1}$)		6.1	78.2	30.1
	High (8.2 $m\ s^{-1}$)		10.3	178.X	54.7
Snoqualmie Pass	Low (1.5 $m\ s^{-1}$)		5.9	26.7	13.9
	Medium (4.1 $m\ s^{-1}$)		12.8	48.3	26.1
	High (8.2 $m\ s^{-1}$)		22.4	99.6	44.5
Cedar Lake	LOW (1.5 $m\ s^{-1}$)	Simulated WAR minus	-17.5	38.0	5.9
	Medium (4.1 $m\ s^{-1}$)	precipitation (excess	-12.7	71.8	20.3
	High (8.2 $m\ s^{-1}$)	runoff) (mm)	-5.x	1x1.7	46.7
Snoqualmie Pass	Low (1.5 $m\ s^{-1}$)		-15.3	16.1	2.7
	Medium (4.1 $m\ s^{-1}$)		-6.1	40.6	13.3
	High (8.2 $m\ s^{-1}$)		6.9	96.5	34.0
Cedar Lake	LOW (1.5 $m\ s^{-1}$)	Simulated melt	4	48	18
	Medium (4.1 $m\ s^{-1}$)	as a percent of	6	87	34
	High (8.2 $m\ s^{-1}$)	precipitation (mm)	9	197	62
Snoqualmie Pass	Low (1.5 $m\ s^{-1}$)		6	27	12
	Medium (4.1 $m\ s^{-1}$)		12	57	22
	High (X.2 $m\ s^{-1}$)		21	117	38
Cedar Lake	LOW (1.5 $m\ s^{-1}$)	Simulated WAR minus	-21	36	6
	Medium (4.1 $m\ s^{-1}$)	precipitation (excess	-14	78	24
	High (8.2 $m\ s^{-1}$)	runoff) as a percent of precipitation	-6	197	53
Snoqualmie Pass	Low (1.5 $m\ s^{-1}$)		-15	15	2
	Medium (4.1 $m\ s^{-1}$)		-5	48	12
	High (X.2 $m\ s^{-1}$)		6	113	33

Presumed 24-hour rain events that were extracted from the synthetic Cedar Lake and Snoqualmie Pass records represented a wide range of rain-on-snow conditions. Average air temperatures for the events ranged from 0.9 to 11.7°C, dewpoint temperatures from 0 to 10.0°C, and precipitation from 3.1 to X.2 mm h^{-1}. In the 51 and 19 events that were identified in the Cedar Lake and Snoqualmie Pass records, respectively, many different combinations of these, average values occurred. All 76 events were simulated to determine possible ranges of WAR (both based on simulated melt and simulated excess runoff) that could occur.

Median values of simulated WAR (based on melt estimates) ranged from 112 to 118 percent of precipitation for low, 24-hour average wind speeds (1.5 m s^{-1}), from 122 to 134 percent of precipitation for medium, 24-hour average wind speeds (4.1 m s^{-1}), and from 138 to 162 percent of precipitation for high wind speeds (8.2 m s^{-1}). In one extreme, snowmelt increased WAR to almost three times the precipitation depth. Simulated melt ranged from 4.2 to 47.0 mm for low wind speeds and from 10.3 to 178.8 mm for high wind speeds. The average of the median simulated 24-hour melt depths at Cedar Lake and Snoqualmie Pass was IS. 1, 2X. 1 and 49.6 mm at low, medium, and high wind speeds, respectively.

To avoid over-interpretation of the results of the high-wind simulations, it should be realized that these simulations represent worst-case scenarios, that is, a thick, ripe snowpack that never entirely melts during 24-hours and an hourly wind speed of 8.2 m s^{-1} sustained for 24 hours. How often these extreme conditions actually did occur is not known. As described previously, hourly wind speeds equal to or exceeding 7.7 m s^{-1} and X.7 m s^{-1} were observed 10 percent of the time from October through March in the SeaTac and Stampede Pass records, respectively, without consideration of the number of consecutive hours that those high wind speeds were sustained

In spite of all data assumptions and unknowns, the simulations strongly suggest that rain-on-snow conditions can increase the WAR significantly. On average, for the medium and high-wind simulations turbulent heat was the dominant source of energy, and net all-wave radiation and advective heat were of similar importance. For the low-wind events, however, both net all-wave radiation and advective heat were more important than turbulent heat. For some of the events, net thermal radiation was negative because of losses of thermal radiation from the snowpack to the atmosphere. For these events, shortwave radiation dominated the all-wave radiation component of the energy budget. Even though rain itself is not a dominant source of energy to generate snowmelt during warm, moist, and windy conditions. the amount of water it contributes t" the WAR is significant. No estimate was made of the frequency of occurrence of particular rain-on-snow conditions.

SUMMARY

Rain-on-snow events on mountain slopes in the tran-Gent-snow zone of the Pacific Northwest result in snowmelt and condensation that increase the amount of water available for runoff (WAR) and increase the potential for downstream flooding and erosion. In forest openings (such as those resulting from clearcut logging), snow accumulation and microclimate conditions differ from those in forest stands; and these differences may lead to increased WAR during rain-on-snow events.

A conceptual model was described of snow accumulation and melt processes that occur in forest stands and forest openings. The high degree of unpredictability of precipitation-interception processes in forested stands precluded the creation of a numerical model to mimic those processes without greatly simplifying the conceptual model. A simplified numerical model of interception processes would have to be tested against a statistically significant number of plot-scale observations of hourly lysimeter outflow representative of an entire forested plot and frequent measurements of snowpack properties (at least every few days). Neither data type was available in sufficient quality or quantity to create and test a numerical precipitation-interception model. As a result, only snow accumulation and melt in a forest opening were analyzed in this study.

Although hourly, clearcut, plot-scale data collected as part of previous rain-on-snow studies were available for various locations and altitudes throughout the western Cascade Range of the Pacific Northwest, these data could not be used to simulate snow accumulation and melt over extended periods of time because they were incomplete and inadequate for this purpose. Because an objective of the present study was to characterize snowmelt in a typical clearcut forest opening during rain-on-snow events for different storm conditions, two S-day periods with some of the best hourly clearcut data were selected for numerical simulation using the physically-based. energy-balance model of Marks (1988). These data were collected in the H.J. Andrews Experimental Forest in Oregon during the 1983-84 winter and included three rain-on-snow events, two of which bad precipitation depths so small that they were not identified as rain-on-snow events in previous

studies. Observed excess runoff (defined as WAR minus precipitation) was compared with simulated snowmelt to evaluate the adequacy of Marks' model for use in rain-on-snow conditions.

Variables used as input to Marks' model were precipitation depth, density, and temperature, net solar radiation, incoming thermal radiation, wind speed, air temperature, vapor pressure, soil temperature, and snowpack conditions at the start of the simulation. Model output consisted of snowmelt, evaporation (or condensation), and WAR. Two of the input variables, thermal radiation and precipitation density, were computed as a function of observed air temperature. The observed precipitation depth and wind speeds were suspected of being too low. As a result, wind speed was increased by 0.9 m s^{-1}, which is the threshold of the anemometer used in the clearcut of the H.J. Andrews Experimental Forest, but no adjustments were made for precipitation catch deficiencies. Snowpack conditions at the start of each 5-day simulation were assumed. Observed WAR was not adjusted, although it too was suspected of containing error. No observations of snowmelt or condensation were available.

When simulated snowmelt was compared with observed excess runoff, it was found that Marks' model accurately predicted the timing of snowmelt generation during rain on snow, but that the depth of simulated melt was consistently smaller than the depth of observed excess runoff. This disagreement between simulated snowmelt and observed excess runoff was attributed to a lack of reliable data rather than to shortcomings in Marks' model, although the model remains unvalidated for rain-on-snow conditions in a transient-snow zone. In a previous study, Marks' model was shown to perform well when simulating snow accumulation and melt for a deep, cold snowpack in the Sierra Nevada. Considering that the available data were not collected for the purpose of performing continuous simulations using an energy-balance numerical model, Marks' model appeared to perform reasonably well for rain-on-snow simulations in the Pacific Northwest.

The sensitivity of WAR during rain on snow to different climate conditions was evaluated by systematically changing input variables and computing the changes in simulated snowmelt during the three selected rain-on-snow events. The sensitivity analysis showed that snowmelt is most sensitive to changes in wind speed and air temperature because they result in changes in turbulent and thermal energy to the snowpack. Although the amount of rain determines the total WAR, it does not contribute a dominant amount of energy to the snowpack to produce melt. Net solar radiation is a minor source of energy during significant rain-on-snow events because extreme cloudiness limits penetration of this radiation and days are short in winter. During extreme rain-on-snow conditions (that is, strong winds and high air temperatures), condensation of water vapor onto the snowpack may increase WAR by up to 6 percent of the snowmelt.

To determine the possible range of WAR that could be produced during rain on snow in typical clearcut forest openings in the western Cascade Range, Marks' model was applied to 24-hour rainstorms exceeding 75 mm of precipitation that were extracted from the historical climate records at Cedar Lake and Snoqualmie Pass NWS stations. Cedar Lake is located near the bottom of the transient-snow zone and Snoqualmie Pass near the top. The climate records, consisting of hourly precipitation and daily temperature extremes, were corrected and expanded through correlations with nearby NWS climate data. To obtain a complete set of hourly model input, assumptions were made regarding the net solar radiation, dewpoint temperatures, wind speed, and the diurnal signal of air temperatures. In addition, the physical settings of the Cedar Lake and Snoqualmie Pass data-collection sites were assumed to be identical to that of the H.J. Andrew Experimental Forest clearcut plot, as this was considered representative of a typical clearcut forest opening. As a result, the same thermal radiation source and sink geometry was assumed at all sites. Simulations of the synthetic historical records showed that if an unlimited amount of snow is on the ground, the 24-hour snowmelt component of WAR can range from 4.2 to 47.0 mm for low wind speeds and from 10.3 to 178.8 mm for high wind speeds. The average of the median 24-hour snowmelt at Cedar Lake and Snoqualmie Pass was 15.1 mm at low wind speeds and 49.6 mm at high wind speeds. Condensation could increase WAR by an additional few percent of the melt.

The numerical simulations of historical climate data at Cedar Lake and Snoqualmie Pass showed that snowmelt during rain on snow can significantly increase the WAR in forest openings over rainfall alone. Although rain itself is not a dominant source of energy to generate melt, it does contribute an important fraction of the runoff that can occur during the warm, moist, and windy conditions.

This study did not address how different the amounts of WAR would be in forest stands and forest openings during identical rain-on-snow events. Instead, only the range in amounts of WAR that may be generated in a typical clearcut forest opening was computed. For land-use management decisions, however, it is important to know the differences in WAR between forest openings and forest

stands. Based on theoretical consideration?,. WAR is thought to be greater in forest openings than forest stands; for this reason, the simulated range in WAR for a typical clearcut forest opening can he used for worst-case-scenario planning.

FUTURE STUDIES

Future studies of rain on snow could bc designed to enable the numerical simulation of snow accumulation and melt in both forest openings and forest stands. A numerical model that can simulate precipitation-interception processes in the forest canopy in addition to the energy and mass balance of a snowpack would be needed. If this expanded model could he tested and validated with high-quality time series of climate and WAR data, it could he applied to historical data at NWS sites to examine the magnitude-frequency relationship of WAR during rain on snow in forest openings versus forest stands. Data would need to he collected at sites of various slopes, aspects, and vegetation densities.

Specifically, data collection for future studies could include frequent visit:; to forest-stand and forest-opening data-collection sites (at least every few days) to obtain measurements of snowpack thickness, density, liquid-water content, and tcmpcraturc and to verify that accurate climate data arc being, collected. In addition to climate variables such as hourly wind speed, incoming solar radiation, air temperature, and dewpoint tcmpcraturc, variables such as incoming thermal radiation, reflected solar radiation, and precipitation density could be measured. For study sites at altitudes where snowpacks remain close to isothermal at 0°C, measurements of soil tcrnpcraturc could he optional. The collection of hourly WAR data in forest stands would have to bc designed to account for the lateral variability in the accumulation and melt of snow below a forest canopy. Unfortunately, no ideal data-collection design exists to account for this heterogeneity. Instead, a combination of two data-collection designs could be used to maximize the advantages and minimize the disadvantages of each.

Measurement of WAR in forested conditions could hc done at both the catchmcnt and plot-scale lysimcter scale. At the catchment scale, streamflow would bc measured as the equivalent of lysimeter outflow. The advantage of this approach is that streamflow integrates the heterogeneities in snow accumulation and melt that occur in the catchment, but the disadvantage is that complications arc added to the determination of WAR, as variables such as evapotranspiration, soil-moisture storage, bank storage, interflow, and baseflow all affect the streamflow measurement. The measurement would need to bc corrected for these variables to derive hourly values of WAR for the catchmcnt, but there would he uncertainty in the size of each of these corrections. At the plot-scale lysimetcr scale, a large surface area of one or multiple lysimcters would need to be installed in the forest stand to measure WAR. The advantage of this approach would he that a direct measurement of WAR is madc, but the disadvantage is that a" unwieldy large number of small lysimeters or a few extremely large lysimctcrs are needed to obtain WAR measurements that average the effects of lateral variability in the accumulation and melt of snow below the forest canopy. Simultaneous analysis of both the plot- and catchment-scale data would allow for a nested, duplicate approach that is more likely to produce useful results for simulating WAR during rain on snow in forest stands than analysis of either data type alone.

REFERENCES CITED

Allis, J.A., Harris, B., and Sharp; A.L., 1963, A comparison of performance of five rain-gage installations: Journal of Geophysical Research, v. 68, pt. 3, p. 4723-4729.

Anderson, E.A., 1976, A point energy and mass balance model of a snow cover: National Oceanic and Atmospheric Administration Technical Report NWS 19, 150 p.

Bcaudry, Pierre, and Golding, D.L., 1983, Snowmelt during rain on snow in Coastal British Columbia, *in* Western snow Conference, 51 st, Vancouver, Washington, 1983, Proceedings: Fort Collins, Colorado, Colorado State University, p. Y-66.

Bcrris, S.N., 1984, Comparative snow accumulation and melt during rainfall in forest and clearcut plots in western Oregon: Corvallis, Oregon, Oregon State University, Master's thesis, 152 p.

Berris, S.N., and Han-, R.D., 1987, Comparative snow accumulation and melt during rainfall in forested and clear-cut plots in the western Cascades of Oregon: Water Resources Research, v. 23, no. 1, p.135-142.

Bruncngo, M.J., 1990, A method of modeling the frequency characteristics of daily snow amount, for stochastic simulation of rain-on-snowmelt events, in Western Snow Conference, 58th, Sacramento, California, 1990, Proceedings: Fort Collins. Colorado, Colorado State University, p.110-121.

Brutsaert, Wilfried, 1975, On a derivable formula for long-wave radiation from clear skies: Water Resources Research, v. 11, p. 142.744.

____1982, Evaporation into the atmosphere-Theory, history, and applications: Dordrecht and Boston, D. Reidel Publishing Co., 299 p.

Ca'Zorzi, F., and Dalla Fontana, G., 1986, Improved utilization of maximum and minimum daily temperature in snowmelt modclling, in Morris, E.M., ed., Modelling Snowmelt-Induced Processes, Budapest, Hungary, 1986, Proceedings: International Association of Hydrological Sciences, Publ. no. 155, p. 141-150.

Coffin, B.A., and Harr, R.D., 1992, Effects of forest cover on volume of water delivery to soil during rain-on-snow, Timber/Fish/Wildlife Report No. SH1-92-001: Olympia, Washington, Washington Department of Natural Resources, 118 p.

Colbeck, S.C., 1978, The difficulties of measuring the water saturation and porosity of snow: Journal of Glaciology, v. 20, p. 189-201.

Conway, H., and Benedict, R., 1994, Infiltration of water into snow: Water Resources Research, v. 30, no. 3, p. 641-649.

Elder, Kelly, Dozier, Jeff, and Michaelsen, Joel, 1991, Snow accumulation and distribution in an alpine watershed: Water Resources Research, v. 27, no. 7, p. 1541-1552.

Gary, H.L., 1975, Airflow patterns and snow accumulation, in Western Snow Conference, 43rd, Coronado, California, 1975, Proceedings: Fort Collins, Colorado, Colorado State University, p. 106-l 13.

Goodison, B.E., Ferguson, H.L., and McKay, GA., 1981, Measurement and data analysis, in Gray, D.M., and Male, D.H., eds., Handbook of snow: New York, Pcrgamon Press, p. 191-274.

Harr, R.D., 1981, Some characteristics and consequences of snowmelt during rainfall in western Oregon: Journal of Hydrology, v. 53, p. 277.304.

____1986, Effects ofclearcutting on rain-on-snow runoff in western Oregon--a new look at old studies: Water Resources Research, v. 22, no. 7, p. 1095~1100.

Larson, L.W., and Peck, E.L., 1974, Accuracy of precipitation measurements for hydrologic modeling: Water Resources Research, v. IO, no. 4, p. 857.863.

Leonard, R.E., 1967, Mathematical theory of interception, in Advanced science seminar on forest hydrology, University Park, Pennsylvania, 1965, Proceedings: Oxford, Pergamon Press, p. 131-136.

Linslcy, R.K., Jr., Kohler, M.A., and Paulhus, J.L.H., 197.5, Hydrology for engineers (2nd ed.): New York, McGraw-Hill. 482 p.

Male, D.H., and Granger, R.H., 1981, Snow surface energy exchange: Water Resources Research, v. 17, no. 3, p. 609.627.

Marks, Danny, 1988, Climate, energy exchange, and snowmelt in Emerald Lake Watershed, Sierra Nevada: Santa Barbara, California, University of California, Ph.D. dissertation, 149 p.

Marks, Danny, and Dozier, Jeff, 1979, A clear-sky longwave radiation model for remote alpine areas: Archiv für Meteorologie Geophysik und Bioklimatologie, set. B, no. 27, p. 159-187.

____1992, Climate and energy exchange at the snow surface in the alpine region of the Sierra Nevada 2—Snow cover energy balance: Water Resources Research, v. 28, no. 1 1, p. 3043.3054.

Marks, Danny, Dozier, Jeff, and Davis R.E., 1992, Climate and energy exchange at the snow surface in the alpine region of the Sierra Nevada l-Meteorological measurements and monitoring: Water Resources Research, v. 28, no. II, p. 3029.3042.

Marks, Danny, Kattelmann, R.C., Dozier, Jeff, and Davis, R.E., 1986, Monitoring snowcover properties and processes in a small alpine watershed, in Santeford, H.S., ed., Proceedings of the Sixth International Northern Research Basins Symposium/Workshop, Houghton, Michigan, 1986: Houghton, Michigan, Michigan Technological University, p. 259-275.

McKay, G.A., 1970, Precipitation, in Gray, D.M., cd., Handbook on the principles of hydrology: Port Washington, New York, Water Information Center, Inc., p. 2.1-2.111.

McKay, (;.A., and Gray, D.M., 1981, The distribution of snowcover, in Gray, D.M., and Male, D.H., cds., Handbook of snow: New York, Pergamon Press, p. 153-190.

Miller, J.F., Frederick, K.H., and Tracey, R.J., 1973, Precipitation-frequency atlas of the western United States-Volume IX Washington, NOAA Atlas 2: Silver Spring, Maryland, U.S. Department of Commerce, 43 p.

Morris, E.M., 1982, Sensitivity of the European Hydrological System snow models, in Glen, J.W., cd., Hydrological aspects of alpine and high-mountain al-ens, Exeter, United Kingdom, 1982, Proceedings: International Association of Hydrological Sciences Publication no. 138, p. 221-231.

Morris, E.M., 1986, Modelling of a seasonal snowcover, in Kukla, G., Barry, R.G., Hecht, A., and Wiesnet, D., eds., Snow watch 'X5, Glaciological Data Report GD-18: Boulder, Colorado, World Data Center for Glaciology, p. 225-240.

Owenby, J.R., and Ezell, D.S., 1992, Monthly station normals of temperature, precipitation, and heating and cooling degree days, 1961-1990, Climatography of the United States no. 81: Asheville, North Carolina, National Oceanic and Atmospheric Administration, [30] p.

Pacific Northwest River Basin Commission, 1969, Water Resources, Columbia-North Pacific region comprehensive framework study, Appendix II: Vancouver, Washington, Pacific Northwest River Basin Commission, 147 p.

Schmidt, R.A., and Pomeroy, J.W., 1990, Bending of a conifer branch at subfreezing temperatures: implications for snow interception: Canadian Journal of Forest Resources, v. 20, p. 1250-1253.

Schmidt, R.A., and Troendle, C.A., 1992, Sublimation of intercepted snow as a global source of water vapor, in Western Snow Conference, 60th, Jackson, Wyoming. 1992, Proceedings: Fort Collins. Colorado, Colorado State University, p. 1-Y.

Stanhill, G., 1992, Accuracy of global radiation measurements at unattended, automatic weather stations: Agricultural and Forest Meteorology, v. 61, p. 151-156.

U.S. Army Corps of Engineers, 1956, Snow hydrology-~ summary report of the snow investigations: Portland, Oregon, North Pacific Division, U.S. Army Corps of Engineers, 437 p.

Warren, S.G., and Wiscomhe, W.J., 1980, A model for the spectral albedo of snow, II, snow containing atmospheric aerosols: Journal of the Atmospheric Sciences, v. 37, no. 12, p. 2734-2745.

Washington Forest Practices Board, 1994, Standard methodology for conducting watershed analysis (version 2. I), Forest Practices Board Manual: Olympia, Washington, Washington Forest Practices Board, [about 500] p.

Wigmosta, M.S., Connelly, B.A., and Cundy, TW.. 1993, Simulating the effects of forest cover on snowmelt during rain-on-snow events [abs.]: Eos Transactions, American Geophysical Union, v. 74, no. 43, p. 23X.

Wigmosta, M.S., Vail, L.W., and Lettenmaier, D.P., 1994, A distributed hydrology-vegetation model for complex terrain: Water Resources Research, v. 30, no. 6, p. 1665- 1679.

Wiscomhe, W.J., and Warren, S.G., 1980, A model for the spectral albedo of snow, I, pure snow: Journal of the Atmospheric Sciences, v. 37. no. 12, p. 2712-2733.

Zinke, P.J., 1967, Forest interception studies in the United States, *in* Advanced science seminar on forest hydrology, University Park, Pennsylvania, 1965, Proceedings: Oxford, Pergamon Press, p. 137-16 1.